CERTIFICATO DI FIRMA DIGITALE

Si certifica che questo documento informatico

phd_unisi_107263.pdf

composto da n°81pagine

È stato firmato digitalmente in data odierna con Firma Elettronica Qualificata (FEQ), avente l'efficacia e gli effetti giuridici equivalenti a quelli di una firma autografa, ai sensi dell'art. 2702 del Codice Civile e dell'art. 25 del Regolamento UE n. 910/2014 eIDAS (electronic IDentification Authentication and Signature).

PROCESSI INFORMATICI COMPLETATI

- **Apposizione di Firma Elettronica Qualificata Remota** emessa da Intesi Group S.p.A. in qualità di prestatore di servizi fiduciari qualificati autorizzato da AgID, per garantire con certezza l'autenticità, l'integrità, il non ripudio e l'immodificabilità del documento informatico e la sua riconducibilità in maniera manifesta e inequivoca all'autore, ai sensi dell'art. 20 comma 2 del CAD - D.lgs 82/2005.
- **Apposizione di Marca Temporale Qualificata** emessa da Intesi Group S.p.A. in qualità di prestatore di servizi fiduciari qualificati autorizzato da AgID, per attribuire una data e un orario opponibile a terzi, ai sensi dell'art. 20 comma 3 del CAD - D.lgs 82/2005 e per far sì che la Firma Elettronica Qualificata apposta su questo documento informatico, risulti comunque valida per i prossimi 20 anni a partire dalla data odierna, anche nel caso in cui il relativo certificato risultasse scaduto, sospeso o revocato.
- **Apposizione di Contrassegno Elettronico**, l'unica soluzione tecnologica che permette di prorogare la validità giuridica di un documento informatico sottoscritto con firma digitale e/o marcato temporalmente, rendendolo inalterabile, certo e non falsificabile, una volta stampato su supporto cartaceo, ai sensi dell'art. 23 del CAD - D.lgs 82/2005.

  Per risalire all'originale informatico è necessario scansionare il Contrassegno Elettronico, utilizzando l'applicazione HONOS, disponibile per dispositivi Android e iOS.


Regione Toscana
GIOVANISÌ


University of Siena

Department of Biotechnology, Chemistry and Pharmacy

PhD in Biochemistry and Molecular Biology BIBIM 2.0

XXXVI Cycle

"Study of role of sulphated proteoglycans in cancer"

Scientific-disciplinary sector: BIO/10

Coordinator:

Prof. Lorenza Trabalzini

Supervisor:

Prof. Chiara Falciani

Doctoral Thesis of

Giulia Marianantoni

Academic Year 2022/2023

In a time of deceit, telling the truth is a revolutionary act.

George Orwell

Abstract

Pancreatic cancer is projected to become the second leading cause of death by 2030, due to an extremely immune-suppressive tumour environment and lack of early-stage markers. Over the last decade, new insights have emerged regarding the mechanism and biological significance of the interactions between heparan sulphate proteoglycans (HSPGs) and their ligands. HSPGs are found in cell surface and extracellular matrix (ECM) and contribute to the binding of growth factors and chemokines to their receptors, thus HSPGs can modulate cell-growth, proliferation and play an important role in cell migration. HSPGs overexpression in some tumours has enabled the concrete hypothesis of their use as possible new markers and target treatment. In this study, we investigated the tumour specificity and the bioactivity of different tetra-branched peptides that could target HSPGs and be effective as new cancer drugs. Particularly, we focused on peptide's specificity on pancreatic cancer cell lines. The use of the tetra-branched structure overcomes the sensitivity to proteolytic degradation of the linear monomeric structure, increasing their half-life and maintaining their target specificity. BOPs proved to be selective in binding and killing tumour cells, particularly pancreatic cancer cells, PANC-1 and Mia Paca-2, compared to cells with no tumoral origin RAW 264.7 and PgsA-745. The promising cancer selectivity exhibited by the two peptides (BOP7 and BOP9) is likely attributed to their repeated cationic sequences, enabling multivalent binding to heparan sulphate proteoglycans (HSPGs) bearing anionic sulfation patterns in cancer cells, that typically exhibit increased surface negativity. This interaction of BOPs with HSPGs not only fosters an anti-metastatic effect *in vitro*, as evidenced by reduced adhesion and migration of PANC-1 cancer cells, but also demonstrated promising specific tumour cytotoxicity and low haemolytic activity. A preliminary *in vivo* assay in nude mice, showed an encouraging ability of BOP9 to inhibit tumour grafting and growth by 20% in a pancreatic cancer model. In the perspective of increasing the chances of early diagnosis of pancreatic cancer, tumour conditioned medium of pancreatic cell cultures was analysed for whole RNA from exosomes. Lastly, to understand the regulation of proteoglycans intracellular pathways on pancreatic cancer cells, we investigate Syndecan-1 (Sdc-1) and Glypican-1 (Gpc-1) role in mTOR signalling. mTOR is involved in migration, proliferation, autophagy, survival and catabolism processes and its inhibition led to proliferative arrest in KRAS/PTEN deficient tumours, but not in KRAS/p53 mutated. On the other hand, Sdc-1 and Gpc-1 seem to be related to AKT and ERK pathway in several tumours. So, we first treated all the primary pancreatic cell lines with AZD2014 (mTORC2 inhibitor) and Rapamycin (mTORC1 inhibitor) to verify the effect of the drug on proteoglycans cell surface expression. Then, we overexpressed Sdc-1 to investigate its role in AKT/ERK cascade in PA14C cells. In fact, the ability of syndecan-1 to enhance TGFβ binding on cell surface receptors let us suppose its involvement in the AKT/ERK pathway. Furthermore, AKT overactivation is present in 33% ductal carcinoma in situ lesions, while phosphorylation of ERK1/2 is known to be necessary for TGFβ-induced epithelial–mesenchymal transition (EMT) in pancreatic cancer cells, and their inhibition reduce CDK2 levels and prevent EMT due to the downstream regulation of c-MYC, with effects on cancer cell growth suppression and cellular senescence. To summarize, peptides demonstrated a great specificity for cancer cells and the ability to reduce their migration and proliferation properties. BOPs target, HSPGs, could play a role in mTOR signalling opening new perspectives in cancer treatment.

Table of contents

Chapter I

Introduction

Proteoglycans overview

Proteoglycans consist of a core protein to which one or more glycosaminoglycan chains are covalently attached, resulting in a brush-like structure. Most of the glycosaminoglycans bind the core through a tetrasaccharide linker that consist of glucuronic acid (GlcA), two galactose (Gal) and a xylose (Xyl) residue via glycosidic bonds. The core proteins are highly conserved in the animal kingdom, and they are rich in amino acids such as serine and threonine. Glycosaminoglycans are long, unbranched molecules that contain repeating disaccharide units of a uronic acid such as glucuronic acid (GlcA) or iduronic acid and an amino sugar (either N-acetylglucosamine, or N-acetylgalactosamine). These glycosaminoglycans impart a negative charge on proteoglycans giving them specificity. In fact, proteoglycans can be classified based on glycosaminoglycans they possess. There are four basic types of glycosaminoglycans: chondroitin sulfate (CS), heparan sulfate, dermatan sulfate (DS), and keratan sulfate (KS). These glycosaminoglycans give rise to several proteoglycans like decorin, biglycan, aggrecan, neurocan, testican, fibromodulin, lumican, etc. Lastly, proteoglycans can form large complexes with other proteoglycans, fibrous proteins (like collagen), and other components (hyaluronan) of the extracellular matrix [1].

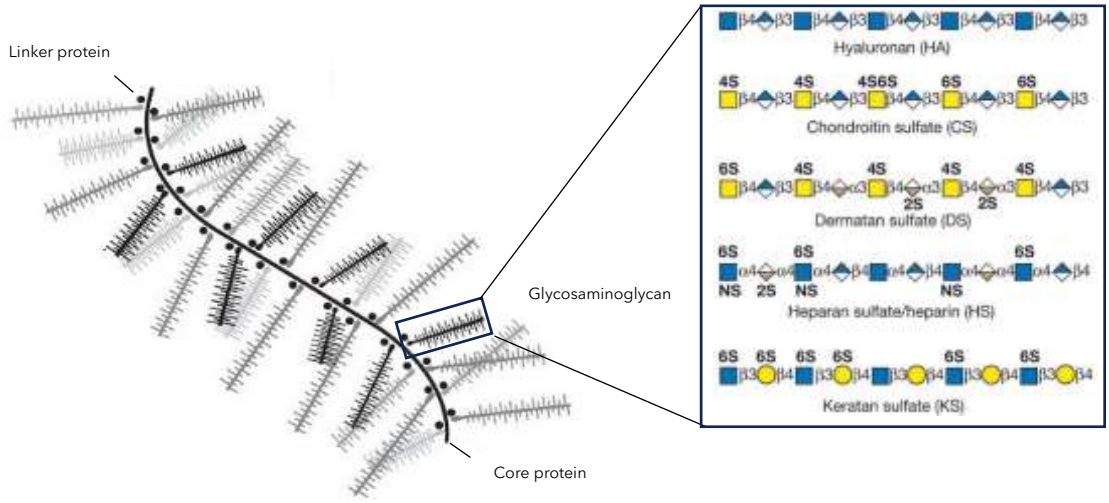

Fig. 1 Proteoglycans general structure: *GAG can be characterized by different disaccharides units which are connected to a tetrasaccharide linkage made by GlcA, Gal, Xyl that directly bind the serine residue of the core protein.*

Intracellular proteoglycans

Serglycin occupies a class of its own as it is the only proteoglycan that is covalently substituted with heparin, due to its consecutive and unique Ser-Gly repeats, resulting essentially a silk-like sequence. It has been utilized primarily by mast cells for the proper assembly and packaging of the numerous proteases that are released upon inflammation. In fact, serglycin promotes granular storage via electrostatic interaction between its highly anionic heparin chains and basic residues within the various proteases of the secretory granules. All inflammatory cells express serglycin and store it within intracytoplasmic granules where, in addition to proteases, serglycin binds and

modulates the bioactivity of several inflammatory mediators, chemokines, cytokines and growth factors. More recently, serglycin has been found in a wide variety of non-immune cells such as endothelial cells, chondrocytes, and smooth muscle cells. Cell-surface serglycin promotes adhesion of myeloma cells to collagen I and affects the expression of matrix metalloproteases (MMPs). It correlates with a more aggressive malignant phenotype, and it has been recently proposed that serglycin protects breast cancer cells from complement attack, thereby supporting cancer cell survival and progression [2].

Cell surface proteoglycans

Syndecans are a transmembrane class of HSPGs that connect the surface of the cells to the underlying extracellular matrix, and it comprises a single-pass transmembrane protein cores with an ectodomain and intracellular domain. The ectodomains exhibit the lowest amount of amino acid sequence conservation, no more than 10–20%, in contrast to the transmembrane and cytoplasmic domains, which are 60–70% identical. This allows syndecans to interact with a variety of proteins and ligands, thereby providing enrichment in their biological function. The transmembrane domain contains a dimerization motif (GxxxG) that mediates both homo-dimerization and hetero-dimerization. The intracellular domain is composed of two regions of conserved amino-acids sequence (C1 and C2), separated by a central variable sequence of amino acids that is distinct for each family member (V). Notably, the C-terminus of all the four syndecans harbours a unique signature (EFYA) that binds PDZ-containing proteins. Generally, PDZ-containing proteins contribute to a proper anchor of transmembrane proteins to the cytoskeleton, thereby holding together large signalling complexes. Briefly, syndecans bind numerous growth factors, especially through their HS chains, and dictate morphogen gradients during development. Many, if not all the syndecans, can also act as soluble HSPGs via partial proteolysis of their juxtamembrane region, releasing their whole ectodomains. This shedding is considered a powerful post-translational modification that can regulate the amount of HSPG linked to the cell surface and their presence in the pericellular microenvironment. Several inflammatory cytokines can induce syndecans shedding by triggering outside-in signalling and by activating several metalloproteinases [3].

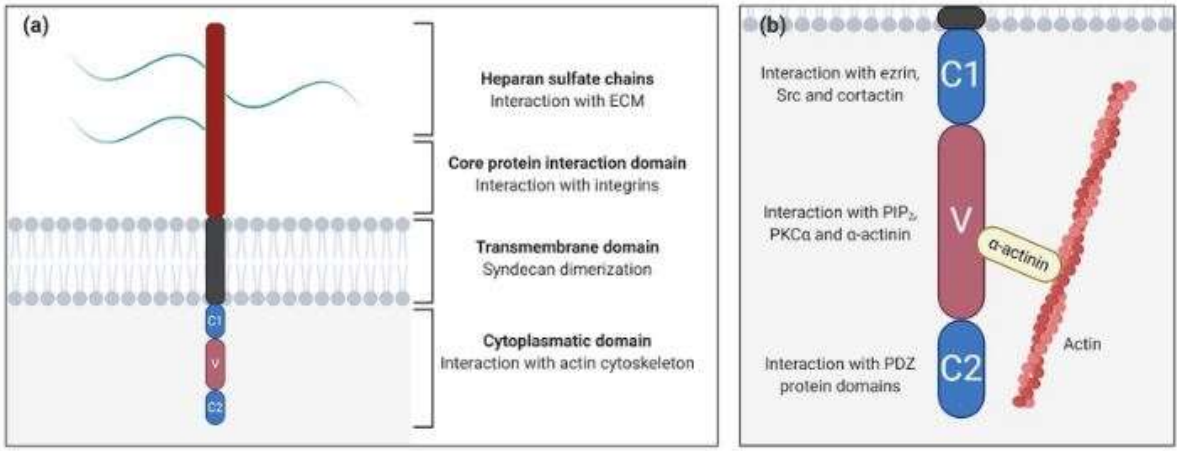

Fig. 2 Syndecan structure: *(a) Schematic representation of syndecan domains and their functions; (b) Close-up of the syndecan cytoplasmatic domain showing the constant (C1/C2) and the variable (V) regions and their potential interactions. The interaction between the variable region with α-actinin links syndecans to the cytoskeleton [3].*

Another surface proteoglycan is CSPG4. More in details, the melanoma-associated chondroitin sulphate proteoglycan (MCSP) was discovered over 30 years ago as a transmembrane proteoglycan and a highly immunogenic tumour antigen of melanoma tumour cells. It is a single-pass, type I transmembrane proteoglycan carrying one chondroitin sulphate chain, and harbouring a large ectodomain composed of three subdomains. Indeed, the central subdomain modules bind to collagens V and VI, FGF and PDGF; the transmembrane domain has a unique Cys residue, generally not found in transmembrane regions and the intracellular domain harbours a proximal region with numerous Thr phospho-acceptor sites for PKCα and ERK1/2. Functionally, CSPG4 proteoglycan promotes tumour vascularization, and due to the binding to collagen VI in the tumour microenvironment, it promotes cell survival and adhesion via the PI3K pathway *[4]*. Betaglycan is a co-receptor of TGFβ superfamily which is a large group of structurally related growth factors, that include TGFβs, activins, inhibins, bone morphogenetic proteins (BMPs), and growth and differentiation factors (GDFs). These factors take part in the regulation of multiple cellular processes, including cell survival, proliferation, migration, and differentiation *[5]*. Phosphacan is a secreted alternative splice variant of the full-length receptor protein tyrosine phosphatase β (RPTPβ), a transmembrane receptor with intracellular tyrosine phosphatase activity. Produced by both neurons and glia, it is a major component of brain matrix and can inhibit or promote axon growth, depending on the neuronal lineage *[6]*. Glypicans are a family of proteoglycans that are bound to the cell surface by a glycosylphosphatidylinositol anchor. They are highly conserved during evolution, and the mammalian genome contains six members of the family. In contrast to syndecans, the attachment of the GAG chains – mostly HS chains – is located near the juxtamembrane region. This allows the three linear HS chains to span a great deal of plasma membrane surface, thereby presenting various morphogens and growth factors in an active configuration to their cognate receptors. Glypicans are dually processed via partial proteases and lipases. In the former case, the ectodomain of glypicans is processed via endoproteolytic cleavage by a furin-like convertase. This processing generates two subunits that are then bound via disulfide bonds, in a way like the Met receptor. In the latter case, the entire glypican is released from the plasma membrane via an extracellular lipase (Notum) that cleaves the GPI anchor. Lastly, one of the main functions of these proteoglycans is the regulation of the signalling pathways triggered by hedgehogs, Wnts, fibroblast growth factors, and bone morphogenetic proteins *[7]*.

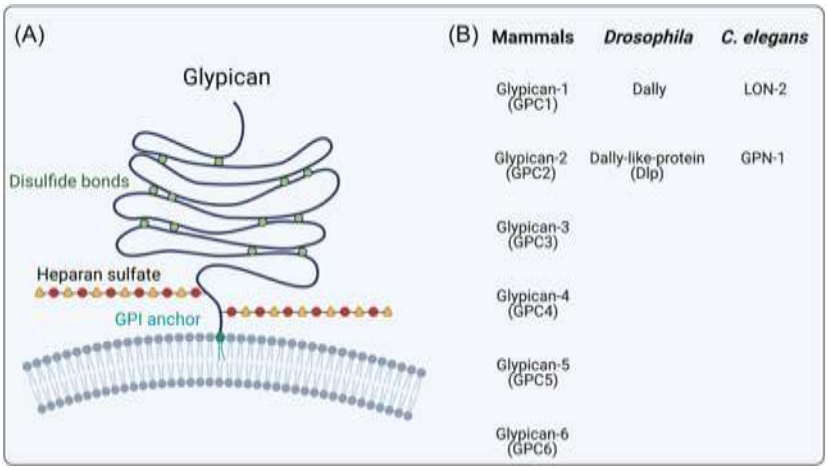

Fig. 3 A) *Representation of a glypican structure GPI anchored* ***B)*** *Members of the glypican family along the three main research models: Mammals, Drosophila and C. elegans. Particularly mammals are the one having more members of this family [7].*

Pericellular proteoglycans

This group of four proteoglycans is closely associated with the surface of many cell types anchored via integrins or other receptors, but they can also be a part of most basement membranes. Perlecan is one of the largest proteoglycans discovered, possessing a protein core of approximately 500 kDa that can be modified by the addition of N-terminal heparan sulfate (HS) side chains, measuring ~65 kDa each. It is a major basement membrane component, as are type IV collagen, laminin and nidogen. Perlecan has a ubiquitous distribution and occurs in vascular, poorly vascularized cartilaginous, fibro-cartilaginous, adipose, lymphoreticular systems, neural, bone and bone marrow stromal tissues. Via the N-terminal HS chains, perlecan acts as pro-angiogenic by binding and presenting VEGFA and various FGFs to their cognate receptors. In contrast to this property, the C-terminal processed form of perlecan domain V, named endorepellin, has a nearly opposite function: it inhibits endothelial cell migration, capillary morphogenesis, and *in vivo* angiogenesis [8].

Another important component of this family is agrin, which has a multimodular structural organization that is homologous to perlecan. The N-terminal region can be spliced to generate either a type II transmembrane form (TM) of agrin, highly expressed in nervous tissue, or an isoform associated with most basement membranes that contains the N-terminal-agrin (NtA) domain. Following the N-terminal domain, there is a stretch of nine follistatin-like (FS) repeats, then there are two Ser/Thr (S/T)-rich domains. The N-terminal and central regions of agrin protein core contain the attachment sites for HS chain. Lastly, The C-terminus of agrin is structurally organized as perlecan domain V/endorepellin, with three LG domains separated by EGF-like modules. Most of the research on agrin in mammalians has focused on agrin's contribution to the control of the postsynaptic apparatus in the neuromuscular junction [2]. Collagens XVIII and XV, two members of the "multiplexin" gene family, harbour structural features of collagens and proteoglycans, being substituted with HS and CS, respectively. Collagen XVIII is a homotrimer comprised of three identical α1 chains and consists of ten interrupted collagenous domains, flanked by eleven non-collagenous domains at their respective N- and C-termini. Collagen XVIII also harbours three Ser-Gly consensus binding sites for the attachment of HS chains. Both collagens XVIII and XV contain a C-terminal no collagenous domain harbouring the antiangiogenic endostatin and endostatin-like modules. Endostatin interacts with numerous receptors including integrins α5β1, αvβ3 and αvβ5 and VEGFR2.

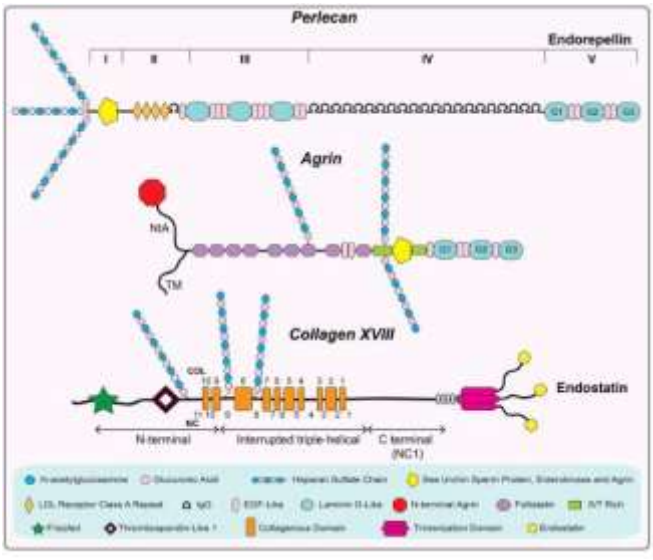

Fig. 4 Principal pericellular proteoglycans *structure and domains that are responsible for their specific role. The C-domain of perlecan and agrin is similarly structured [2].*

Extracellular proteoglycans

Hyalectans comprise a distinct family of proteoglycans with structural similarities at the genomic and protein levels. This family contains four distinct genes, namely aggrecan, versican, neurocan, and brevican. They have a tri-domain structure: an N-terminal domain that binds hyaluronan, a central domain harbouring the GAG side chains, and a C-terminal region that binds lectin.

Aggrecan has the propensity to aggregate into large supramolecular complexes > 200 MDa together with hyaluronan and link proteins. It is the principal load-bearing proteoglycan of cartilage, in fact, these large aggregates generate a densely packed, hydrated gel enmeshed in a network of reinforcing collagen fibrils and other proteoglycans and glycoproteins. Aggrecan is a multi-modular molecule expressed by chondrocytes. Its core protein is composed of three globular domains (G1, G2, and G3) and a large extended region (CS) between G2 and G3 for glycosaminoglycan chain attachment. G1 comprises the amino terminus of the core protein and this domain has the same structural motif as a link protein. Functionally, the G1 domain interacts with hyaluronan acid and link protein, forming stable ternary complexes in the extracellular matrix. G2 is homologous to the tandem repeats of G1, and it is involved in product processing. G3 makes up the carboxyl terminus of the core protein. The three globular domains, G1, G2, and G3 are involved in aggregation, hyaluronan binding, cell adhesion, and chondrocyte apoptosis *[9]*.

Versican, has highly versatile functions. There are at least five different isoforms of versican: V0, V1, V2, V3, V4, due to the alternative splicing of the major exons that code for the attachment regions for the chondroitin sulphate (CS) glycosaminoglycans (GAG) in the core protein. V0, V1, V2, and V3 differ in the size of the core proteins and the size and number of the GAG chains. The C-terminal domain of versican is also very similar to that of aggrecan and other hyalectans harbours similar structural motifs, including two EGF-like repeats, a C-type lectin domain, and a complement regulatory protein-like module. Versican is involved cell adhesion regulation, migration, and inflammation *[10]*.

The third member of the hyalectans is neurocan, a developmentally regulated CSPG originally cloned from rat brain, thus its name reminds its neuronal origin. As other hyalectans, neurocan has an N-terminal domain with structural homology to the typical arrangements found in link protein, harbouring a G1 domain and an Ig repeat. Functionally, recombinant N-terminal module of neurocan interacts with hyaluronan in solution and isolated complexes compromising gel permeation and hyaluronan profile. The C-terminal module of neurocan shares significant homology to the G3 domain of aggrecan and versican. By analogy to the other hyalectan members, this domain could bind several brain glycoproteins. Brevican is one of the most important hyalectans of the central nervous system and it harbours a typical hyalectan configuration with N- and C-terminal homologous domains, but with the shorter GAG-binding domain. Although sequence homology with the other hyalectan members is quite uniform (~60% overall), the GAG-binding domain is poorly conserved and contains a high content of acidic amino acid residues (mainly glutamic acid). This structural feature, shared with the link protein-like module of versican, could mediate binding to cationic proteins and minerals. Brevican has been implicated in glioma tumorigenesis, nervous tissue injury and repair, and in Alzheimer's disease *[2]*.

Small leucine rich proteoglycans (SLRPs) are widely distributed in various tissues and are characterized by tandem arrays of leucine-rich repeats, a cysteine-rich region in the N-terminus, and characteristic “ear repeats” at the C-terminus. SLRPs are involved in matrix organization of tissues,

sequestering growth factors of the TGF-β/BMP superfamily and mediating cellular and immune responses through various receptors. Decorin, biglycan, lumican, and fibromodulin are the most well-characterized SLRPs, typically associated with genetic diseases. Decorin and biglycan contain one and two GAG attachment sites, respectively, which, depending on the tissue type, can be either chondroitin or dermatan sulfate. During collagen assembly, their respective GAG chains regulate the interfibrillar diameter, compactness of fibrils, and form a steric barrier against degradation by collagenases. Biglycan is highly expressed in cartilage and bone, where it maintains the bone marrow stem cell niche, modulates BMP-2 and -4 activities, and regulates bone mass and post-natal skeletal growth. Fibromodulin bind to active TGF-β and sequester its activity. Finally, lumican is a keratin sulfate proteoglycan that confers corneal transparency, and loss-of-function mutations lead to excessive lateral growth of collagen fibrils that cause corneal opacification, myopia, and additionally skin laxity and fragility [11].

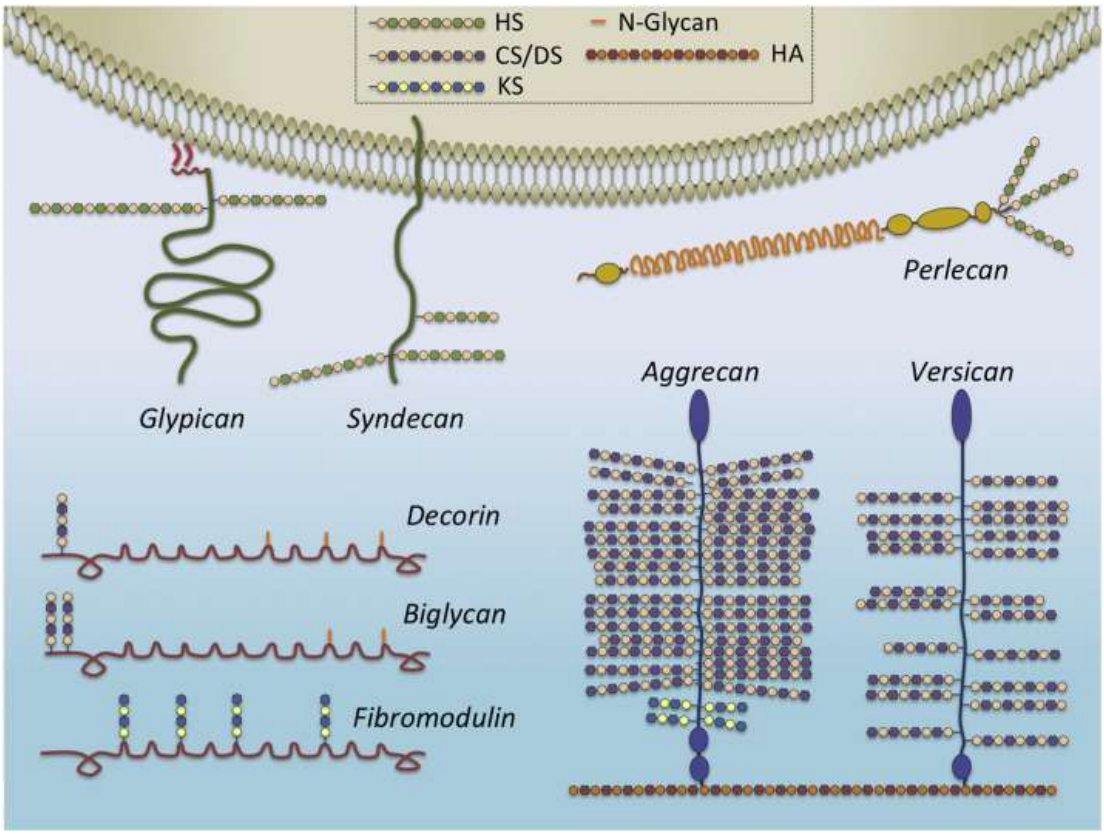

Fig. 5 Proteoglycans families: *short resume of the main proteoglycan's families such as pericellular, extracellular and cell surface families classified by their location [12]. Starting with the extracellular proteoglycans, versican is one of the largest (>1000kDa) and has a role in cells adhesions, migrations and proliferation, while aggrecan is the most abundant proteoglycan found in the cartilage due to its ability to absorb water. Perlecan can interact with laminin, fibronectin and collagen type IV and integrins in cell adhesion. Fibromodulin is a small protein (42kDa) part of the family of SLRPs that shares sequence homology with decorin and biglycan and participates in collagen fiber assembly. Biglycan is part of SLRPs and interact with collagen and has a role in bone's mineralization. Decorin is found in all connective tissues and is able to contribute to the assembly and solidity of collagen fibers. Lastly, glypican is attached to cell membrane thanks to GPI anchor on C-terminus and it's involved in Wnt and Hedgehog pathway. Syndecan has a transmembrane domain and acts as co-receptor especially for G-coupled receptors binding FGF, TGF, fibronectin, VEGF.*

Role in the extracellular matrix

Proteoglycans are major components of the extracellular matrix. In cartilage, the matrix constitutes more than 90% of tissue dry weight, primarily composed of fibrous proteins and proteoglycans. The ECM functions are to provide mechanical and biochemical support to cells within tissues, and help drive key cellular events such as differentiation, migration, and proliferation. Various proteins, such as collagens and elastin, are synthesized as monomers in cells, post-translationally modified in the Golgi, packaged, released via secretory vesicles, and assembled into macromolecules in the extracellular space. The resulting macromolecules commonly form fiber structures, such as elastic fibers - formed from elastin combining with glycoproteins like fibrillins and fibulins and fibrillar collagens like collagens I, II, III, V, and XI. The collagen IV and laminin are crosslinked to form the main architecture of the thin ECM surrounding cells, also known as basement membranes, while the fibrous proteins form 3D networks in the interstitial spaces. This 3D network also acts as a scaffold providing anchor points for other ECM proteins and cells to adhere to, allowing for transduction of extracellular mechanical forces such as stress and strain into signals for the cells to understand. Furthermore, many proteoglycans have the inherent ability to bind growth factors to regulate their stability and diffusion within the ECM and facilitate their interactions and signalling with cell surface receptors. For example, HS proteoglycans can facilitate fibroblast growth factor 2 (FGF2), hepatocyte growth factor (HGF), and transforming growth factor beta (TGF-β) signalling by immobilizing them via their heparin-binding domains. To summarize, cell-surface receptors bind to the ECM and their associated biomolecules (growth factors, cytokines, etc.) to regulate key biological events such as cell adhesion, survival, and tissue morphogenesis. These receptors include membrane-embedded proteins such as integrins (activated by fibronectin, vitronectin, collagen, and laminin), growth factor receptors, discoidin domain receptors (activated by various types of collagens), and CD44 (receptor for HA). Spatially, the ECM can be divided into two categories: interstitial matrix and pericellular matrix. Interstitial matrix makes up the bulk of ECM and contains most ECM components (collagens, fibronectins, proteoglycans) that are assembled into a GAG-rich matrix. Pericellular matrix describes the ECM immediately surrounding cells, which possesses properties and compositions different from interstitial matrix and unique to the said cells; basement membranes can be considered a form of pericellular matrix unique to endothelial and epithelial cells and is composed of specific ECM components such as laminins, nidogens, perlecan, agrin, and collagen IV [13].

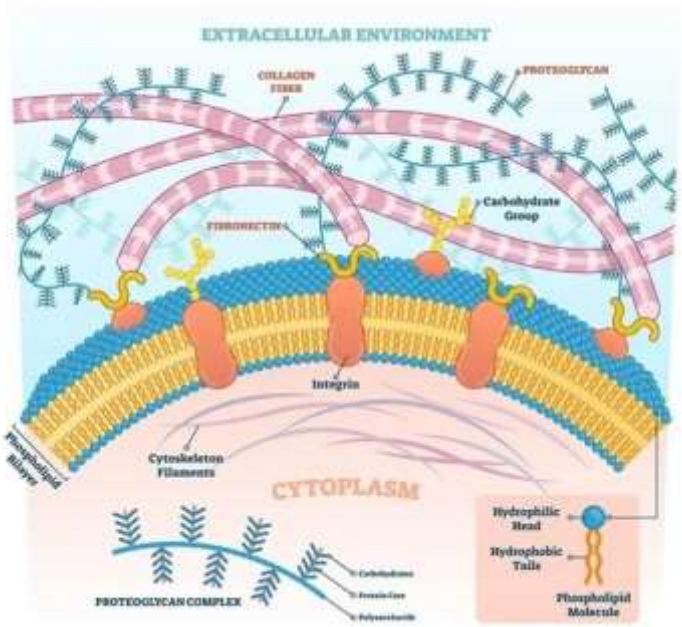

Fig. 6 ECM: *overview of the main component in the extracellular matrix such as fibronectin, collagen fibers, proteoglycans that interact with transmembrane integrins to modify the actin cytoskeleton response [14].*

Heparan-sulphate proteoglycans involvement in cancer

An important milestone for cancer cells is to gain migratory capacities to leave the primary tumour and invade the surrounding tissue. In fact, molecular changes in transcription factor networks and gene expression facilitate the loss of cell polarity and cytoskeletal reorganization, resulting in an increased migratory capacity. Cancer cells imitate this developmental EMT (epithelial mesenchymal transition) program, and several studies suggest that proteoglycans are actively involved in this part of cancer progression, thus supporting the relevance of proteoglycans as targets for CTC (circulating tumour cells) capture. Situated in the glycocalyx of cancer cells, proteoglycans provide a contact link between the cell membrane and the surrounding ECM, thereby playing a central role in regulating cancer cell adhesion and migration. Some proteoglycans are downregulated to enable detachment from the basement membrane facilitating invasion, others are shed from the surface as a different mode of regulation, and some maintain their function throughout the invasive phase [15] .

One important modulator of EMT processes is the transforming growth factor β (TGFβ), which is known to drive progression of late state malignancies by promoting invasion. Indeed, TGFβ regulates a multitude of genes with potential cancer-specific effects. Several proteoglycans are connected to TGFβ-signalling. An example is syndecan-4, that binds to fibronectin to activate a series of signals, including the MAPK pathways, leading to cell proliferation and migration, in fact it is positively regulated by TGFβ in lung cancer A549 cell. Expression of this proteoglycan further induced upregulation of the EMT transcription factor zinc finger protein SNAI1. Another example is syndecan-1, a coreceptor and cooperator with HGF and HER2, respectively, activates proliferative signals and improves cancer cell survival, can be affected by TGFβ and it is correlated to poor prognostic factor in breast cancer. Moreover, incubation of mouse mammary epithelial cells with TGFβ changed the GAG composition of syndecan-1 from being mainly HS modified to carry nearly equal amounts of HS and CS. More in general, proteoglycans might affect cancer cell migration independently of TGFβ signalling [15].

Another important role is the regulation of several angiogenic factors such as VEGF and FGF-2, for example HA overproduction within the ECM rapidly develops aggressive breast carcinomas in which cancer cells engage in more vascularization. Generally, HA interacts with versican, the most abundant type of PG, to affect angiogenesis. Matrix versican, secreted by stromal cells, promoted cancer growth by inducing angiogenesis in lung cancer. Also, agrin matrix levels result to be vital for angiogenesis; also confirmed by a study in which agrin stimulated angiogenesis by upregulating VEGFR2 levels in liver cancer. Lastly, perlecan interacts with various cytokines including FGF and VEGF families too, through its core protein and the HS chains to affect angiogenesis and cell growth. Via interactions with signalling molecules, PGs cooperate with ECM proteins and cell proliferation-related signalling events, including NF-κB and EGFR signalling pathways, to regulate tumour growth. Serglycin, the only intracellular PG, promoted tumour cell growth through interacting with CD44, and it is found that combining targeting serglycin and CD44 could be an effective therapy against tumour growth. In addition, some proteoglycans are considered anti-proliferative such as, lumican and perlecan due to their binding to EGFR able to block downstream pathway resulting in an inhibited cell proliferation in melanoma, lung, and breast cancer.

Lastly, proteoglycans can interact with the immune system. In fact, for example versican is known to reduce the tumour-infiltrating level (TIL) of CD8+ T-cells and promote cell migration in cervical cancer. Also, decorin is involved in immune modulation reducing the abundance of anti-inflammatory molecules and increasing proinflammatory molecules, thereby boosting the immune response and reducing tumour growth. Decorin signalling was able to suppress tumour growth by stimulating PDCD4, shifting the immune response toward a proinflammatory phenotype in a tumour xenograft model. Also, serglycin can carry up to eight CS or HS chains and is widely expressed by hematopoietic cells as well as embryonic stem cells, where it serves functions in storage of intracellular granules and secretion of inflammatory mediators. In fact, elevated serglycin expression are reported in cancer cells derived from patient tissues and has been linked to aggressive cancer cell phenotypes *in vitro* for glioblastoma, liver, and lung cancer [16].

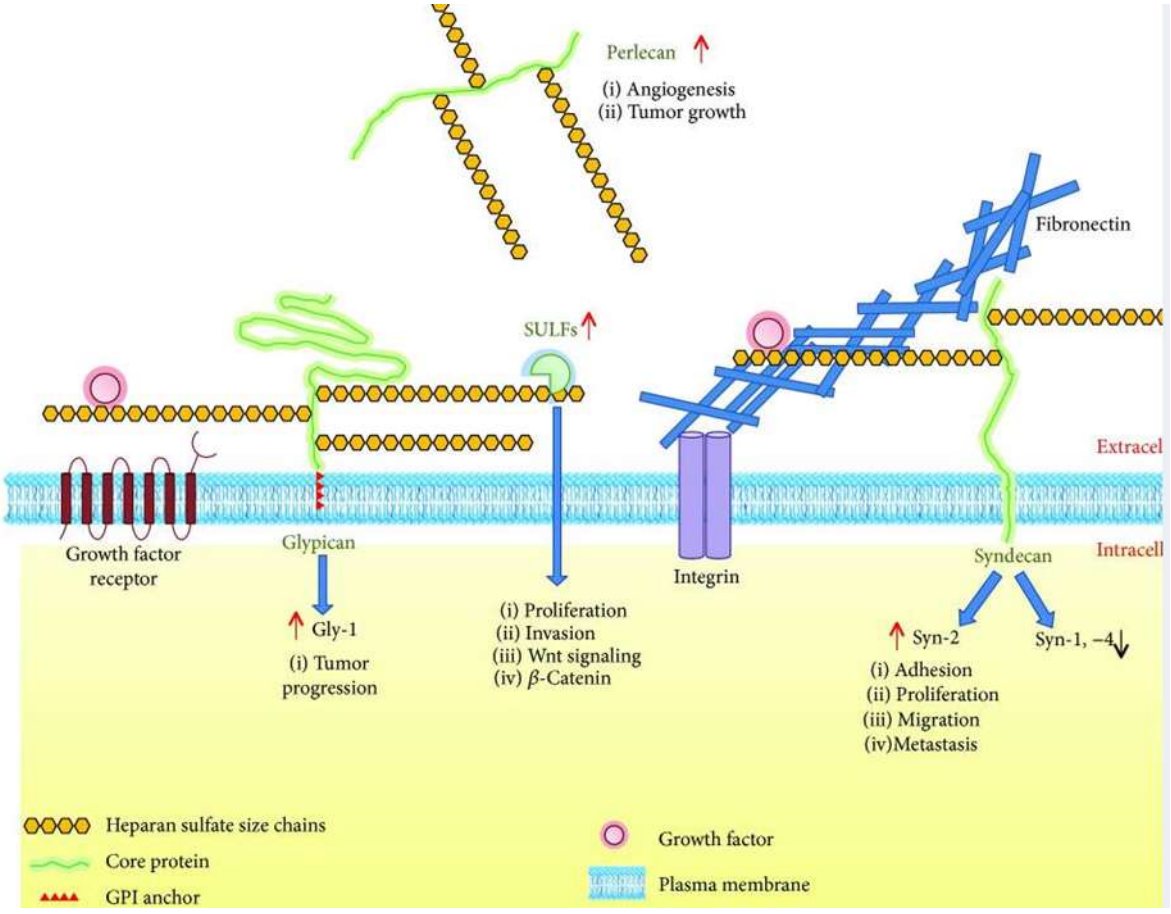

Fig. 7 Functions of proteoglycans in cancer: *The cell surface HSPG syndecan-2 (Sdc-2) is upregulated and promotes cancer cell adhesion, proliferation, migration, and metastasis. Syndecan-1 and syndecan-4 (Sdc-1; Sdc-4), generally anti-tumor molecules, are reduced in colon carcinoma cells. The cell surface HSPG glypican-1 (Gpc-1) is increased in CRC and it is involved in tumour progression. The augmentation of matrix HSPG perlecan favours angiogenesis and tumour growth. The SULF enzymes are upregulated, and the edition of HS chains promotes proliferation and invasion of CRC cells. In addition, SULFs release growth factors that were bound to HS, stimulating the Wnt signalling pathway and the activation of β-catenin [17].*

TABLE I: Role of HSPGs in different tumour types.

Cancer type	*HSPGs roles*	*HSPGs class*	*References*
Brain cancer	*Influence aggregation and activity of AMPA receptors, chemoresistance through PI3K/AKT*	*CS PG4 marker of glioblastoma,*	*Yan et Al, Frontiers in Oncology, 2020*
Breast cancer	*Binding EGFR and IGFR; aggressive phenotype, increased inflammatory environment*	*Sdc-4, Sdc-2, Gpc-1 and versican 3 overexpression*	*Theocharis et Al, Biochimica et Biophysica Acta, 2015*
Colorectal cancer	*Cancer progression, increased heparinase levels and SULF2 that regulate p53*	*Sdc-1 and Sdc-4 downregulated, Sdc-2 upregulated*	*Vicente et Al, Analytical Cell Pathology, 2018*
Hepatocarcinoma	*Binding TGF-β; VEGF, CXCL12*	*Gpc-3; Agrin overexpressed*	*Baghy et Al, World Journal of Gastroenterology, 2016*
Ovarian cancer	*Increased angiogenesis, integrin-related pathways*	*Sdc-1 and Sdc-4 upregulated*	*Oto et Al, Cancers, 2023*
Pancreatic cancer	*Mediation of micropinocytosis, DNA methylation*	*Gpc-1 as marker, Sdc-1 and Gpc-2 overexpressed*	*Chen et Al, Frontiers in Immunology, 2022*
Prostate cancer	*Binding EGF, TGFs and dysregulation Wnt*	*Gpc-1 as marker and Gpc-5 reduced*	*Alves de Moraes et Al, BMC Molecular and Cell Biology*

Focus on pancreatic cancer

The incidence of pancreatic cancer is rising at a rate of 0.5% to 1.0% per year, and pancreatic cancer is projected to become the second-leading cause of cancer death by 2030 in the US. Pancreatic ductal adenocarcinoma (PDAC) accounts for the majority (90%) of pancreatic neoplasms, and the other subtypes include acinar carcinoma, pancreatic blastoma, and neuroendocrine tumours. Most patients with pancreatic cancer present with nonspecific symptoms at an advanced stage with disease that is not amenable to curative surgery. No effective screening exists. The 5-year survival rate approached 10% for the first time in 2020, compared with 5.26% in 2000.

Epidemiology

The median age at diagnosis in the US is 71 years, and PDAC is slightly more common in men than in women (5.5 vs 4.0 per 100 000 individuals). At presentation, 50% of patients have metastatic disease, 10% to 15% have localized disease amenable to surgery, and the remainder (30%–35%) have locally advanced mostly unresectable disease due to the extent of tumour-vascular involvement. Pancreatic intraepithelial neoplasms (PanINs) refer to precancerous lesions, of which a small fraction may progress to high-grade dysplasia and PDAC. Low-grade PanINs are common and their

potential to transform into a malignancy is unclear. In a retrospective review of 584 patients who underwent a pancreatectomy for non-PDAC (median age, 59 years), 153 patients (26%) were identified with PanINs; most patients had low-grade PanIN-1 (50%) or PanIN-2 (41%) and 13 (8%) had PanIN-3. None of the patients with PanIN-3 developed cancer, whereas one patient with PanIN-1B developed cancer in 4.4 years. Intraductal papillary mucinous neoplasms are more common precancerous cystic lesions than PanINs and can arise in either the main or branch pancreatic duct [18].

Risk factors

The unmodifiable risk factors are: ovarian and breast cancer syndromes whose mutations are the BRCA1 and BRCA2 that explain 17-19% of hereditary pancreatic cancer; people who have Lynch syndrome, because of the microsatellite instability (MSH2, MSH6, MLH1, PMS2 and EPCAM genes); familial adenomatous polyposis, caused by a mutation in the APC gene, is characterized of early-onset polyps in gastrointestinal tract that can be develop in malignant neoplasia; Peutz-Jeghers syndrome, where the STK11/LKB1 genes mutation characterize an hamartomatous polyposis syndrome and this condition can determine gastrointestinal neoplasia and other tumours like pancreatic cancer; familial atypical multiple mole melanoma syndrome which is characterized by malignant melanoma in one or more first-degree or second-degree relatives. In 38% of cases this pathology is caused by a p16INK4a gene mutation, which dysregulates the normal cellular cycle; hereditary pancreatitis due to PRSS1 gene mutations is responsible of the chronic inflammation and higher risk of tumour development and lastly, cystic fibrosis, caused by CFTR gene mutation, has the same pathogenetic mechanisms explained in hereditary pancreatitis, because recurrent acute pancreatitis can be involved in pancreatic cancer onset [19].

Regarding, the environmental risk factors: smoking is the main demonstrated environmental risk factor for the development of pancreatic cancer; the pathogenetic mechanisms include genes mutations inducement (KRAS, p53) and, on the other hand, a chronic inflammation. These two factors can induce cytokines and growth factors output, providing the right pathway to cellular transformation. Alcohol and its metabolites make a pro-carcinogenetic pathway through chronic inflammation (considering alcohol consumption is responsible of 60-90% of chronic pancreatitis) and cellular gene instability. The chronic inflammation causes the production of TNFα, IL-6, IL-8, PDGF, TGFβ and other cytokines that can induce cellular proliferation and reduce immune-surveillance. The main damage on DNA is caused by ROS production, promoting the progression to cellular transformation. Another risk is obesity, in fact in obese people the pathogenesis is characterized by adiposopathy, a chronic adipose disease in which macrophages product pro-inflammatory cytokines and there is a dysregulation of hormonal level consisting in high level of leptin and low level of adiponectin. About diabetes mellitus about 80% of people with pancreatic cancer also have glucose intolerance or diabetes. The association between these two diseases is clear but it is important to define the relationship. In fact, many patients with pancreatic cancer have diabetes in close to the diagnosis of the tumour, validating the hypothesis which support that diabetes is a consequence of the neoplasia. There is a relevant association also with diabetes mellitus type 2, in fact the pathogenetic mechanisms that sustain this relationship are the hyperinsulinemia, often

detected in DMT2, and high level of IGF1, whose modification can induce pancreatic glandular proliferation and specific cellular interaction [19].

Molecular profile of pancreatic cancer

The KRAS gene is mutated in ~93% of pancreatic cancers. This protein is a small GTPase responsible for interacting with cell membrane growth factor receptors and controlling the switch of multiple signalling pathways and cellular processes. The proteins in the human RAS family usually consist of two functional domains: the G domain and the membrane-targeting domain. Different isoforms of the RAS family have a similar G domain but vary in the membrane-targeting domain. GTP-bound RAS prompts the membrane-targeting domain, to interact with effector proteins and activate downstream signalling pathways. GDP-bound RAS inactivates the process, and GTP/GDP conversion is catalysed by the SOS1 protein. The most frequent mutation of KRAS in pancreatic cancer occurs in codon G12 of exon 2 (e.g., G12D (40%) and G12C (33%)). Point mutations in codon 12 of the KRAS oncogene prevent the conversion from GTP to GDP, resulting in the constitutive activation of downstream signalling pathways [20].

Pancreatic cancers are derived from a series of precursor lesions, among which pancreatic intraepithelial neoplasia (PanIN) is the most common lesion and oncogenic KRAS mutations drive the initiation and progression of different stages of PanINs. In addition, factors that promote and activate KRAS, such as inflammation, oxidants and TGF-β, all contribute to the initiation and development of pancreatic tumours. However, a KRAS mutation alone is insufficient to drive carcinogenesis, moreover, due to the consecutive activation of oncogenic KRAS, the RAF/MEK/ERK pathway, PI3K/AKT/mTOR pathway, RalA/B pathway and NF-κB pathway are all activated to promote the proliferation of PDAC [20]. Another mutated gene is CDKN2A, which encodes two proteins, $p16^{INK4a}$ and $p14^{ARF}$. $p16^{INK4a}$ inhibits CDK4 activity, that is a regulator of cell cycle progression, but in addition to its role in aging, CDKN2A is also one of the most frequently mutated tumour suppressor genes, and genetic alterations in CDKN2A have been detected in many types of cancers (30%–50% of pancreatic cancer cases). The inactivation of CDKN2A cooperates with KRAS mutations and drives the malignant transformation of the pancreas and the main genetic alterations include deletions, mutations, and promoter hypermethylation [21]. Likewise, TP53 mutations that are prevalent in subsequent steps of pancreatic carcinogenesis. The TP53 gene encodes the p53 protein, which binds to specific sequences through its DNA binding domain and regulates the transcription of downstream molecules to exert its functions in various biological processes, including the cell cycle, mitochondrial respiration, cell metabolism, autophagy and stem cell maintenance and development. TP53 is commonly activated by oncogenic mutations or cellular stress, such as DNA damage and oxidative stress, preventing p53 from interacting with MDM2/4 and therefore stabilizing p53. As its level increases, p53 increases the transcription of downstream genes, such as P21 and Bcl-2, thus driving cell cycle arrest and repairing or eliminating damaged cells to inhibit the accumulation of oncogenic mutations [22].

The inactivation of SMAD4, an important tumour suppressor involved in transforming growth factor β (TGFβ) signalling and associated with altered mitochondrial activity, is also one of the main driving mutations in PDAC. TGFβ signalling has emerged as an important player in antitumor drug resistance, which is linked to its ability to induce EMT in cancer cells. The TGFβ signalling pathway

is compromised in the absence of its crucial signalling mediator SMAD4, which is inactivated by gene deletion or by mutations in up to 50% of advanced-stage PDACs. SMAD4 is mutated in half of PDAC cases, with homozygous deletions occurring in 30% of cases and chromosome allelic loss existing in 20% of cases, and the mutations remarkably decrease immunohistochemical staining for the SMAD4 protein. In addition, loss of SMAD4 expression has been detected in high-grade precursor lesions rather than in low-grade lesions, suggesting that the inactivation of SMAD4 promotes progression to a later stage of tumorigenesis [23].

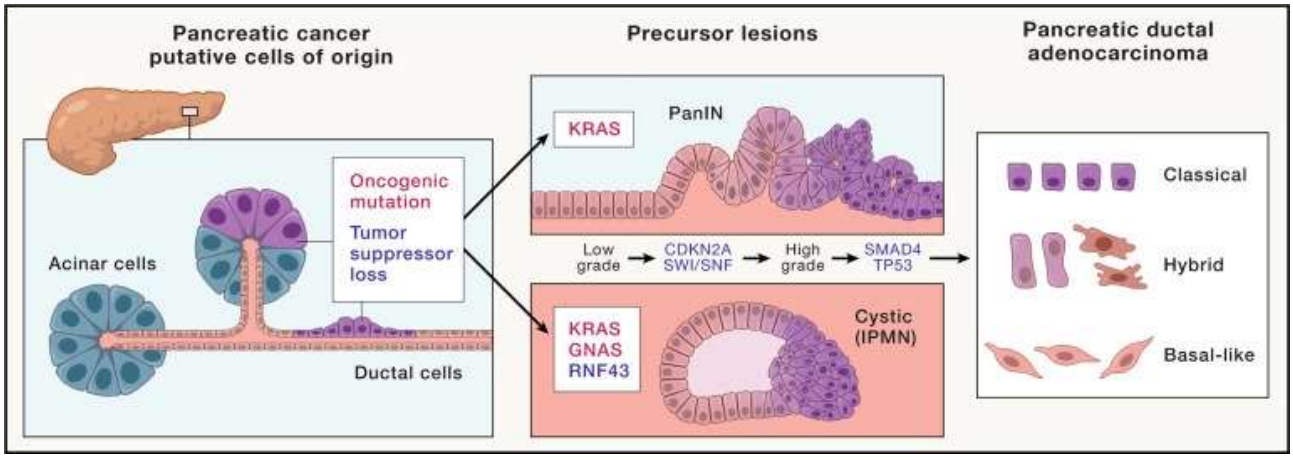

Fig. 8 Description of pancreatic cancer precursor lesions: *PanIN, which is a microscopic (usually <5 mm) flat or papillary lesion arising in the small intralobular pancreatic ducts. This class of lesions is characteristically asymptomatic. PanINs are composed of columnar to cuboidal cells with varying amounts of mucin and varying degrees of cytological and architectural atypia. High-grade PanINs (PanIN-3) are characterized by severe cytological and architectural atypia. PanIN-3 is also referred to as "carcinoma in situ". In this scenario the first gene to be mutated is KRAS, subsequently CDKN2A mutation takes place and starst to increase the severity of the lesion. Lastly, when SMAD4 and TP53 started to disfunction the high grade of the lesion is already reached. IPMNs are mucinous cystic lesions of the pancreas that are characterized by neoplastic, mucin-secreting, papillary cells projecting from the pancreatic ductal surface. They arise from the epithelial lining of the main pancreatic duct or its side branches. They are usually found in the head of the pancreas as a solitary cystic lesion, but in 20% to 30% of the cases they may be multifocal [24].*

Tumour environment

The tumour microenvironment (TME) contains fibroblasts, macrophages, and endothelial cells, increased numbers of extracellular matrix (ECM) compounds, elevated interstitial fluid pressure, and a high number of compressed tumour blood vessels. In addition, pancreatic TME has an abundant fibrotic stroma, rich in various cell types and extracellular components including collagen, fibronectin, and hyaluronic acid. Hyaluronan binds to its receptor CD44 and induces angiogenesis, epithelial-to-mesenchymal transition (EMT), and chemoresistance via receptor tyrosine kinase regulation and small GTPase. In a healthy state, stellate pancreatic cells are latent, while in pancreatic pathological situations, stellate cells are capable of transitioning into a myofibroblast phenotype, playing a key role in the desmoplastic reaction. PDAC stromal desmoplasia is the main histological hallmark, containing pancreatic stellate cells, ECM proteins, inflammatory cells, growth factors, and cytokines. PDAC stromal desmoplastic reaction leads to the accumulation of a

significant amount of type I collagen. Moreover, via integrin $\alpha 2\beta 1$, type I collagen is involved in cancer cell adhesion, proliferation, and migration. This cocktail of molecules and cells induces PDAC aggressiveness by promoting tumour growth, metastasis, and even chemoradiotherapy resistance. PDAC patients have an excessive production of ECM proteoglycans and glycosaminoglycans. The cancer-associated fibroblasts (CAF) via various cytokines have an activated phenotype, promoting inflammation, angiogenesis, tumour growth and proliferation, invasion, metastasis, and regulation of the tumour metabolism. The immune system is also involved by releasing cytokines, chemokines, and growth factors, which can mediate the neoplastic transformation. In the periphery of PDAC, tumour-associated macrophages are accumulated, being correlated with a M2 phenotype. This type of phenotype is characterized by extra-pancreatic and lymph vessel invasion, lymph node involvement, and shortened survival time [25].

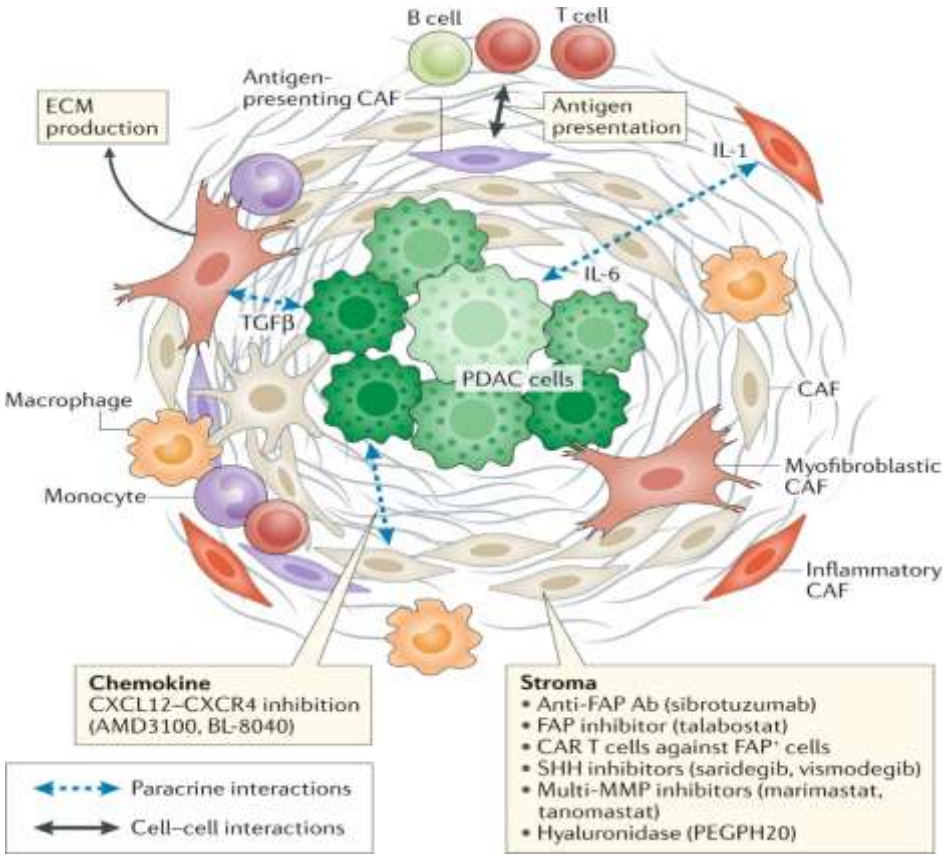

***Fig. 9 Tumour environment overview**: The role of the stroma to either promote or resist tumour formation and progression is influenced by the surrounding signals. Both cell–cell and paracrine interactions between cancer-associated fibroblasts (CAFs) and cancer cells are involved in programming the stroma. CAFs, key constituents of the pancreatic ductal adenocarcinoma (PDAC) stroma, are heterogeneous, and include myofibroblastic, inflammatory and antigen-presenting subtypes. Fibroblasts in proximity to cancer cells are induced by transforming growth factor-β (TGFβ) from cancer cells into myofibroblastic CAFs, producing the mechanical barrier that can be both tumour promoting and antitumour. Inflammatory CAFs, located in the stroma away from the cancer cells, are reprogrammed by cancer-secreted IL-1 to produce cytokines and chemokines (for example, IL-6), which further promote cancer growth. The subsequently developed antigen presenting CAFs, which express MHC class II molecules, modulate the immune cells in the stroma. Approaches to deconstruct the stroma have included the use of matrix metalloproteinase (MMP) inhibitors, hyaluronidase, Sonic hedgehog (SHH) inhibitors, fibroblast activation protein (FAP) targeting agents and CXCR4 inhibitors. Ab, antibody; CAR, chimeric antigen receptor; ECM, extracellular matrix [26].*

Diagnosis

A latency period of about 10 years between the start of pancreatic carcinogenesis and symptomatic disease has been shown. Prospective observational studies of screening have included patients at high risk and have used a combination of endoscopic ultrasound, computed tomography (CT) imaging, magnetic resonance imaging (MRI) or endoscopic retrograde cholangiopancreatography. Biomarkers that have been evaluated include: CA19-9 which has poor positive predictive value in both asymptomatic (0.9%) and symptomatic patients (72%), and carcinoembryonic antigen, which also has a low diagnostic yield. Abdominal ultrasound is often used as an initial diagnostic test for patients with nonspecific abdominal pain. The sensitivity and specificity of ultrasound in diagnosing pancreatic tumours is 90% and 95%, respectively, but worsens for masses smaller than 3 cm. The putative diagnosis and stage of pancreatic cancer is usually made with triphasic contrast-enhanced abdominal CT. Endoscopic ultrasound is warranted in cases where malignancy is uncertain (autoimmune or chronic pancreatitis) and in unresectable disease before chemoradiation therapy [27].

Pancreatic cancer exosomes

Exosomes, small vesicles with a double-layered structure, are generated by nearly all cells to facilitate intercellular communication and maintain equilibrium within the body. These vesicles transport a variety of materials such as proteins, lipids, and nucleic acids, delivering them to target cells through fusion and altering the characteristics of these cells upon arrival. They originate in the endosomal compartment after inward budding of the plasma membrane with subsequent endosome self-invagination and a role for membrane-associated PGs in the biogenesis of exosomes has been described as part of Sdc1-syntenin-alix axis. Syntenin is essential for the membrane availability of SDCs by controlling their endocytosis and recycling to the cell membrane. The recycling of SDC1 through syntenin occurs *via* its direct interaction with phosphatidylinositol 4,5-bisphosphate (PIP2) and depends on the activation of the small GTPase ARF6 . The cytoplasmic protein syntenin binds to the cytoplasmic domain of SDC1 with one of its PDZ domains and can bind to alix with its other PDZ (Post synaptic density protein (PSD95), Drosophila disc large tumor suppressor (Dlg1), and Zonula occludens-1 protein) domain. Alix associates with the endosomal-sorting complex required for transport (ESCRT) through interactions with TSG101 and CHMP4, which have been shown to be important for exosome cargo selection and loading. In addition, heparanase mediated exosome production may occur through enhanced SDC1 clustering and formation of the SDC1–syntenin–alix complex. For example, EV-associated SDC1 (EV-SDC1) was recently identified as a plasma biomarker that could non-invasively differentiate malignant, high-grade gliomas (glioblastoma) from low grade gliomas. HSPGs also play a role about the functional effects of exosomes, in fact both exosome-induced ERK1/2 signalling as well as exosome-dependent cancer cell migration were attenuated in PG-deficient mutant cells as well as when parental cells were treated with PG inhibitory xylosides [28]. In general, Tumour cells, like other cell types, utilize exosomes to communicate within the tumour microenvironment, modifying surrounding cells to promote

tumour growth. Notably, exosomes derived from tumour cells exhibit varying compositions, including distinct microRNAs, at different stages of tumour progression. These unique components hold promise as potential markers for diagnosing and monitoring pancreatic cancer treatment efficacy, progression, and regression. Consequently, there is a growing need to study and isolate exosomes originating from tumour cells as they serve as valuable biological tools for comprehending tumour development stages [29].

Lastly, exosomes originating from tumor cells can influence target cells, thereby promoting conditions favorable for tumor cell proliferation, metastasis, drug resistance, tumor-specific immune suppression, and angiogenesis, ultimately driving tumor progression. These exosomes typically exert their effects on target cells through three primary mechanisms. Exosomes from pancreatic cancer cells, are notably elevated in pancreatic cancer patients compared to healthy individuals and non-pancreatic cancer patients. This significant increase in exosome levels in the serum suggests their potential utility as diagnostic and monitoring tools for pancreatic cancer. Exosomes, particularly their RNA content, especially microRNAs, are commonly utilized for diagnostic purposes. When compared to free RNAs circulating in the peripheral blood, exosomal RNAs typically exhibit greater diagnostic value in terms of both quantity and quality [29].

Treatments

The recommended adjuvant chemotherapy after resection of PDAC is either modified FOLFIRINOX (Fluorouracil, Oxaliplatin, Irinotecan, Leucovorin) for individuals with high functional status or Gemcitabine and Capecitabine or Gemcitabine alone for individuals with poorer functional status. The main chemotherapy agents are DNA-damaging agents, which directly affect DNA synthesis and repair (Oxaliplatin, Irinotecan), and antimetabolites, such as Gemcitabine and Fluorouracil. Current standard first-line regimens for patients with metastatic disease include Gemcitabine and albumin-bound paclitaxel or modified FOLFIRINOX. Novel combination strategies evaluating targeted agents and immune therapy combinations are undergoing testing for patients with PDAC associated with impaired DNA damage repair. Single-agent PD-1 blockade has US Food and Drug Administration approval for mismatch repair deficiency in any tumour. Mismatch repair deficiency occurs in approximately 1% of individuals with PDAC and it is defined by either germline or somatic alterations or loss in mismatch repair deficiency genes, such as MLH1 and MSH2. KRAS missense variants in codon G12C in PDAC occur in 1% to 2% of patients with PDAC and single or combination immune checkpoint blockade inhibitors, such as Durvalumab and Tremelimumab, are ineffective for PDAC. However, an early efficacy signal of an objective response rate of 67% (8 of 12 participants in all cohorts and median overall survival of 20.1 months among 24 dose-limiting toxicity-evaluable participants) has been observed for the combination of the CD40 agonistic antibody Sotigalimab with the checkpoint inhibitor Nivolumab and chemotherapy. Adenosine is an immunosuppressive metabolite in the TME. Depleting adenosine, using both small molecule–targeting agents (eg, AB680) or with antibody therapy (eg, oleclumab), represent novel metabolism-directed approaches being investigated in PDAC [18].

Proteoglycans in pancreatic cancer

The ECM is known to play an integral role in development, tissue repair, and metastasis. Proteoglycans seems to be related with the tumour environment also in pancreatic cancer. In this introduction, several families of proteoglycans will be underlined to report their activity in pancreatic cancer.

Syndecan-1

Syndecan-1 has a critical role in regulating metastasis due to its part in EMT and ECM- actin cytoskeleton rearrangement. The precise mechanisms of relevant signal transduction to target cells, however, remain unknown. Due to the variability of the Sdc-1 domain, changes in its location have been speculated to correlate with the occurrence of metastasis. Highly expressed on epithelial cells, the heparan-binding domains of Sdc-1 are capable of binding laminin, collagen, fibronectin, and thrombospondin, resulting in activation of focal adhesion kinase (FAK) signalling. In addition, Sdc-1 regulates focal adhesion dynamics *via* control of Rap1 (a small GTPase that switches integrins to a high-affinity state) to slow cell adhesion and suppress migration [30]. Syndecan-1 seems to be upregulated on the cell surface from KRAS and localization of Sdc-1 at the cell surface—where it regulates macropinocytosis, an essential metabolic pathway that fuels PDAC cell growth—is essential for disease maintenance and progression. Among the top-ten most-enriched surfaceome proteins modulated by KRAS, three belonged to the heparin sulphate proteoglycan family (Sdc-1, Sdc-4 and Gpc-1). Membrane Sdc-1 expression is primarily modulated via shedding (proteolytic cleavage of the N-terminal domain into the extracellular space) and endocytosis (internalization through the endocytic route), which is balanced by endosomal recycling that returns much of the endocytosed proteins back to the cell surface. Whereas KRAS extinction did not affect Sdc-1 internalization, the rate of Sdc-1 recycling back to the plasma membrane was significantly inhibited in the absence of KRAS. Recovery of surface Sdc-1 expression was significantly delayed upon KRAS inactivation, further supporting that KRAS promotes Sdc-1 membrane localization by enhancing Sdc-1 recycling. Trafficking of syndecans to the plasma membrane is orchestrated by the small GTPase, ARF6. KRAS inactivation resulted in redistribution of Sdc-1 from the cell surface to the juxtanuclear ARF6 endocytic recycling compartment, a characteristic of reduced ARF6 activity. Expression of the dominant-negative ARF6(T27N) inhibited Sdc-1 membrane localization in the presence of KRAS, so KRAS signalling stimulates ARF6 activity to promote Sdc-1 trafficking to the plasma membrane. Sdc-1 is involved in macropinocytosis process due to the collaboration with RAC1, in fact this small GTPase has an essential role in the formation of the initial membrane ruffles. Depleting RAC-1 in SDC1 defected cells result in inhibition of macropinocytosis, which is recovered after ectopic expression of RAC-1 [31].

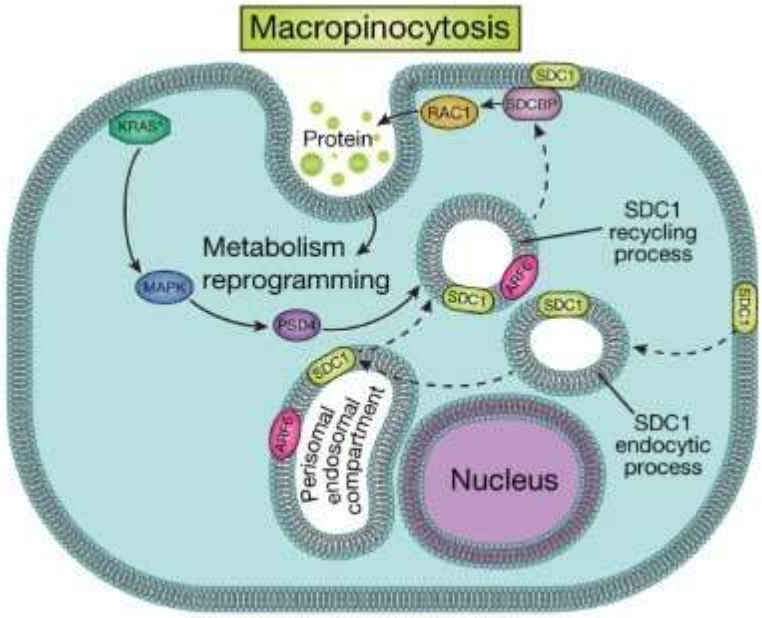

Fig. 10 Macropinocytosis mediated by Syndecan-1: *KRAS promote through PSD4 signalling Sdc-1 recycling on the cell surface which induce itself protein and extracellular materials endocytosis via RAC1 [31].*

Syndecan-1 could be used also, as a new marker since, during infection, inflammation, and tissue injury, serum levels of Sdc-1 increase sharply, contributing to diverse pathophysiological events. In fact, the median serum Sdc-1 level was significantly higher in the PDAC group compared with healthy controls, unfortunately its levels were not significantly different among the different stage group, but it was higher in patients with tumour location in the head of pancreas vs body/tail localization [32]. Lastly, syndecan-1 seems to increase chemoresistance, in fact treatment with doxorubicin, dexamethasone, cisplatin and carfilzomib was found to significantly increase levels of shed SDC-1. The HS chains of shed and full-length Sdc-1 compete to bind downstream epithelial growth factor receptor (EGFR), subsequently facilitating resistance to chemotherapy in colorectal cancer cells via PI3K/AKT signalling [30].

Syndecan-4

Evidence showed that Sdc-4 regulates cell migration, cell adhesion, and cytoskeleton development in tumorigenesis and progression. Sdc-4 was highly expressed in PDAC and was related to clinicopathological features and poor prognosis [33]. Since TGF-beta1 increases Sdc-4 expression whereas Sdc-4 modulates TGF-beta1 actions and interacts with EGFR [34]. Syndecan-4 has been involved in focal adhesions (FAs) formation through the binding and activation of PKCα. The absence of syndecan-4 not only generates smaller FAs, but also shows an impaired actin-cytoskeleton and defective smooth muscle actin incorporation [3].

Glypican-1

Gpc-1 is known to interact with heparin-binding growth factors, such as FGF-2, VEGF, heparin-binding EGF-like growth factor, and TGF-beta. The involvement of Gpc-1 in the signalling pathways of these heparin-binding growth factors contributes to cancer cell proliferation, metastasis, and angiogenesis and its expression in PDAC appears to be associated with promoter hypomethylation, as Gpc-1 mRNA levels in PDAC samples are inversely proportional to DNA methylation [35]. The overexpression of Gpc-1 was both at the mRNA as at protein level in PDAC, whereas it was absent or very low in normal pancreas and chronic pancreatitis. In fact, immunohistochemistry showed a weak Gpc-1 signal in cells within the tumour, but a strong Gpc-1 signal was observed in fibroblasts surrounding the cancer cells. It is likely that the Gpc-1 signal observed in the fibroblasts could originate from the cancer cells. In situ hybridization revealed that Gpc-1 mRNA expression levels were high in cancer cells and adjacent fibroblasts (CAF). Gpc-1 could be used as a specific marker in cancer exosomes, which are lipid-bilayer-enclosed extracellular vesicles that contain proteins and nucleic acids [35]. In fact, Gpc-1 is a membrane-anchored protein that is overexpressed in pancreatic cancer exosomes compared to the non-cancer ones and the percentage of them increased with tumour size. Studies on sera from PDAC patients report high levels of Gpc-1-positive circulating exosomes compared with healthy sera. The presence of these exosomes made it possible to distinguish with absolute specificity and sensitivity healthy individuals and individuals with benign lesions from PDAC patients. The level of Gpc1-positive circulating exosomes was also associated with tumour burden and survival, with higher levels detected in distant metastases of patients. These results indicated that Gpc1-positive circulating exosomes used as a diagnostic tool are better than carbohydrate antigen 19-9 (CA 19-9), the main tumour biomarker used in the clinic for PDAC patients [36]. Lastly, knockdown of Gpc-1 in the human pancreatic cancer cell line PANC-1 resulted in a reduction in tumour growth, metastasis, and angiogenesis compared to the PANC-1 cell line without knockdown, due to its interaction with the Hedgehog signalling pathway [35].

Glypican-5

It was recently observed that mRNA and protein expression levels of Gpc-5 were significantly down-regulated in PDAC cell lines, including AsPC-1, Panc-1, BxPC-3 and SW1990, compared to the normal pancreatic ductal epithelial cell line. This indicate that the low expression of Gpc-5 may contribute to PDAC development, which could be explained by the concomitantly reduced expression of catenin and the reduced transcriptional activity of Wnt/β-catenin signalling. Gpc-5 directly bound to Wnt3a and could compete with Frizzled-8 for binding to Wnt3a, at the cell surface. Normally expressed Gpc-5 could bind to Wnt3a and subsequently inhibit the Wnt pathway activity. When the Gpc-5 expression is inhibited, Wnt3a would activate Wnt/β-catenin signalling, and lead to cell proliferation, migration, and invasion [37].

Why targeting mTOR complex in pancreatic cancer?

Pancreatic cancer has a high prevalence of KRAS mutations and downstream signalling pathways, such as RAF/MEK/ERK, PI3K/AKT/mTOR, and RalA/B, and all enhance cancer progression, proliferation, and differentiation [24]. Downstream players of KRAS include phosphatidylinositol 3-kinase (PI3K) and AKT, which link ligation of growth factor receptors to the phosphorylation and activation of the serine/threonine kinase, mammalian target of rapamycin (mTOR), further downstream. This effector plays a role in cell survival, growth, proliferation, and motility, as well as a regulation of apoptosis. mTOR exists as two complexes: mTORC1 that is rapamycin sensitive and mTORC2 that is largely rapamycin insensitive. mTORC1 interacts with the accessory protein RAPTOR to phosphorylate effectors S6 kinase 1, which ultimately enhances the translation of mRNAs, including ribosomal proteins, elongation factors, and insulin growth factor 2. mTORC1 also phosphorylates 4EBP1 promoting dissociation of eIF4E from 4EBP1, thus relieving the inhibitory effect of 4EBP1 on eIF4E-dependent translation initiation, which again ultimately leads to increased translation of mRNAs (Fig. 11). mTORC2 interacts with its companion RICTOR to phosphorylate PKC alpha and AKT contributing to cell survival, migration, and regulation of the actin cytoskeleton. The mTOR complex is also closely related to the insulin/IGF-1 pathway. Decrease of adenosine triphosphate (ATP) production by metformin, for example, leads to AMPK activation and disruption of insulin/IGF-1 signalling through inhibition of mammalian target of rapamycin. Upstream of mTOR, the PI3K/AKT pathway is influenced by PTEN, the negative regulator of PI3K signalling, which decreases its expression in many cancers including pancreatic, and may be downregulated through several mechanisms including mutation, deletion, and methylation. Genomic alterations analysis via next generation sequencing have detected PI3K/AKT/mTOR pathway aberrations in patients suffering from pancreatic cancer with a frequency of 19%, including PI3K mutations (3.7%) and AKT amplifications (2.8%) [38] . Most of these aberrations have been listed as actionable molecular alterations, defined as genomic biomarkers that may predict the benefit from a specific targeted therapy. Regarding mTOR inhibitors, Rapamycin bind FKBP-12 in mTOR and inhibit mTORC1 downstream signalling, preventing S6K1 and 4EBP1 phosphorylation. While FKBP12-rapamycin complex cannot bind directly to mTORC2, prolonged treatments can disturb mTORC2 assembly and inhibit the phosphorylation of its downstream substrate AKT. However, inhibition of mTORC1 without mTORC2 inhibition may stimulate tyrosine kinase activity leading to AKT upregulation, a feedback loop that has been thought to contribute to mTOR resistance. Animal models have demonstrated that agents targeting the mTOR pathway can lead to significant inhibition of proliferation, differentiation, and tumour progression in specific PDAC subpopulations. Enhanced inhibition of tumour differentiation and progression by rapamycin was demonstrated to be specifically dependent on loss of PTEN in KRAS-mutant mice [39].

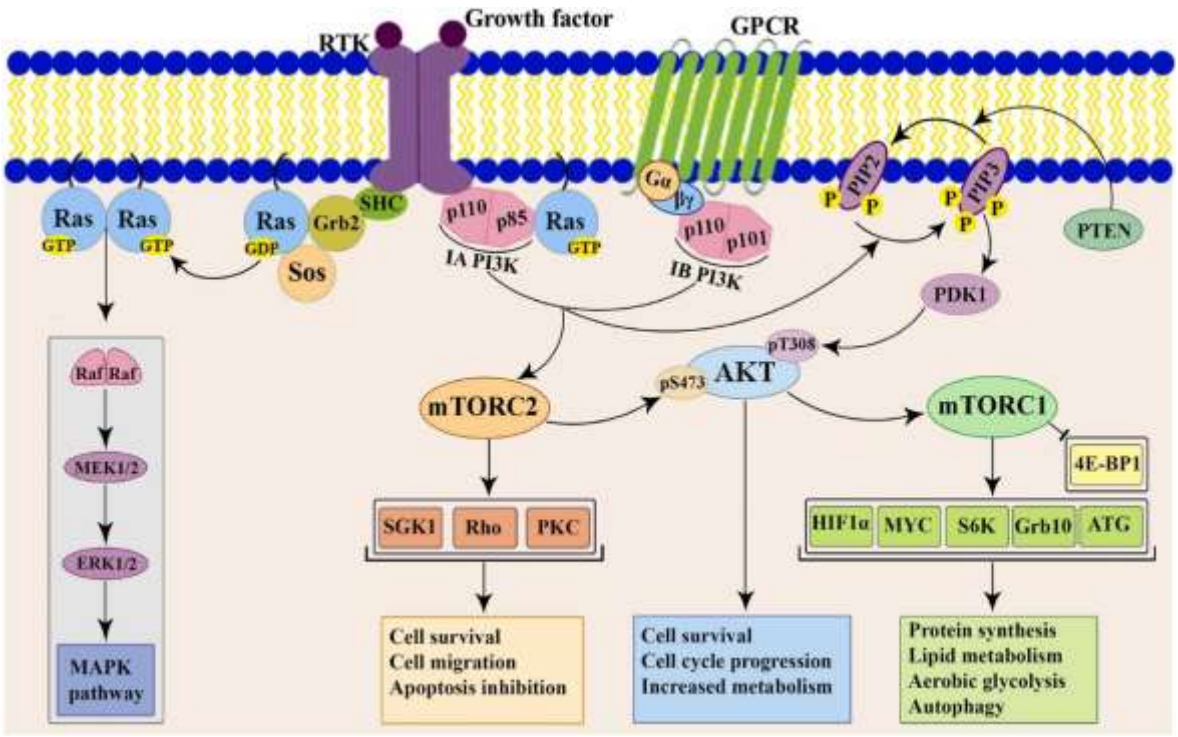

Fig. 11 PI3K/AKT/mTOR signalling pathway in normal and cancerous cells. *Stimulation of different RTKs and GPCRs by extracellular signals, causes the activation of class IA and IB PI3Ks, respectively. Active PI3Ks produce PIP_3 from PIP_2 that recruits AKT to the cell membrane rendering it susceptible to phosphorylation on Thr308 and Ser473 by PDK1 and mTORC2, respectively. Meanwhile, PTEN negatively regulates AKT activation through dephosphorylation of phosphoinositides. AKT phosphorylation and activation consequently leads to the activation of mTORC1 complex consisting of multiple proteins affecting many downstream targets. On the other hand, activation of RAS cause initiation of MAPK pathway [40].*

Peptides as novel cancer therapeutics

The anticancer effects of a peptide can be the direct result of the peptide binding on its intended target, or the peptide may be conjugated to a chemotherapy drug and used to target the agent to cancer cells. Peptides can be targeted to proteins on the cell surface, where the peptide–protein interaction can initiate internalization of the complex, or the peptide can be designed to directly cross the cell membrane. Peptides can induce cell death by numerous mechanisms including membrane disruption and subsequent necrosis, apoptosis, tumour angiogenesis inhibition, immune regulation, disruption of cell signalling pathways, cell cycle regulation, DNA repair pathways, or cell death pathways [41]. Compared with antibodies, peptides exhibit certain disadvantages, such as lower affinity, rapid excretion from the body (or shorter half-life in the body), and vulnerability to protease-mediated degradation. The bioavailability and stability of therapeutic peptides have been increased due to the development of several formulation and delivery methods including prodrug approaches, direct chemical modifications, applying special drug delivery systems, co-administration of enzyme inhibitors, and absorption enhancers. One method is cyclization that

dramatically reduced proteolytic degradation by amino- and carboxypeptidases, because of masking both the N-terminal amino and C-terminal carboxyl groups and adopt a limited number of conformations in solution, mainly β-turns, which can allow them to bind more efficiently to the active site of the desired target. Also, multiple copies of peptides assembled in branched molecules may be used as drugs, by virtue of their effect on the affinity and stability of bioactive peptides to proteolytic degradation. Another strategy is the manipulation of the amino acid sequence for example, partially substituting L-amino acids to D-amino acids or loading the peptides in nanoparticles [42]. Lastly, Sarko et al. also demonstrated that arginine and arginine bonds (RR bonds) could lead to degradation susceptibility of peptides, thus showing that the ones not containing RR bonds had more stability that those with RR bonds in the sequence [43].

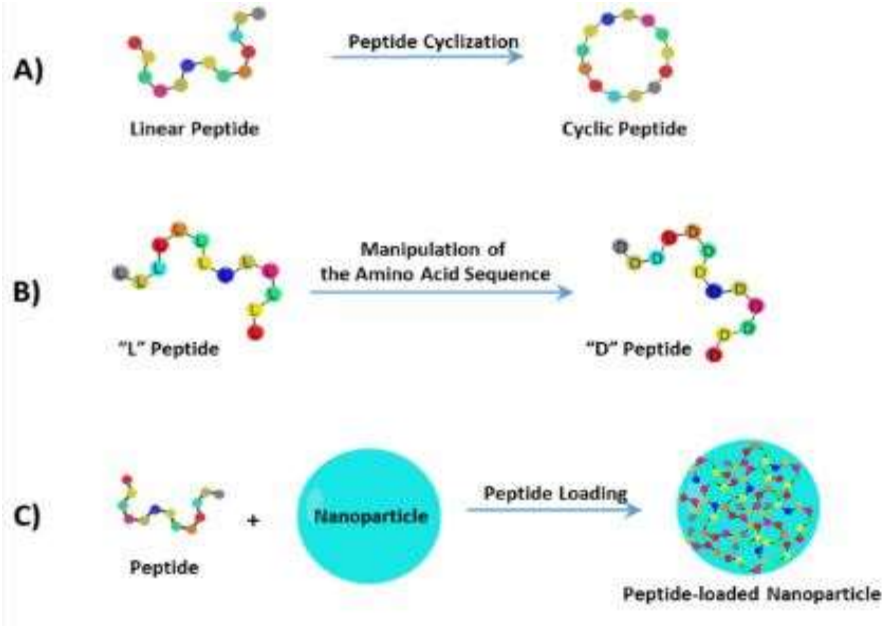

Fig. 12 Scheme of all the mechanisms that could be used to avoid proteolytic degradation: ***A****)Peptide cyclization* ***B****) manipulation converting L-amino acids into D-amino acids* ***C****) Use of nanoparticles [41].*

Focus on tetra-branched peptides

Branched peptides are characterized by a central branched scaffold (core) to which a variable number of peptide sequences are linked. Their molecular size ranges from about 2 kDa to large protein-like structures with molecular weight over 100 kDa depending on their adjustable generation numbers [44]. Chemosynthesis of these peptides can be achieved through solid-phase peptide synthesis (SPPS). Over the recent years the automation of SSP strongly reduced the costs and allowed continuous synthesis, in fact Fmoc solid phase helped the synthesis of longer and more complex peptides in shorter duration of time. The solid support is used to bind and immobilize the synthetized peptide and during synthesis, the peptides are chemically modified with protecting groups at their N-terminus or side chains. [45]. Generally, peptide multimers can be composed of branching poly amino acids, such as lysine multimeric structures (Fig. 13A) or containing a branching core with either unnatural amino acids or acids or organic groups (e.g., poly-amidoamine (PAMAM core) which produces higher molecular weight) and surface groups modified by peptide or proteins (Fig. 13B). These last are generally referred as dendrimers.

Tetra-branched derivatives are very versatile peptides because they balance low molecular with multivalent binding, giving good synthetic yield and optimal performances in binding [46]. The higher *in vivo* activity of oligo-branched form compared with corresponding monomeric sequences, was reported and demonstrated as being due to acquired resistance to protease and peptidase activity. Moreover, all the endogenous peptides tested, retained the full biological activity of the native sequences when synthesized as tetramers [47]. Available examples were obtained using the sequences of different peptides including enkephalins ,neurotensin and melanocyte stimulating hormone [46]. Finally, the advantages of tetramer chemical structures are: I) increased receptor binding by multivalent interaction; II) maintenance of a low molecular weight; III) low multimericity, which means controls non-specific interactions; and IV) retention of peptide biological activity by keeping the tumor targeting unit, that is the peptide, far from the effector moiety, which is linked to the branched core rather than directly to the peptides [44].

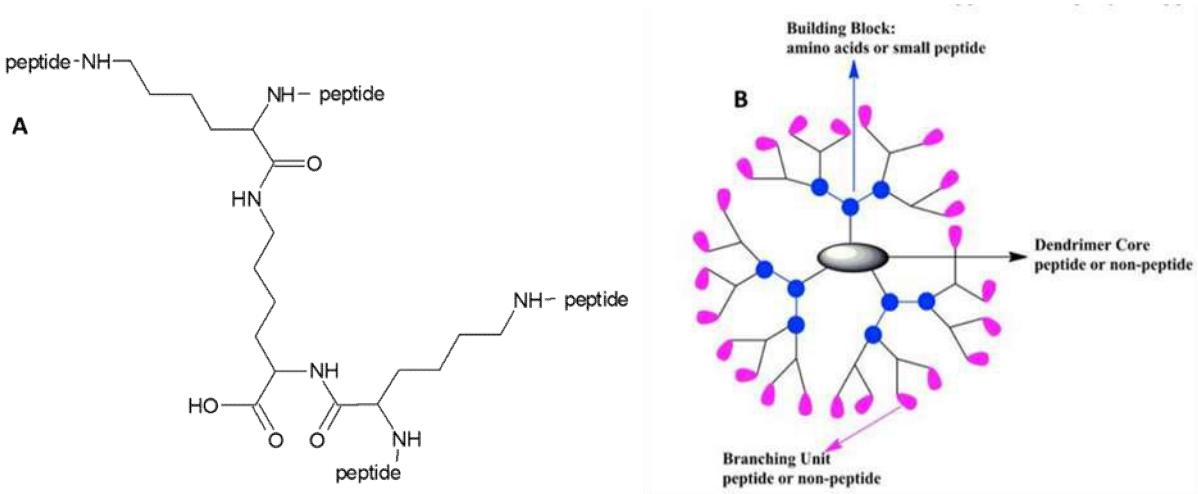

***Fig. 13 Multimeric peptide general structure: A**) Tetra branched peptide **B**) Dendrimeric peptide [68].*

Mechanism of action

Oncolytic peptides can target cancer cells specifically, giving alternate strategy to traditional treatments by common chemotherapy. Their specificity is due to increase negative charge on the cancer cell membrane. In fact, in healthy cells, negatively charged phospholipids are mainly found in the inner membrane leaflets, but in cancer cells, this asymmetry is disrupted, causing overexpression of negatively charged phosphatidylserine on the cell membrane surface. Additionally, other anionic molecules, such as O-glycosylated mucins, and the glycosaminoglycan side chains mainly in the form of heparin sulphate, further increasing the negative charges on cancer cells. Furthermore, in healthy cell membranes, cholesterol serves as a crucial regulator of fluidity, contributing to the inhibition of cationic peptide entry or translocation. The lower cholesterol content in cancer cell membranes compromises this protective mechanism. Oncolytic peptides have a cationic amphipathic structure, which contain both non-polar and polar amino acid regions, thanks to which they can interact with the lipid bilayer of cancer cell membranes, causing disruption and destabilization. This disruption leads to increased permeability, leakage of intracellular components,

and, ultimately, cell lysis. Moreover, the higher abundance and aberrant morphology of microvilli on cancer cells augment the cell surface area and contact with the peptides, further enhancing their interaction [48]. Different model mechanisms have been proposed to explain cellular peptide's penetration, such as transient pore formation or membrane destabilization. The pore formation consists in the initial interaction of the peptides with the cell surface that allow them to assume an amphipathic α-helix structure with basic residue interaction. After this surface interaction, they penetrate the cell bilayer, with the hydrophobic region interacting with the lipid core and the hydrophilic region facing the interior of the transient pore and forming a barrel-like structure. On the other hand, membrane destabilization is divided in two possible models: the inverted micelle model and the carpet model. The inverted micelle model proposes that peptide interaction with the membrane promotes a migration of negatively charged phospholipids to the site, which allows the formation of an inverted micelle, and subsequently the release of peptides into the intracellular compartment. The carpet model has a different mechanism concept, which describes positively charged amphipathic peptides distributed horizontally through the membrane surface by binding the acid phospholipids head groups to the cell membrane, which leads to the gradual destabilization of the cell membrane and peptides uptake. Lastly, endocytosis is still the main mechanism for cellular uptake, characterized by phagocytosis and pinocytosis, that differ in the endosome size obtained, the nature of the cargo and the mechanism of endosome formation [48].

Their intrinsic effects consist in the induction of cell death by DNA damage or mitochondrial membrane disruption and stop of the cell cycle through cyclin/CDK complexes modulation, which trigger G1 phase arrest [45]. Peptides are also known for modulating the immune response against cancer cells by stimulating the activation and proliferation of immune cells, such as T cells and NK cells, leading to enhanced recognition and elimination of cancer cells by the immune system. Particularly for the immune response, several proteins are involved on cell surface that interact with one another, forming the immunological synapse, where peptides act as a mimicking surface of one of the proteins, modulating the signalling especially through cytokine expression profile alterations, re-programming of M2 tumour associated macrophages and reduction on Treg cells activation [49]. Finally, peptides have effectively inhibited or reduced cancer cells' migratory, invasive, and metastatic capabilities by regulating pathways such as PI3K/AKT/mTOR and Wnt [45]. They can also inhibit angiogenesis, a process in which new capillaries are formed from pre-existing blood vessels, and it has a vital function in cancer by providing oxygen and nutrients necessary for tumour growth and metastasis. Their effect occurs by various signalling pathways, such as vascular endothelial growth factor (VEGF), fibroblast growth factor (FGF), platelet-derived growth factor (PDGF) [50].

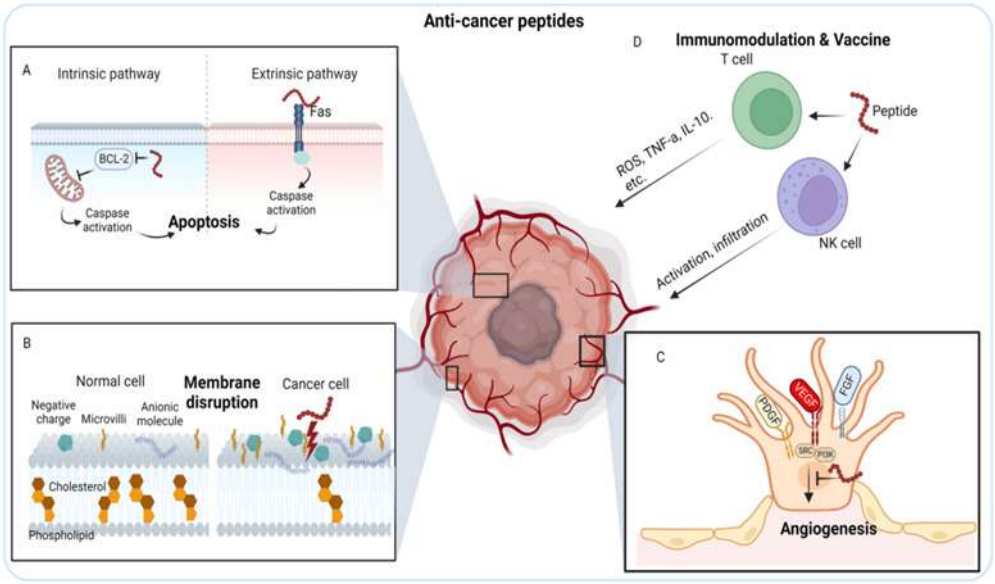

Fig. 14 Mechanisms of anti-cancer peptides *(**A**) Apoptosis induction. (**B**) Membrane disruption. (**C**) Inhibition of tumour angiogenesis. (**D**) Immunomodulation and peptide vaccine [50].*

Aim of the project

In this PhD project, we examine the role of branched-oncolytic peptide in pancreatic cancer. In fact, their amphipathic and cationic nature demonstrated high affinity for negative charged molecules, such as heparan-sulphate proteoglycans. HSPGs are mostly overexpressed in pancreatic cancer cells, such as Syndecan-1 and Glypican-1, and participate in growth, proliferation, metastatic and angiogenesis processes. The ability to overcome peptides proteolytic degradation was reached by the modification of their original linear structure into a tetra-branched form, which increased half-life.

The first part of the thesis was focused on the characterization of the cancer specificity and efficacy of oncolytic peptides against pancreatic cancer cells.

Peptides were then tested for their ability to interfere with the metastatic phenotype of pancreatic cancer cells, such as the ability to migrate and invade. A metastatic mouse model of pancreatic cancer was also employed to test efficacy of one of the peptides.

In the second part of the thesis, with the collaboration of Dr. Brian C Lewis of the UMass Chan Medical School, we investigated the possible connection between mTOR pathway and Syndecan-1/Glypican-1 overexpression in primary pancreatic cancer cells, with particular attention on ERK/AKT pathway, through experiment of endogenous expression and knockout of both proteoglycans.

Lastly, we then focused on harvesting exosomes from pancreatic tumour cell cultures and analysis of RNAs, in comparison to exosomes from non-tumour origin, in order to find new markers for liquid biopsies and to investigate HSPGs role in tumoral exosomes.

Chapter II

Materials and Methods

Peptide identification

Branched Oncolytic Peptides were screened from the "Database of Antimicrobial Activity and Structure of Peptides" (DBAASP v3.0) a comprehensive database containing information on amino acid sequences about peptides. BOP2 is a derivative of Gaegurin 5 (GGN5), a 24-residue cationic amphipathic membrane-active antimicrobial peptide isolated from the skin of an Asian frog (*Rana rugosa*). BOP7 and BOP9 were selected for their cationic amphipathic structure, which is well-established to give anticancer activity. All peptides were synthesized in a branched structure, in fact major features were about stability, half-life, toxicity, and efficacy compared to monomeric peptides.

Peptide synthesis

Peptides were synthesized on an automated multiple synthesizer Syro (MultiSynTech, Germany) by standard Fmoc chemistry. Protected L-amino acids, TentaGel resin, and Fmoc4-Lys2-Lys-β-Ala-Wang resin were purchased from Iris Biotech, Germany. The coupling reagent HBTU (O-benzotriazole-N,N,N,N-tetramethyluronium hexafluorophosphate) was from MultiSynTech, and the base DIPEA (N,N-diisopropylethylamine) was from Merck. Tetrabranched peptides were synthesized on Fmoc4-Lys2-Lys-beta-Ala-Wang resin or built using two consecutive Fmoc-Lys (Fmoc)-OH coupling steps to form the branched core on TentaGel resin. For the synthesis of BOP2, BOP7 and BOP9 the resin used was a TentaGel-PHB 4 branch β Ala Wang-type resin (Rapp Polymere, Germany) which was already functionalized with the branching lysine core in L-form (Fmoc4-Lys2-Lys-β-Ala). In the case of biotinylated BOPs, the coupling step involved the insertion of the amino acid Fmoc-Lys (Biotin)-OH, followed by Fmoc-Peg12-OH as a second, and Fmoc-Lys (Fmoc)-OH to build the lysine core. Peptides were then cleaved from the resin, deprotected, and lyophilized. HPLC purification was performed on a C18 Jupiter column (Phenomenex). Water with 0.1% TFA (A) and acetonitrile (B) were used as eluents. Linear gradients of B in 30 min were run at flow rates of 0.8 and 4 mL/min for analytical and preparatory procedures, respectively. All compounds were also characterized on a Bruker Ultraflex MALDI TOF/TOF mass spectrometer.

Human serum protease stability

Serum from different patients (n=5) was heat-inactivated at 56°C for 35 minutes, filtered with 0.2 μm filters and mixed with 25% of RPMI 1640. BOPs were dissolved in 2 mg/ml DMSO-H_2O at the concentration of 180 μM added to the serum and were incubated in the oven at 37°C. Samples withdrawn after 0, 4 and 16 h were precipitated with 200 μl of trichloroacetic acid and centrifuged for 5 min at 10,000 x *g*, and the crude solution was used for the MALDI-TOF analysis (2 μL) and part (250 μL) for the HPLC (series 200CR3A, Perkin Helmer) analysis, after being diluted with 1% TFA (750 μL). Time-zero HPLC and MS-spectroscopy spectra were obtained immediately after mixing the peptide with 50% serum. The presence of the intact peptide was determined in HPLC by spotting and integrating the peptide peak at the correct retention time. The identity of the peptide peak was further also confirmed by MALDI mass spectrometry.

Cell lines

PANC-1, 293T, MIA-PACA2, TE671 RAW 264.7 and PsgA-745 were obtained from ATCC (Rockville, MD, USA). hTERT-HPNE were a gift from Dr. J. Wu (UMass Chan Medical School, USA) and primary pancreatic cell lines (PAO1C, PAO2C, PAO3C, PAO4C, PA14C, PA16C, PA18C) were provided by Dr. B.C. Lewis (UMass Chan Medical School, USA). PANC-1, MIA-PACA2, TE671, RAW 264.7, 293T and all the primary pancreatic cell lines were maintained in DMEM (Dulbecco's Modified Eagle Medium), while PsgA-745 were cultured in Kaighn's Modification of Ham's F-12 Medium (F-12K), both media were purchased from GIBCO ®. All media were supplemented with 10% Fetal Bovine Serum (FBS), 200 μg/ml glutamine, 100 μg/ml streptomycin and 60 μg/ml penicillin from Euroclone S.p.A (Milan, Italy). 2.5% of Horse serum (HS) were added to MIA-PACA2 medium. hTERT-HPNE medium was made of 75% DMEM w/o glucose and phenol red (Sigma-Aldrich ®), 25% Medium M3 Base (InCell Corporation), 5% FBS (GIBCO ®), 750 ng/ml puromycin, 5.5mM D-glucose (Sigma-Aldrich ®) and 10ng/ml human recombinant EGF (Prepco, NH, USA). Human cardiac fibroblasts were cultivated in Fibroblast Medium M-2 (Innoprot Bizkaia, Spain). Cell lines were maintained at 37°C, 5% CO_2 and 95% of humidity. Human cardiac fibroblasts were kept in culture for a maximum of 15 passages, as well as pancreatic primary cell lines, due to their loss of morphological characteristics.

BOPs binding to cancer cells

5 x 10^4 cells/ well of PANC-1 and MIA-PACA2 were plated on round cover glass slides placed on 24-well plate the day before the assay and incubated at 37°C and 5% CO_2 overnight. Fixation was performed using 4% PFA-PBS 1x (cod. 47608 Sigma Aldrich ®) for 15 minutes at RT. To avoid unspecific binding of the peptides, a saturation step was carried out using 5% BSA-PBS 1x (cod. A9418 Sigma Aldrich ®) for 1h at 37°C. Biotinylated peptides were used at the concentration of 2 μM in 1% BSA-PBS 1x for 30 minutes incubation at 37°C, then probed with Streptavidin-Atto 550 (0.5 μg/ml in 1% BSA-PBS 1x) (cod. 96404, Sigma Aldrich) for 30 minutes at room temperature. To empathize the binding of the peptides on the cellular membrane, the latter was stained by 10 minutes of incubation at room temperature with wheat germ agglutinin Alexa Fluor 647 conjugate (2.5 μg/ml in 0.3% BSA-PBS 1x) (cod. W32466 Molecular Probes). As last step, cover glass slides were mounted on microscope slides using Fluoroshield with DAPI (cod. F6057, Sigma Aldrich) which turned out the nuclei visible. In between the different incubations with antibodies, three washing steps with PBS 1x were repeated to remove the previous signal excess. Samples were analyzed using confocal microscope (Leica TCS SP5) with 380 λ ex and 450–470 λ em; 550 λ ex and 570-590 λ em; and 633 λ ex and 660–680 λ em for DAPI, Atto 550, and Atto 647, respectively. The experiment was repeated three times, and three different fields were acquired for each sample.

BOPs flow cytometry

2 x 10^5 cells/well were seeded in a 96 well U bottom plates and incubated at three different concentrations (10 μM, 2 μM and 0.4 μM) of biotinylated peptides for 30 minutes at room temperature and probed with Streptavidin-FITC diluted 1:1000 (cod. A2901, Sigma Aldrich). All the dilutions were performed in FACS Buffer (1% BSA-5mM EDTA/PBS). 7.000 events were evaluated in a Guava EasyCyte Flow Cytometers (Millipore). The results were analyzed by FCS Express 6 Flow cytometry software. A variation in the protocol occurred, when heparin (Sigma Aldrich ®) was used to assess the binding of BOPs to the HS of proteoglycans on the cell surface, in fact, heparin was added at two concentrations (10μM and 5μM) together with the peptides during the incubation step.

Cytotoxicity assay

2.5 x 10^5 cell/ml of PANC-1 were seeded in a volume of 200 μl/well in two different 96-well flat plate, one for testing the cytotoxic effect of the drug after 24h. Cells were incubated at 37°C overnight to let them attach on the bottom of the wells. The next day once removed the media, serial dilution (1:2) of the peptides were added to the cells, starting from 100 μM to 0.08 μM. The control is only culture medium (DMEM). Cells were then incubated for the established time points and at the end, fixed with 100 μl/well of 4% PFA-PBS (cod. 47608 Sigma Aldrich ®) for 15 minutes at room temperature. The plates are then washed with PBS 1x and then stained with 100 μl/well of 0.1% Crystal Violet (cod. 46364 Sigma Aldrich ®) and incubated for 1h in the dark. After several wash in PBS, 10% of Acetic Acid was added to dissolve Crystal Violet and they were read after 5 minutes at 595nm (Multiskan, Thermo Scientific Waltham, MA, USA). Experiments were repeated twice in quintuplicate and the values from untreated gave 100% cell viability.

Haemolysis assay

Whole human blood was centrifuged at 1507 *x g* for 10 minutes to separate plasma from erythrocytes. Several additional centrifugation steps using PBS 1x were performed to wash red blood cells. Isolated cells were diluted 1:50 in PBS and added to a 96-well flat plate (100μl/well). Serial dilutions of the peptides, from 160μM to lowest at 0.25μM, were added. 100% hemolysis was obtained with 1% TritonX 100 in PBS. The plate was incubated at 37°C for 30 minutes, centrifuged at 492 *x g* for 5 minutes and the supernatant analyzed using the plate spectrophotometer (Multiskan, Thermo Scientific Waltham, MA, USA) at 405 nm and 490nm wavelengths.

Heparin ELISA assay

A 96-well flat plate was sensitized using BOPs at the concentrations of 10μg/ml, 5μg/ml and 1μg/ml in carbonate buffer (pH=9) at 4°C overnight. Uncoated wells constituted negative controls. The next day, the plate was rinsed three times using washing buffer (PBS 1x + 0.05% Tween20) and other three times with only PBS 1x. The blocking of unspecific binding was performed by using 3% Non-Fat Milk-PBS 1x and followed by incubation at 37°C for 2h. Another round of washing steps was done before the incubation at room temperatures for 30 minutes with heparin-biotin sodium salt (cod. B9806 Sigma Aldrich, St. Louis, MO, USA) diluted in 0.3% BSA-PBS 1x at the concentration of 5μg/mL and, the negative control, was incubated with only 0.3% BSA-PBS 1x. After rinsing the plate, 100 μL/well of Streptavidin-POD (cod. S5512 Sigma Aldrich, St. Louis, MO, USA) diluted 1:500 in PBS-milk 0.3% were added to the plate and incubated in the dark for 30 minutes at room temperature. As final step 150 μL/well of substrate solution composed of phosphocitrate buffer, TMB, DMSO, glycerol and H_2O_2, were added and incubated for 5 minutes. The reaction was stopped adding 50 μL/well of HCl 1M and then the plate was read at 450 nm and 650 nm using a microplate spectrophotometer (Multiskan, Thermo Scientific, Waltham, MA, USA).

Adhesion assay

PANC-1 were seeded at the concentration of 2×10^6cell/ml in a 96-well flat plate together with BOP7 and BOP9 at the working concentration of 0.2 μM and 0.08 μM. The positive control was made by incubating the cells with culture media only (DMEM). The plate was then incubated at 37°C for 4h, followed by a fixation step using 4% PFA-PBS 1x (cod. 47608 Sigma Aldrich ®) for 15 minutes at room temperature. The plates were then washed with PBS 1x and then stained with 100 μl/well of 0.1% Crystal Violet (cod. 46364 Sigma Aldrich ®) and incubated for 1h in the dark. After several wash in PBS, 10% of Acetic Acid was added to dissolve Crystal Violet and the signal was read after 5 minutes at 595nm (Multiskan, Thermo Scientific Waltham, MA, USA).

Migration 2D assay

2-wells silicone inserts (cod. 80209 Ibidi GmbH Gräfelfing Germany) were placed with sterile tweezers in a 24-well plate and 3×10^4 cells/well were plated in a final volume of 70 μl of culture media for each side of the insert. Cells were let attached to the well for 24h at 37°C and 5% CO_2. The next day, the inserts were removed to create the gap between the two wells and 1ml of DMEM with BOP2, BOP7 and BOP9 at the concentration of 1μM and 10μM was added as a treatment to inhibit the migration of the cells. Negative control was only incubated with DMEM. The closure of the gap was followed by using DFC 7000T microscope (Leica) and the camera recorded pictures every 30 minutes for 16h for each sample.

3D migration assay

According to the manufacturer instructions, 24-well Transwell insert (cod. 833932800 Sarstedt Nümbrecht, Germany) were re-hydrated in DMEM w/o FBS for 2h at 37°C. Once removed the medium, the inserts were coated with Collagen type I (167µg/ml cod. CLS354231 Corning®) overnight at 37°C. PANC-1 were seeded at the concentration of 5x 10^5 cells/ml together with BOP2, BOP7 and BOP9 at 0.1µM, 1µM and 10µM dissolved in DMEM w/o FBS in the upper chamber of the insert. As chemoattractant 600µl complete media were used in the lower chamber, to allow cells to migrate through the Transwell membranes after 24h of incubation at 37°C and 5% of CO_2. The next day, the media was removed, and cells were then fixed with 4% PFA-PBS 1x (cod. 47608 Sigma Aldrich ®) for 15 minutes at room temperature, washed with PBS 1x and then stained with 100 µl/well of 0.1% Crystal Violet (cod. 46364 Sigma Aldrich ®) and incubated for 1h in the dark. The samples were washed several times with PBS 1x to remove the Crystal Violet staining until they were totally clean and ready to analyse with confocal microscope used in brightfield mode to capture the images (Leica TCS SP5).

Luciferase transfection PANC-1

6.6 x10^5cells/ml of PANC-1 were seeded in a final volume of 3ml per well using culture media without antibiotics and incubated overnight at 37°C at 5% CO_2. The next day, according to the manufacturer instructions (Lipofectamine 3000 reagent, cod. L3000015 Invitrogen, ThermoFisher, USA) 125µl of Opti-mem (reduced serum medium, cod. 31985062 ThermoFisher, USA) were added to three 1.5ml centrifuge tubes. In the first, 7.5µl of Lipofectamine were added, in the second only 5.5µl and in the last, which was the negative control, the highest concentration of lipofectamine used (7.5µl). In another 1.5ml centrifuge tubes, the stock of plasmid DNA (PGL45LUC2CMVNEO) was prepared adding 250µl of Opti-mem, 5µl of plasmid DNA and 10µl of Lipofectamine and 125µl of this mixture were added to the Lipofectamine 7.5 and 5.5 tubes but not in the control tubes. Once the reagents were ready to be added on the plate, the media was replaced with a fresh one w/o antibiotics and 250µl of the solution contained in the Eppendorf tubes were added to the corresponding wells. After 48h, the media was replaced with a complete cell culture media supplemented with 1mg/ml of Geneticin (G418 Sulfate cod. 10131035 Gibco, ThermoFisher, USA). Fresh selective media was replaced every two days to avoid lack of transfection due to antibiotic inactivity.

Luciferase assay

Transfected PANC-1 cells were seeded at serially diluted (1:2) concentrations starting from 10^6 to 3.12x 10^4cell/ml in 96-well black plate. Cells were then incubated for 4h at 37°C and 5% CO_2 to let them attach to the plate and then 0.15mg/ml of D-Luciferin sodium salt (cod.6882 Sigma Aldrich ®) were added to every well. The plate was incubated for others 15 minutes at 37°C and then analysed

using Victor Nivo Multimode Plate Reader (PerkinElmer) with an emission wavelength of 700nm. The experiment was made twice in quintuplicates.

Mouse model

A total of 15 nude mouses was divided into in two groups: the first treated with BOP9 (28 mg/kg) and the control group injected with saline solution. Mice were injected with $1.5x10^6$ PANC-1 Luc each, in the tail vein, to create a metastatic model of infection. The next day, the drugs were administered consistently every 24 hours for the first five days through intraperitoneal injections in a volume of 150µl. Other three treatment cycles were repeated after two days of interval. D-Luciferin (150mg/kg) in PBS 1x was intraperitoneal injected 15 minutes prior imaging. Pictures of the different groups were taken using IVIS Lumina X5 (PerkinElmer).

Exosome mRNA Extraction

PANC-1 and human cardiac fibroblasts cells were starved changing the complete media with a media w/o FBS 24h before the exosome extraction. Human cardiac fibroblasts were selected as negative control due to their no-tumoral phenotype. The extraction was performed using ExoRneasy Kit (cod. 77023 Qiagen, Germantown, MD) according to the manufacturer instructions and the samples were sequenced and analysed by BMKGENE (Münster, Germany).

Immunoblotting Assay

Primary cell lines protein lysates were obtained using RIPA Buffer (50 mM Tris, pH 7.2; 150 mM NaCl; 1% Triton X-100; and 0.1 % SDS cod. R0278 Sigma Aldrich ®) supplemented with protease and phosphatase inhibitors (1:100) from Roche (Laval, QC). Protein concentration of each sample was determined using the BCA kit from Pierce (Rockford, IL) per manufacturer's instructions. 25ng of protein were separated by SDS-PAGE and transferred (Bio-Rad, USA) to polyvinyl difluoride (PVDF) membranes (Millipore, USA). Proteins expression was quantified using rabbit polyclonal antibody Gpc-1 1:1500 in 3% BSA-TBST (cod. GTX104557, GeneTex, USA), rabbit monoclonal antibody Sdc-1/CD138 1:1000 in 3% BSA-TBST (cod. A4174, ABclonal, USA), rabbit polyclonal phospho-p44/p42 MAPK (Erk1/Erk2) antibody (cod. 9101S, Cell Signalling, USA), rabbit polyclonal p44/p42 MAPK (Erk1/Erk2) antibody (cod. 9102S, Cell Signalling, USA), rabbit polyclonal phospho-AKT antibody (cod. 9271S, Cell Signalling, USA), rabbit polyclonal AKT antibody (cod. 9272S, Cell Signalling, USA) diluted 1:1000. The expressions of these proteins were standardized to human α-actin by using rabbit polyclonal α-smooth muscle anti-actin antibody (1:1000 cod. 14968S, Cell Signalling, USA). Primary antibodies were detected using goat anti-rabbit or goat anti-mouse horseradish peroxidase (HRP)-conjugated secondary antibodies (1:2000, cod. Sc-2004; Sc-2005 Santa Cruz Biotechnology, USA). Immunoreactive bands were visualized by ECL Plus Western Blotting Substrate (cod. AR1196-200 Boster Biological Technology, USA) according to the manufacturer's

instructions through ChemiDoc Imaging System (BioRad, USA). Data were analysed using ImageJ Software (National Institutes of Health, USA).

ShRNA and Overexpression transfection

The plasmids Sdc-1 in pLenti6.3/V5-DEST (cod. HsCD00940971 DNASU, Arizona, USA) and empty vector pLenti6.3/V5-DEST (cod. OVT2848 Creative Biogene, USA) were spread in Ampicillin-LB agar plates in serial dilution to obtain single colonies at incubated at 37°C overnight. The next day, a single colony from each plate was picked and let grow in 2ml of LB-Ampicillin media and this overnight culture was then used to grow 50ml of bacteria for plasmid DNA extraction, performed following manufacturer instructions (Qiagen Plasmid Midi kit cod. 12143 Qiagen, MD, USA). Plasmid DNA was stored at -80°C for next uses. To produce the lentivirus, $5x10^5$ cell/ml of 293T were seeded on 6-well plate and incubated at 37°C and 5% CO_2 overnight. Effectene Reagent Kit (cod. 301425 Qiagen, MD, USA) was used to create the transfection mix, according to the instructions, and was then added to the cells after replacing of fresh media. After 24h the media was replaced and after 48h the lentiviruses contained in the medium were collected by filtering it with 0.45nm syringe filters.

ShRNA plasmids were provided from RNAi Core at the UMass Chan Medical School in a number of four different clones for Sdc-1, six for Gpc-1 and an empty vector containing pGIPZ. In this case, the core facility directly provided the lentivirus supernatants, so from this step, both the experiments, silencing and overexpression, followed the same protocol. The cell lines to transfect were seeded at the concentration of $1.5 x10^5$ cell/ml in a 6-well plate and the next day, the cells were infected with 250µl and 500µl of viral supernatants. Fresh media was replaced to reach a final volume of 1ml per well and 10µl of 1µg/µl Polybrene (cod. TR-1003 Merck, Germany) was added to enhance viral infection. After 24h, cells were re-fed with fresh media and after 48h from the infection, silenced cells were selected with Puromycin (cod. ant-pr-1 InvivoGen, USA) and the ovexpressing cells with Blasticidin (cod. ant-bl-05 InvivoGen, USA). After 5-7 days of selection the cells were ready for the use in the assays. The ability of the antibiotics used to select the cells, to kill the parental cell lines, were verified in a seven day of treatment, where cells died after only 4 days.

Statistical Analysis

The data were plotted and analysed using GraphPad Prism version 9.5.0 software (GraphPad Software Inc., USA) and Excel (Microsoft, Redmond, WA, USA). Each experiment was repeated at least three times and performed in triplicate. A *P*-value of 0.05 was considered statistically significant.

Ethic Statement

Animal procedures were approved by the Italian Ministry of Health and complied with EU Directive 2010/63/EU for animal experiments.

Funding Statements

The PhD project was approved and funded by Pegaso Scholarship through POR ESF TOSCANA 2014/2020 within the framework of Giovanisì provided by Tuscany Region FSE+.

Chapter III

Results

BOPs serum stability

Peptides can achieve high target specificity and low toxicity due to an overall positive charge and amphipathic properties, which are particularly important to develop safer and more effective anticancer therapies. The linear structure often renders them less stable, making them susceptible to degradation in serum in most of the cases after only 1h of incubation, and reducing their effective lifespan in the body. Proteases are ubiquitous constituents of cells, tissues, and body fluids, essential for digestion, post-translational processing, and subcellular localization. To enhance peptides effect on the affinity and stability to proteolytic degradation, BOPs were synthesized on Fmoc4-Lys2-Lys-beta-Ala-Wang resin or built using two consecutive Fmoc-Lys (Fmoc)-OH coupling steps to form the branched core on TentaGel resin. To test the resistance of this special tetra branched structure, serum stability of the peptides was performed mixing BOP7 and BOP9 with a pool of 25% human sera in RPMI 1640 and incubated at 37°C for different time points (t=0, t=4h, t=16h). The supernatant has been analysed by HPLC and MALDI-TOF spectrometer. Figure 15 reports BOP7 chromatogram (A) and mass spectrum at different time points of BOP7 (B-C-D), the other peptides showed analogue results.

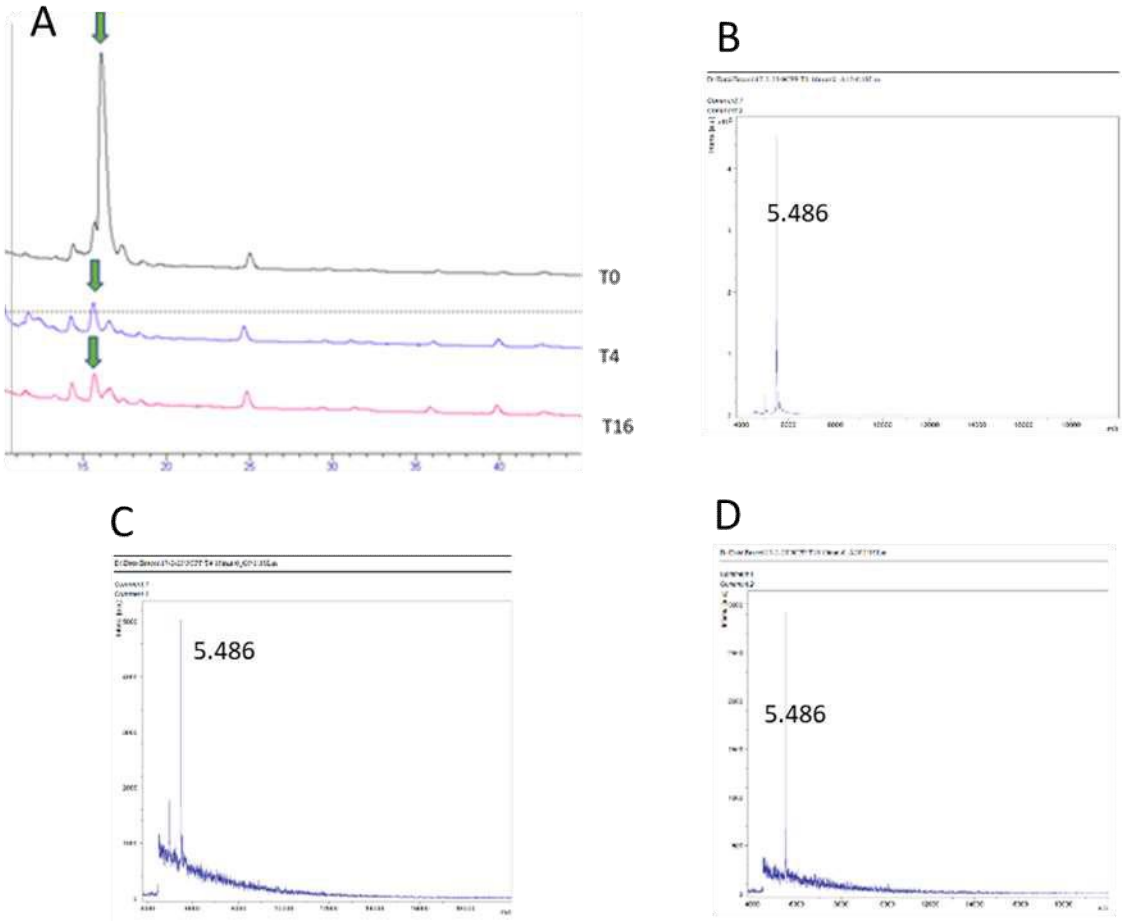

Fig. 15 BOPs degradation in serum: ***A****) BOP7 HPLC chromatogram at different time points (t=0h; t=4h; t=16h). MALDI-TOF mass spectrum of BOP7 at t=0 (****B****), t=4h (****C****) and t=16h (****D****). BOPs molecular weight calculated is reflected in the results obtained by the MALDI-TOF analysis.*

Immunofluorescence binding of BOPs-Bio to PANC-1 and MIA-PACA2

The purpose of this experiment was to observe the ability of BOPs to bind pancreatic cancer cell lines plasma membrane. BOPs were biotinylated and revealed with a fluorescent avidin. BOPs were able to bind plasma membranes at the concentration of 2μg/ml as reported from the green fluorescent label detected in Fig 16 B-C-D and Fig 17 B-C-D. Plasma membranes were stained with lectin, responsible for the red signal obtained, while DAPI highlighted the nuclei with a blue coloration. Comparing the two cell lines, MIA-PACA2 showed a stronger signal.

PANC-1

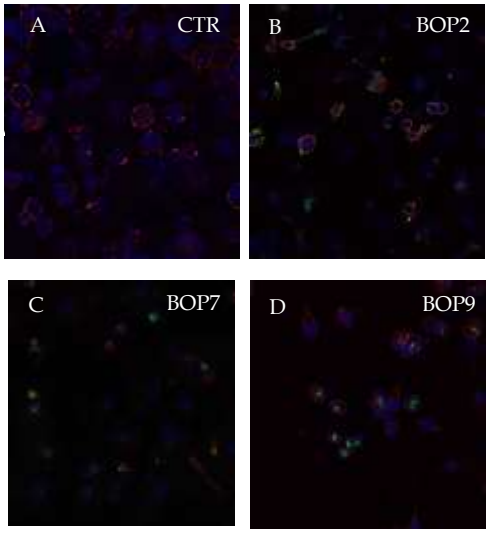

Fig. 16 BOPs binding to PANC-1: *untreated cells as negative control show only DAPI for nuclei and agglutinin for membrane (**A**); BOP2 (**B**); BOP7 (**C**) and BOP9 (**D**) are highlighted by green signal.*

MIA PaCa-2

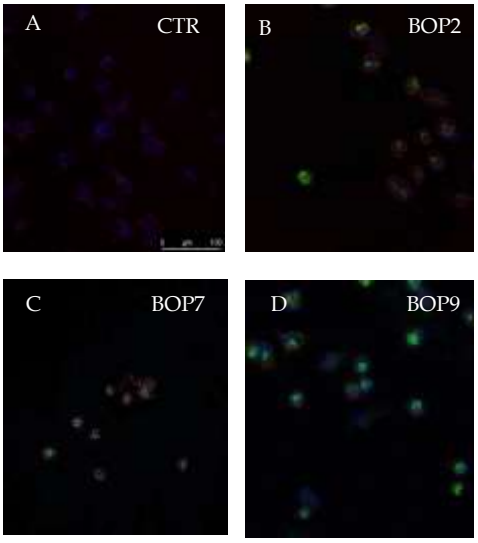

Fig. 17 BOPs binding to MIA-PACA2: *untreated cells as negative control show only DAPI for nuclei and agglutinin for membrane (**A**); BOP2 (**B**); BOP7 (**C**) and BOP9 (**D**) are highlighted by green signal.*

BOPs binding to PANC-1 and MIA-PACA2

To verify the binding of BOP7 and BOP9 on cancer cells, a flow cytometry using PANC-1 and MIA-Paca2 with different concentrations of the peptides was performed. BOP2, showed a dose-manner dependent binding to PANC-1 cells, not fully true for MIA-PACA2 where the highest concentration of the peptide had a halfway binding ability between the lowest and the highest concentration (Fig 18 A-B). Regarding BOP7, the diagraph of MIA-PaCa2 cells showed that both 2μM and 10μM have the same curve, indicating a saturation in the bond that reached an activity plateau after 2μM (Fig. 18 C-D). Lastly, BOP9 was the only one keeping the dose-manner dependent binding also in MIA-PaCa2 cells (Fig. 18 E-F).

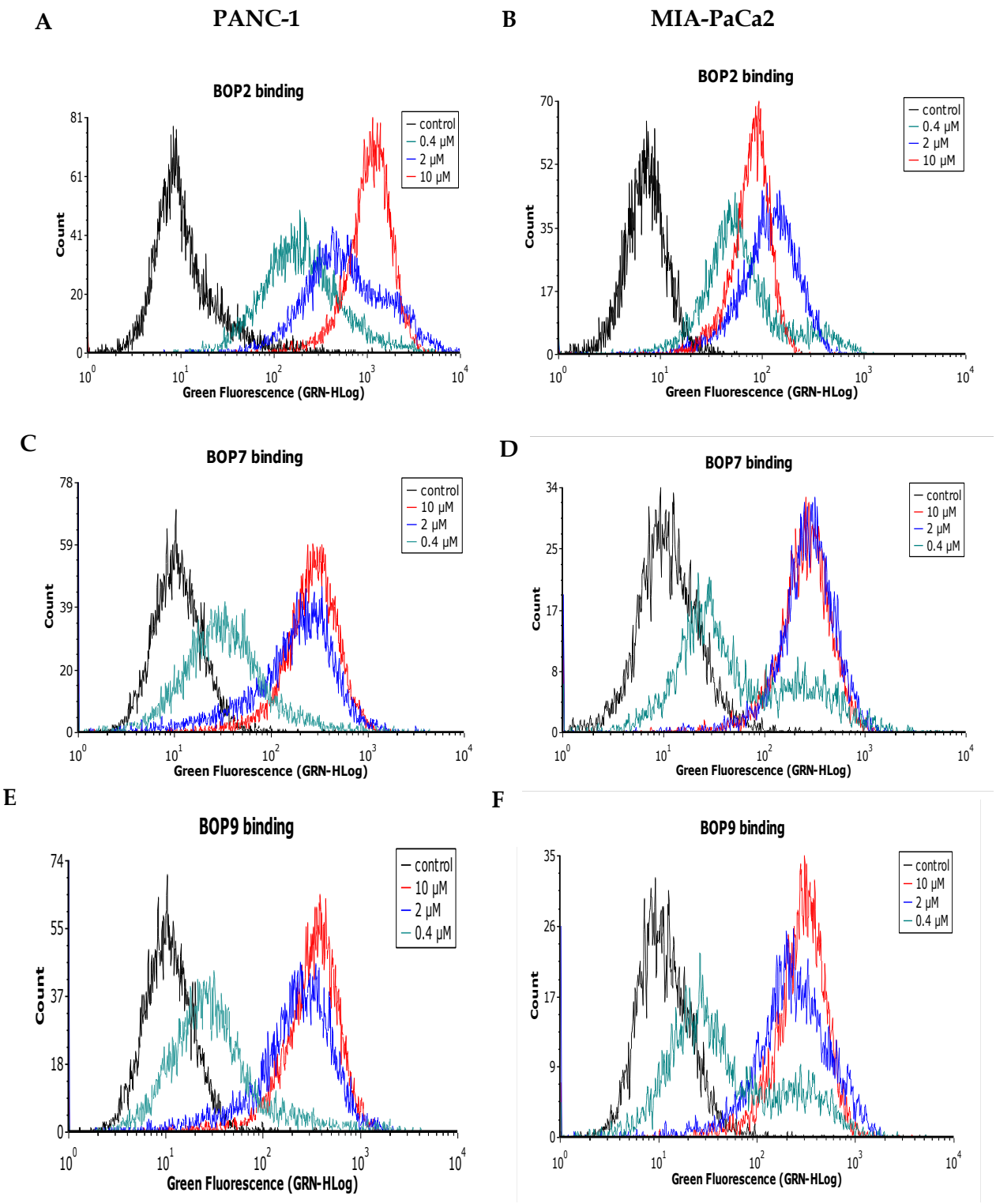

Fig. 18 BOPs FACS analysis in different pancreatic cell lines: *BOP2 analysis at different concentrations (10µM in red, 2µM in blue and 0.1µM in light blue) in PANC-1 (**A**) and MIA-PaCa2 (**B**), the latter shows a no dose-dependent manner behaviour. BOP7 (**C**-**D**) and BOP9 (**E**-**F**) in both cell lines shows ability to bind them if the concentration increases. In fact, lower concentrations follow the same trend as the negative controls in black.*

BOPs binding to RAW 264.7 and PgsA-745

To assess the specificity of the binding, mammalian immortalized cell lines of non-cancer origin were analyzed with the same flow-cytometry conditions. In fact, RAW 264.7 are non-tumoral macrophage cells that in Fig. 19 showed low BOP7 and BOP9 binding, exhibiting fluorescence intensity similar to the isotypic control. Since cationic peptides preferentially bind negatively charged targets and among them HSPGs could be a preferential target, we chose pgsA-745 cell line as a control of selectivity. These cells are mutants of Chinese hamster ovary cells deficient in xylosyltransferase, the enzyme responsible for the first sugar coupling, in the synthesis of heparan sulfate glycosaminoglycans (HSPGs), therefore they lack the heparan sulfate glycosaminoglycans (HSPGs). Thus, the ability of BOPs to bind cells that do not express HS was evaluated. Interestingly, BOP7 and BOP9 exhibited poor binding activity on pgsA-745, suggesting that they may target the heparan sulfate chains of HSPGs. BOP2 could bind PgsA-745 cell line (Fig. 19D). Regarding BOP7, its poor binding was remarkable at the lowest concentration (0.4µM) in comparison with the highest concentrations of 2µM and 10µM (Fig. 19E). BOP9 was also not able to tie up this cell line in a dose dependent manner, in fact cells incubated with 0.4uM of the peptide showed the best result, showing a curve close to the negative control cytogram (Fig.19F).

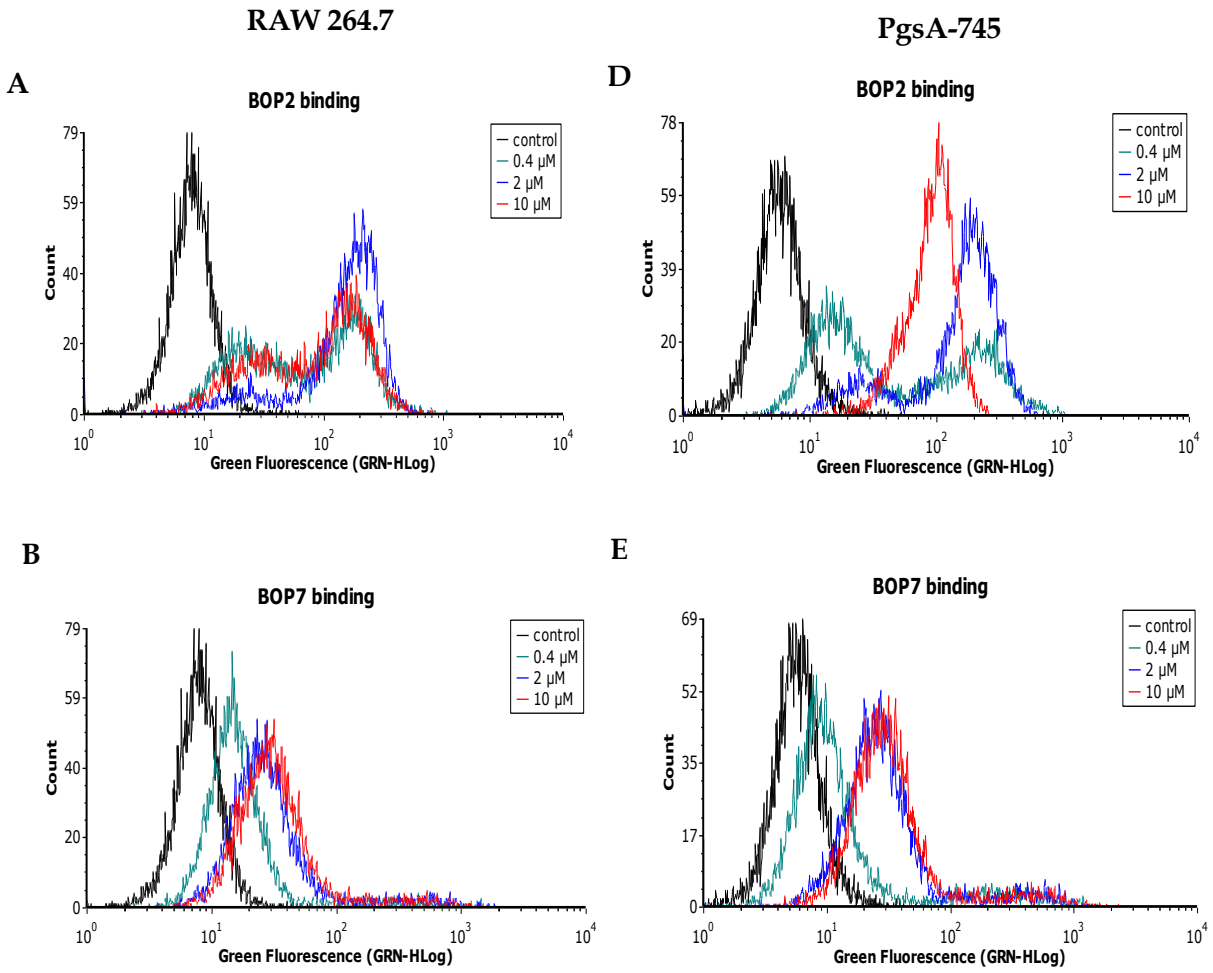

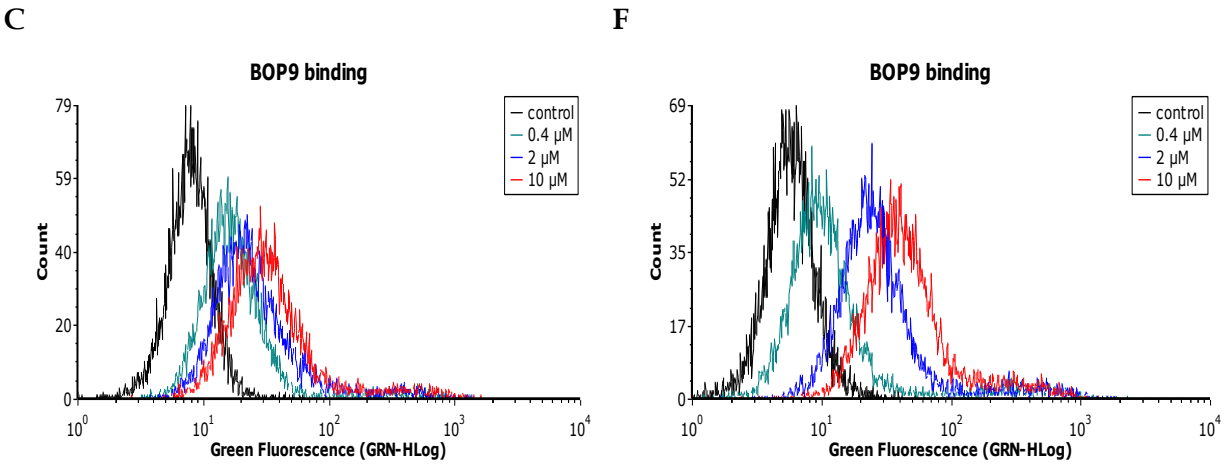

Fig. 19 BOPs flow cytometry in RAW 264.7 and PgsA-745: *Flow cytometry analysis on non-cancer murine macrophages, RAW 264.7 and PgsA745, CHO derived cells defective of HSPGs. Red line corresponds to 10µM concentration, blue to 2 µM and green to 0.4 µM. BOP9 (**C**) and (**D**) show no ability to bind these specific cell lines, as well as BOP7 (**B**) and (E). BOP2 (**A**) and (**B**) show efficiency in cell lines binding at least at the highest concentrations, probably due to some other cell membrane target.*

Cytotoxicity in PANC-1 cells

As a consequence of the previous flow cytometry data, a cytotoxicity assay using a tumoral cells line (PANC-1) was performed. In fact, the purpose of this experiment was to confirm the specific binding of BOPs to the cancer cells and their efficacy after 24h of treatment. More in general, peptides can adopt different structures (i.e., α-helical, β-sheet, or extended), upon interaction with biological membranes and all of which have both a cationic face and a hydrophobic face. The amphipathic nature of such molecules allows their adhesion to the cell membrane and the subsequent translocation into the interior of the cells (in fact, they are sometimes referred to as "cell-penetrating peptides"). Their mechanism of action can be either direct or indirect: in the first case, cell death is caused by irreparable membrane damage and cell lysis, whereas in the second case, cancer cells are killed by intervention in cell death pathways, signal transduction pathways, and/or the cell cycle. As general protocol, cytotoxicity was performed using increasing concentrations of the peptides for 24h of incubation and cell death was verified by using Trypan Blue, which is one of the most common staining able to highlight loss of integrity in cell membrane. The results show an IC_{50} of 4.68 x 10^{-6} M for BOP2, 1.67 x 10^{-6} M for BOP7 and 8.3 x 10^{-6} M for BOP9 (Fig. 20 A-B-C).

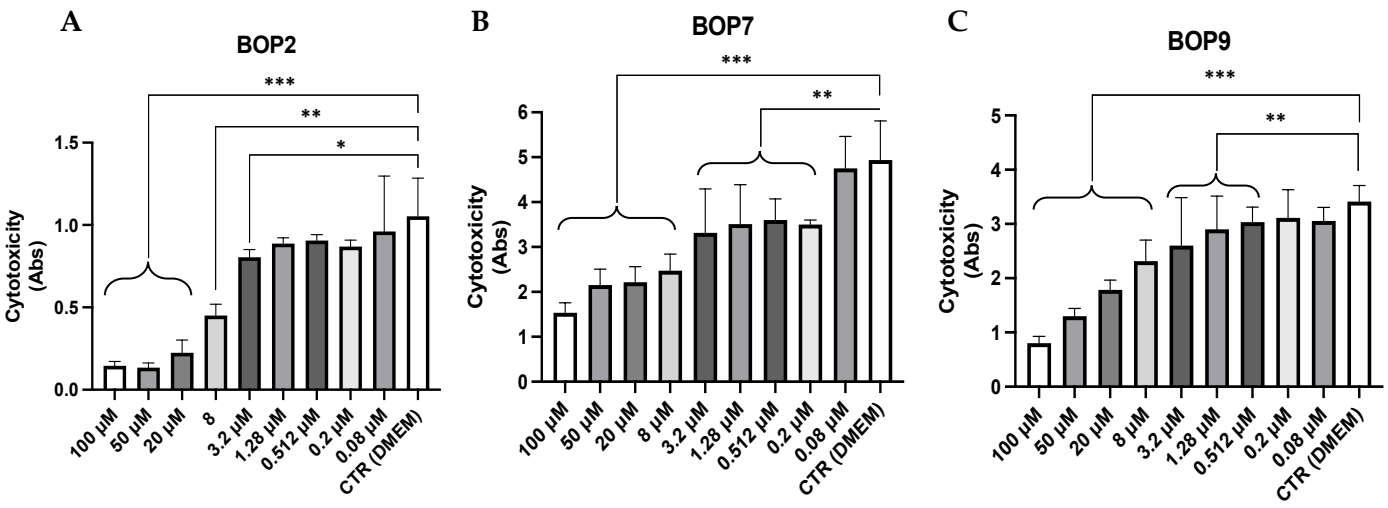

Fig. 20 Cytotoxicity assay: *BOP2 (**A**), BOP7 (**B**) and BOP9 (**C**) at different concentrations and the negative control only include treatment with DMEM media in PANC-1 cells (*** $p < 0.001$, ** $p < 0.01$, * $p < 0.5$; $n = 5$; ANOVA one-way, unpaired, parametric p values).*

Haemolysis assay

The general haemolytic assay procedure is based on the exposure of the erythrocytes to a specific agent (in this case, peptides) at a selected range of concentrations for the subsequent spectrophotometric quantitation of released haemoglobin at a given wavelength. Notably, the human RBCs are a valuable and efficient cellular model to obtain a rapid *in vitro* approximation of the toxic damages of a peptide in the body and reflect their safety. Many cationic peptides studied to date have some toxicity, due to their ability to induce cell membrane disruption, as measured by their tendency to induce lysis of erythrocytes at higher concentrations of some of them such as gramicidins, but other relatively nontoxic peptides include dermaseptins, which safety is probed.

In this assay, serial dilution of anticoagulant treated whole human blood were tested with two-fold dilutions of BOP7 and BOP9, showing low percentage of haemolysis even at the highest concentration compared to the positive control, and reaching the same range of values of the negative control made by PBS 1x (Fig 21 A-B). The positive control was made by incubation of red blood cells with 1% Triton100-PBS1x.

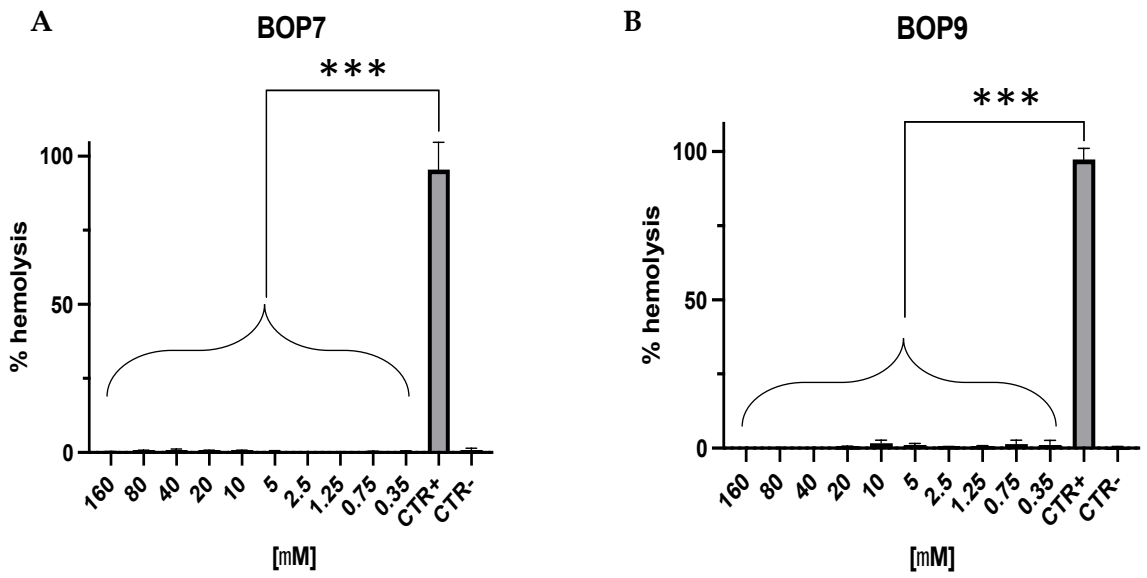

F*ig. 21 In vitro red blood cells lysis: A) BOP7 and **B**) BOP9 shows significant drop in the histogram when compared with positive control made with Triton X-100. Negative controls are only incubated with DMEM. (*** $p < 0.001$, n=3; ANOVA, one-way, unpaired, parametric p-values).*

Heparin-binding ELISA assay

Due to the well-known electrostatic interactions between the cationic anticancer peptides (ACPs), mainly composed of basic and hydrophobic amino acids, and anionic cell membrane components, the lack of interaction with RAW 264.7 and PgsA-745, suggested the hypothesis of a possible interaction between BOPs and the negative charged sulphate groups located on GAGs contained by proteoglycans. Additionally, the vast majority of HS-binding proteins also invariably bind heparin, since its main repeat unit structurally resembles the protein binding sequences in heparan sulphate. For that reason, an enzyme-linked immunosorbent assay (ELISA) was designed. ELISA is an immunological assay commonly used to measure antibodies, antigens, proteins, and glycoproteins in biological samples.

In this case, the sandwich ELISA was performed coating the plate with different concentrations (10 μg/ml; 5 μg/ml; 1 μg/ml) of the BOPs. The two negative controls were made by wells uncoated with the BOPs and wells where heparin-bio wasn't added. When added heparin-bio, BOP2 showed a dose dependent trend but less affinity for the heparin-bio binding. BOP9 and BOP7 had a much stronger binding with heparin-bio and the best results were obtained using a concentration of 5 μg/ml in both cases. Notably BOP9 seemed to be a better candidate in comparison with BOP7 due to the strength of the binding, moreover the 10 μg/ml was decreased, which probably means that a saturation was reached (Fig.22).

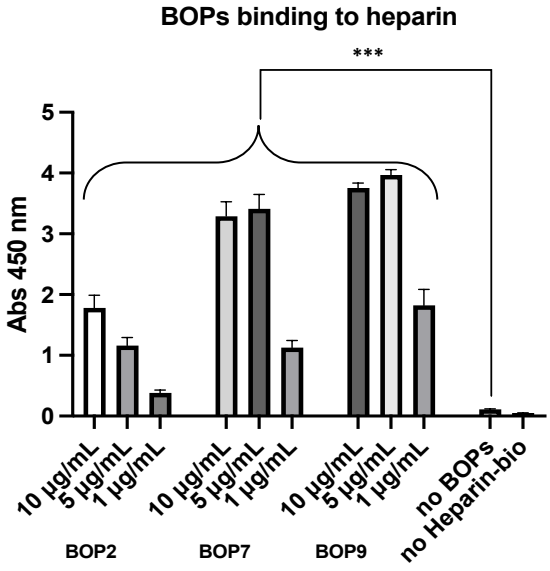

Fig. 22 BOPs ELISA: *BOP2 is the only one having a dose-dependent trend, while BOP7 and BOP9 are less linear, in fact the best concentration in 5µg/ml. In any case all of them are significant in comparison with the negative controls made with no BOPs and no heparin-bio (*** $p < 0.001$; n=3; ANOVA, one-way, unpaired, parametric p-values).*

Inhibition of BOPs binding to PANC-1 using Heparin as antagonist

To verify the ability of BOP7 and BOP9 to bind proteoglycans on PANC-1 cell plasma membrane, FACS analysis was performed using heparin at different concentrations (5µg/ml and 20µg/ml) as antagonist in the cell binding. The previous data, where BOPs were able to link specifically PANC-1, but not PgsA-745, strongly supported the hypothesis of their possible affinity for heparan sulphate proteoglycans, reinforced by heparin-binding ELISA assay results. Heparin and heparan sulphate (HS) are negatively charged, polydisperse linear polysaccharides. They are composed of α1-4 linked disaccharide repeating units containing a uronic acid and an amino sugar and they have been shown to bind and regulate the activities of many proteins, including enzymes, growth factors, extracellular matrix (ECM) proteins, and the cell surface proteins of pathogens. Heparin is found *in vivo* in the granules of connective tissue mast cells, whereas HS is found on the cell surface or in the ECM, covalently attached to several different core proteins forming heparan sulphate proteoglycans (HSPGs). They have been shown to differ in their degree of sulfation, with heparin displaying higher N- and O-sulfation than HS, giving to heparin a higher overall negative charge which is the main reason why it was used as antagonist in this flow cytometry assay.

In this case heparin was used at increasing concentration, to bind BOPs and reduce their ability to link HS on the cell surface. Both the peptides were used at the concentration of 10 µM which resulted to be optimal for PANC-1 binding from the previous data. BOP7 cytogram showed that the incubation of the peptide with 20 µg/ml of heparin was able to shift the curve almost at the level of the negative control, while the concentration of 5 µg/ml wasn't sufficient to reduce the binding of BOP7 to HS and the affinity of the peptide for these sites was still strong enough to give a trend similar to the positive control, made by the incubation of the peptide alone (Fig 23A). BOP9 follows the same trend: the highest concentration of the heparin could eliminate peptide's binding and shift cells signal close to the negative control, while the lowest concentration wasn't able to affect BOP9 affinity for PANC-1 HSPGs (Fig 23B).

A

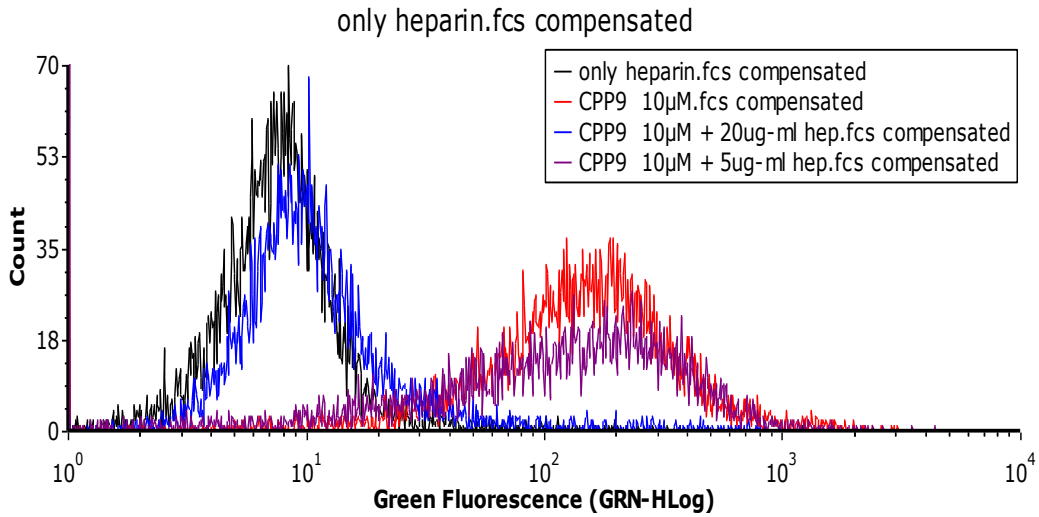

B

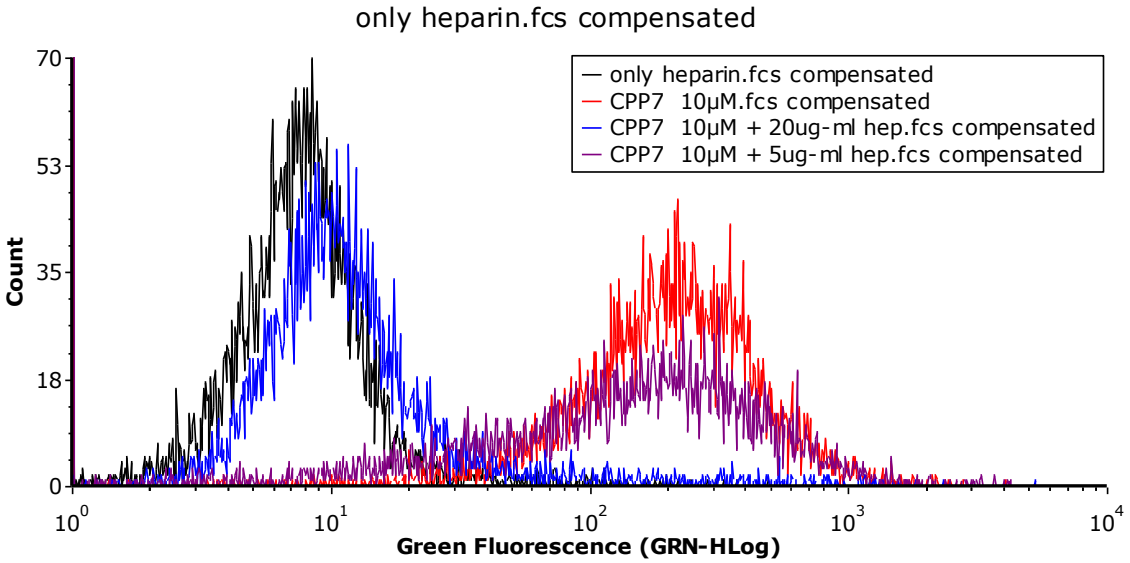

Fig. 23 BOPs cytograms using an antagonist: *the negative controls are made by incubation of the cells with heparin alone at the concentration of 20µg/ml. The red curve of the BOP7 is the positive control made by incubation of the peptide alone at 10µM, while the purple curve is the peptide used in combination with 5µg/ml of heparin and the blue with higher of 20µg/ml (**A**). The same legend is also used for BOP9 (**B**).*

Adhesion assay on PANC-1 cells

Proteoglycans (PGs) are an important component of the extracellular matrix (ECM), where regulate migration, proliferation, and cell adhesion. For example, has been reported that cell surface heparan sulphate proteoglycans are necessary for the formation of stable focal adhesion sites on fibronectin coated substrates such as cover slips or wells in the culture plate.

From there, the initial hypothesis of this assay was to understand if the incubation of the BOPs with PANC-1 cells, could reduce cells attachment to the plastic surface of a 96-well plate during 4h of treatment by interfering with HSPGs. BOP9 showed a dose-dependent significant reduction of cells attachment, if compared with positive control, (Fig.24 A) while BOP7 effect is only valid at the highest concentration of 0.2μM (Fig.24 B).

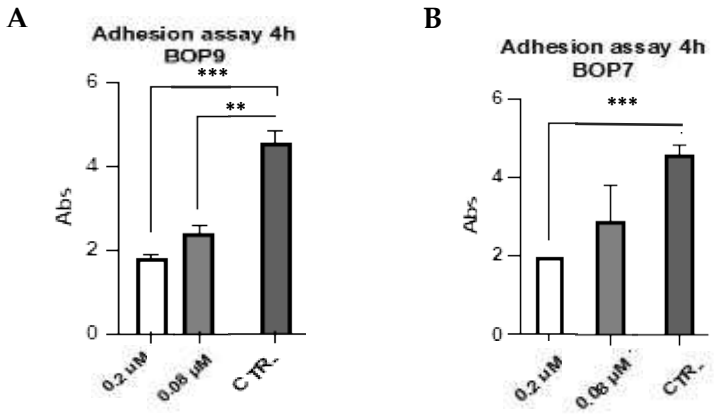

Fig. 24 BOPs adhesion assay: A*) BOP9 histogram after 4h of incubation.* ***B****) BOP7 showed significant reduction only at 0,2μM (*** p < 0.001, ** p < 0.01; n=3; ANOVA, one-way, unpaired, parametric p-values).*

Inhibition of PANC-1 migration in a 2D model

Proteoglycans are responsible for cell movements through enhancing growth factor signals, which rearrange the cytoskeleton of actin. In fact, one important modulator of EMT processes is transforming growth factor β (TGFβ), which is known to drive progression of late state malignancies by promoting invasion. Several proteoglycans are connected to TGFβ-signalling such as syndecan-1.

To investigate this property, a 2D migration model was designed using a silicon insert to standardize the experiment. Once seeded the cells, they were treated with different concentrations of the BOPs and the migration was observed for 16h. As shown in Fig. 25A, the BOPs were able to reduce the speed of PANC-1 closing the gap. The most effective peptide was the BOP7 at the concentration of 10μM (Fig. 25B), but all the three peptides showed significant activity.

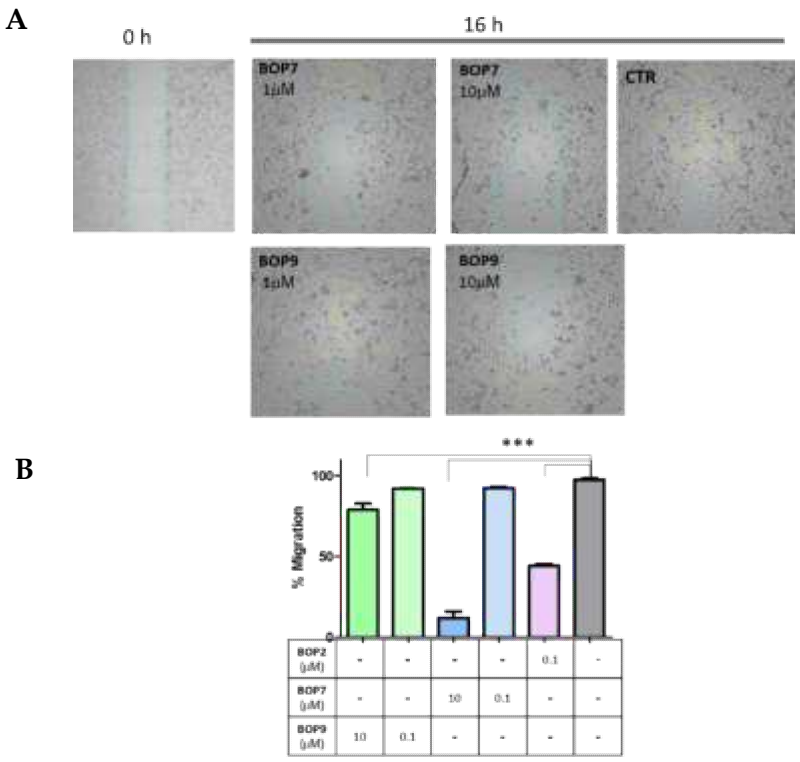

Fig. 25 Migration 2D in PANC-1 cells: A*) Pictures of the BOPs at different concentrations, compared with the untreated negative control and with the t=0,* ***B****) Diagraph of the significant reduction in the closure of the gap especially for BOP7 10µM (*** p < 0.001; n=3; ANOVA, one-way, unpaired, parametric p-values).*

Inhibition of 3D model of migration using PANC-1 cells

Tridimensional migration simulates invasion of tissues by cancer cells. In this setting, cells not only move, but also must degrade a matrix, in this case collagen type I, and have to change their shape to squeeze through the pores of an artificial membrane. Using a standard protocol, cells were seeded on a collagen layer on the insert, upper chamber, and their ability to cross the membrane and reach the lower chamber, was measured. FBS was used to attract cells and induce their migration from the upper chamber to the lower passing through the membrane (Fig. 26B). Focusing on the histogram obtained, BOP7 at the concentration of 10uM was confirmed as the most effective, but also BOP2 was surprisingly good in reducing cells movement (Fig. 26A).

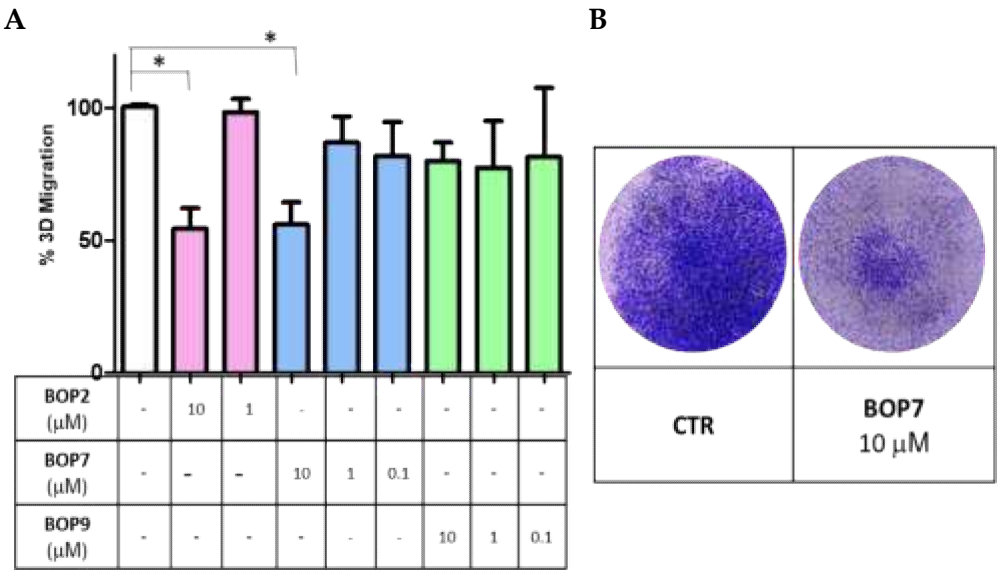

Fig. 26 Migration 3D using PANC-1: A*) histogram of all BOPs used at the concentration 10μM, 1μM and 0.1μM* ***B****) Representative pictures of the Transwell membranes after treatment with the highest concentration of BOP7 and DMEM alone for the negative control (* p=0.0285; n=3; ANOVA, one-way, unpaired, parametric p-values).*

Luciferase transfection of PANC-1 cells

Firefly (*Photinus pyralis*) luciferase is used most commonly for *in vivo* imaging studies because of the sustained kinetics of light emission, favourable pharmacokinetics of the luciferin substrate, and relatively red-shifted emission spectrum. In this case, we transfected pancreatic cells using Lipofectamine3000 reagent (7.5μl and 5.5μl) and selected them with a specific antibody, Geneticin (G418). The consequent addition of D-luciferin allows the ATP-dependent oxidation to oxyluciferin, producing light emission at 560nm. This experiment has been essential to track the speed of cell replication and tumour growth in the mouse model experiment (Fig. 27 A-B).

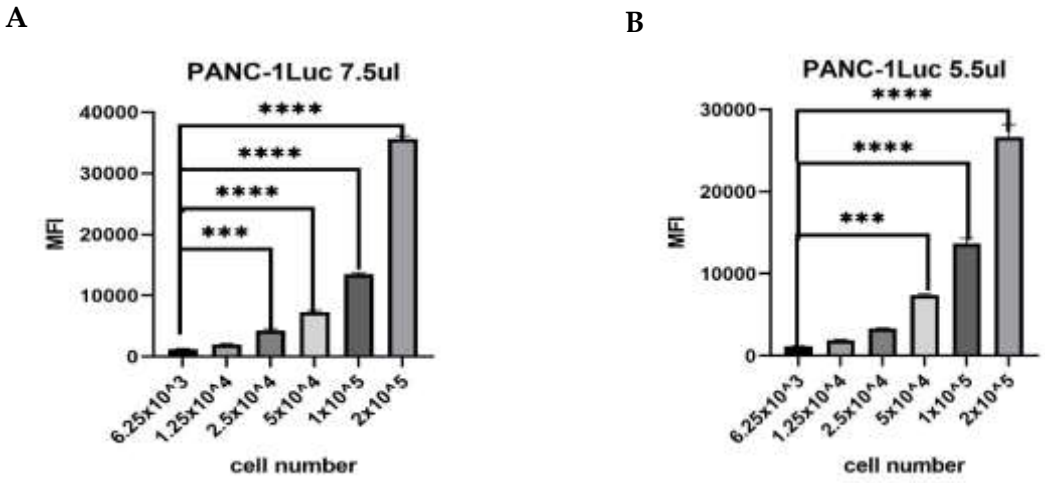

Fig. 27 Luciferin assay: A*) Fluorescent signal coming from PANC-1 transfected with 7.5μl of the reagent, decreasing as long as the number of cells decreases.* ***B****) Signal from the use of 5.5 μl of the reagent to transfect the cells. On the Y axis the MFI (mean fluorescent intensity) and on the X axis the cell number per well (*** p = 0.0004; **** p value < 0.0001; n=3; ANOVA, one-way, unpaired, parametric p-values).*

Mouse model of pancreatic cancer metastasis

In this experiment, PANC-1 Luc cells were injected into mice tails to create a metastatic model. In fact, after entering the bloodstream, tumour cells can disseminate widely throughout the body and are known as circulating tumour cells (CTCs) and on reaching distal organs, surviving tumour cells can be intercepted in small capillaries or actively adhere to larger blood vessels and extravasate through paracellular or transcellular trans-endothelial migration prior to colonization. Pancreatic cancer normally spread to the liver, lungs, or distant parts of the abdomen. This model was performed using nude mice, which lack in thymus development, resulting in an inhibited immune system, which otherwise would have caused the human tumour rejection. As shown in the Fig. 28A the tumour growth was observed for 24 days after PANC-1 Luc2, in the first 5 days the treatment with BOP9 and saline solution was performed every day and repeated in four days long cycles at day 8, 16 and 22. The end point was established at 24 days after the injection and the imaging pictures were taken at day 1, 5, 16, 22 and 24. The bioluminescence from PANC-1 Luc2 metastasis spred in the abdomen of the mice, showed clearly a reduction in the signals of the group treated with BOP9 (Fig. 28C) confirmed by the analysis of radiance, which is the photon emission from the tissue surface. In fact, the photon emission from control mice was significantly higher than the treated group, validating the effect of the peptide in reducing the tumour growth (Fig. 28B).

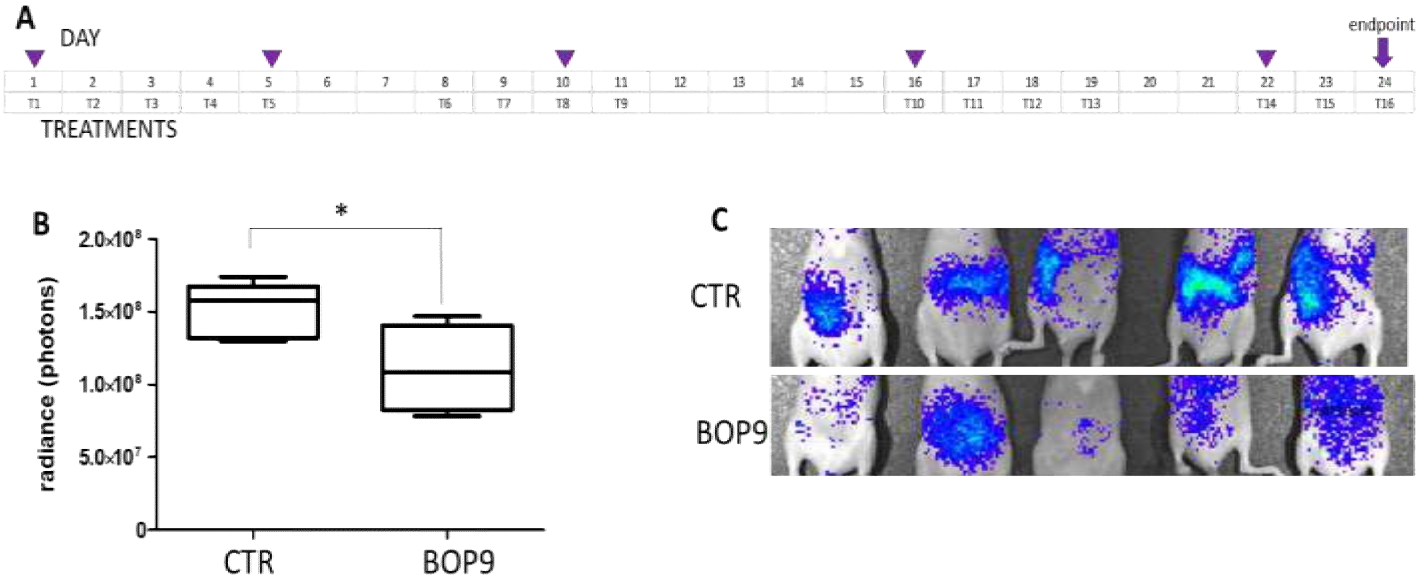

Fig. 28 Bioluminescence analysis of pancreatic cancer orthotopic mouse model: ***A****) Scheme of the treatments in the two mice groups, the arrows indicate the days of in vivo imaging analysis, using D-Luciferin as reagent.* ***B****) Diagraph of the photon's radiance average from the different groups: controls have significant higher signals than BOP9 treated mice (* p value= 0.02; n=5; unpaired, one-tailed t-test).* ***C****) Images taken at the endpoint of the experiment showing higher intensity of luminescence in comparison with the peptide treated mouses.*

The PhD fellowship PEGASO funded by Regione Toscana, provides to the students the opportunity of pursuing their research projects abroad. In my case, the UMass Chan Medical School (Boston, MA, USA) under the supervision of Dr. Brian C. Lewis, allowed me to spend six months in his laboratories investigating the possible connection between proteoglycans, in particular syndecan-1 and glypican-1, with mTOR signalling. Lewis Lab in fact, is involved in uncovering the function of mTOR complex2 in pancreatic cancer and a collaborative project between University of Siena and his lab was established.

Genetic PDAC mutations in primary cell lines

Seven different primary cell lines with different mutations were used (Fig. 29A). HPNE is an hTERT-immortalized epithelial cell that was isolated from the healthy pancreas, and it was used as a negative control since it's not tumoral.

A

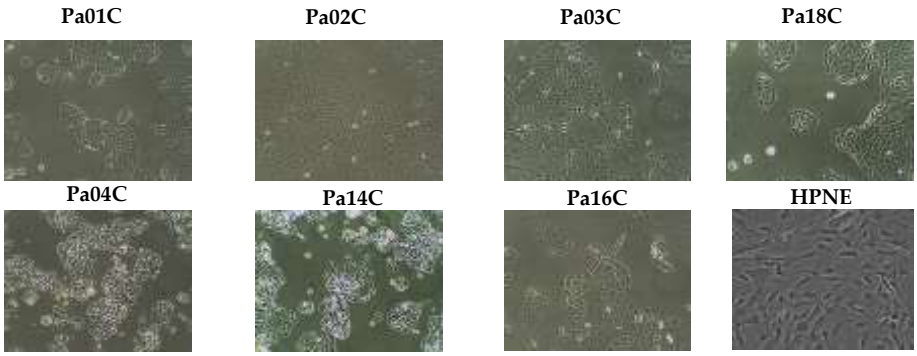

B

Cell line	Origin	KRAS	CDKN2A	TP53	SMAD4
PaO1C	Liver Metastasis	Mutant G12D	WT	Mutant T155P	Homozygous deletion
PaO2C	Liver Metastasis	Mutant Q61H	Homozygous deletion	Mutant L257P	Homozygous deletion
PaO3C	Liver Metastasis	Mutant G12D	WT	Mutant L344P	WT
PaO4C	Lung Metastasis	Mutant G12V	Homozygous deletion	Homozygous deletion	WT
Pa14C	Primary pancreatic tumour	Mutant G12D	Homozygous deletion	Homozygous deletion	Frameshift mutation
Pa16C	Primary pancreatic tumour	Mutant G12D	WT	Mutant I255N	WT
Pa18C	Primary pancreatic tumour	Mutant G12D	Homozygous deletion	WT	Homozygous deletion

Fig. 29 Primary cell lines genetic mutations and phenotypes: A*) Pictures of the different cell lines used and their morphology.* ***B****) Genetic mutations and tissue derivation.*

Mutations in the oncogene KRAS, and in the tumour suppressors CDKN2A, TP53, and SMAD4 are the major genetic mutations that underly PDAC development. The most predominant KRAS mutation site in PDAC occurs at codon 12; most commonly G12D (45%), followed by G12V (35%), and G12R at 17%. In these cell lines, mutant G12D is the most common mutation, especially in the ones coming from the primary pancreatic tumour. CDKN2A inactivation predicts a poorer prognosis in PDAC patients. On the other hand, mutated TP53 leads to cell survival, metastasis, autophagy inhibition and metabolic reprogramming. Lastly, homozygous deletion of Smad4 is found in about 30% of pancreatic cancer patients, inactivation of Smad4 in 20% of patients, data confirmed also in the cell lines used, which showed the deletion as a most common mutation (Fig. 29B).

Expression of Sdc-1 and Gpc-1 in primary cells

To have a clear view of proteoglycans overexpression in PDAC, the first experiment done, was conducted checking Sdc-1 and Gpc-1 signals by western blot analysis. In fact, most patients with PDAC (80%) expressed Gpc-1 in pancreatic cancer cells and stromal cells, suggesting its new role as a potential new marker. Regarding Sdc-1, its expression is increased in PDAC stroma compared to a normal stroma and this shift is correlated with poor prognosis.

As confirmed in Fig. 34, hTERT-immortalized epithelial pancreas cell (HPNE) that should act as a negative control expressed a weak signal of Sdc-1, but higher of Gpc-1. For the primary cell lines: PAO1C, PAO3C and PA16C had high expression of both proteoglycans, while PA18C and PAO2C only showed Sdc-1 signals. Finally, check of β-actin levels was used to confirm no degradation of the lysates and the same loading concentration of the protein during the SDS-PAGE run (25μg/ml). This experiment was essential also for the choice of which cell line to use for overexpression and silencing transfection, in fact for the first purpose PA14C resulted the most suitable due to their low expression of Sdc-1 and Gpc-1, while for silencing aims PAO3C and PAO16C were chosen.

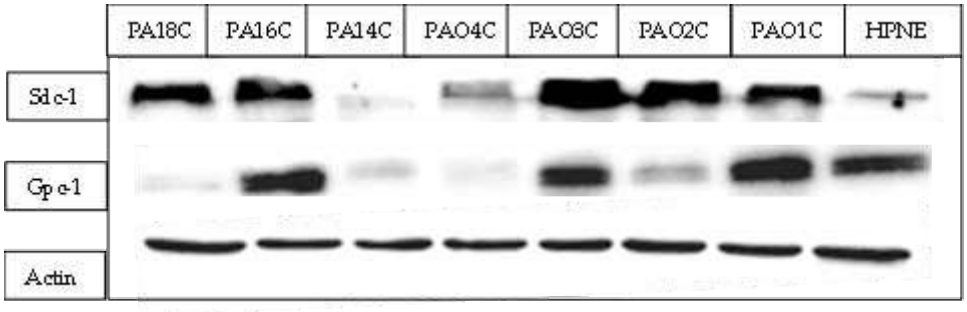

Fig. 30 Western Blot analysis of primary cells: *All the cell lines were probed for Sdc-1, Gpc-1 and β-actin expression. Most of the cells overexpress Sdc-1 (PA18C, PA16C, PAO3C, PAO2C, PAO1C), while only few of them Gpc-1 (PAO1C, PAO3C, PAO16C).*

Exogenous expression of Sdc-1 in PA14C cell lines

The purpose of this assay was to compare the protein expression variations in the growth factor pathways, between parental and overexpressing cell line. In fact, since proteoglycans are known to enhance growth factor binding on the cell surface and their intracellular pathways, the purpose of the transfection was to verify the differences on ERK/AKT expressions and at the phenotype level, performing migration assays.

Lentiviral vector was used to transfect PA14C cell lines using Sdc-1 and Gpc-1 plasmid DNA in order to overexpress these surface proteins. The transfected cells were selected using Blasticidin and Western blot assay was performed to confirm the success of the transfection. The diagraph showed higher expression of Sdc-1 in comparison with the negative control (parental cells) in Fig. 31A, where strongest Sdc-1 are obtained from the transfected cells.

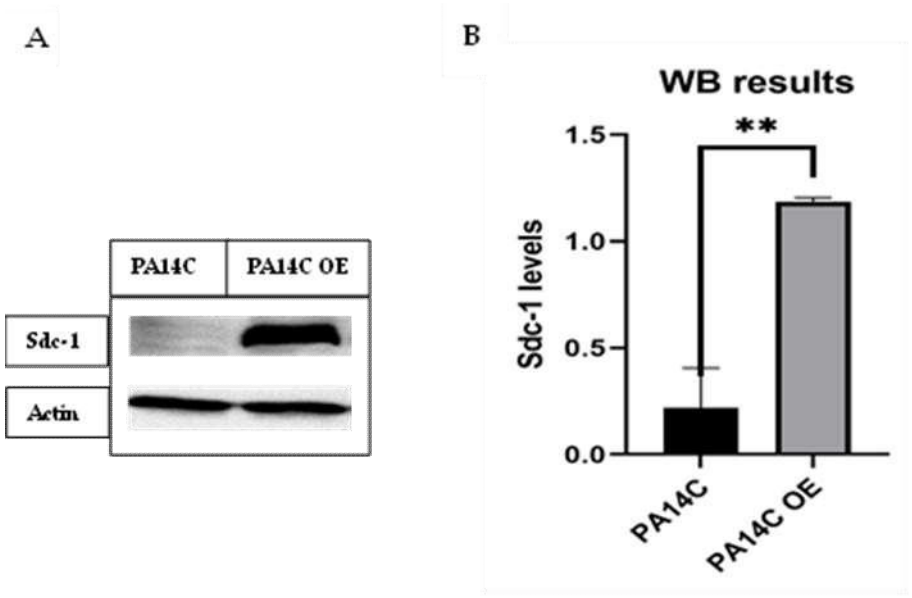

***Fig. 31 PA14C OE Sdc-1 data: A**) WB of parental cell line lysate and the overexpressing cells. **B**) Diagram of WB after normalization of the data with β-actin (** p value = 0.0092; n=3; unpaired, one-tailed t-test).*

ShRNA silencing of Gpc-1 and Sdc-1 expression in PA03C and PA16C cell lines

In parallel with the OE of exogenous Sdc-1, a silencing transfection was performed using shRNA for both proteoglycans (Sdc-1 and Gpc-1) in PAO3C and PA16C. The negative control was made by the transfection of the cells with empty pGIPZ vector that should not affect HSPGs expression. pGIPZ was able to produce a green fluorescence signal when observed on fluorescent microscope (Fig. 32A), characteristic useful to keep track of the success of the transfection. The choice of the two cell lines (PAO3C and PA16C) was a consequence of previous data where they showed consistent expression of both the proteoglycans and the effectiveness of the HSPGs silencing was verified by western blot analysis. In PAO3C, none of the clones used were able to completely knockout the expression of Sdc-1 (Fig. 32C), meanwhile Gpc-1 levels were strongly reduced by clones 4 (Fig. 32D).

Regarding PA16C, the clone 4 was able to reduce the expression of Sdc-1 (Fig. 32B) and clone 1 was effectively reducing Gpc-1 levels (Fig. 32E). The efficacy of the shRNA clones was evaluated selecting only the ones showing a reduction on HSPGs levels higher than 20%.

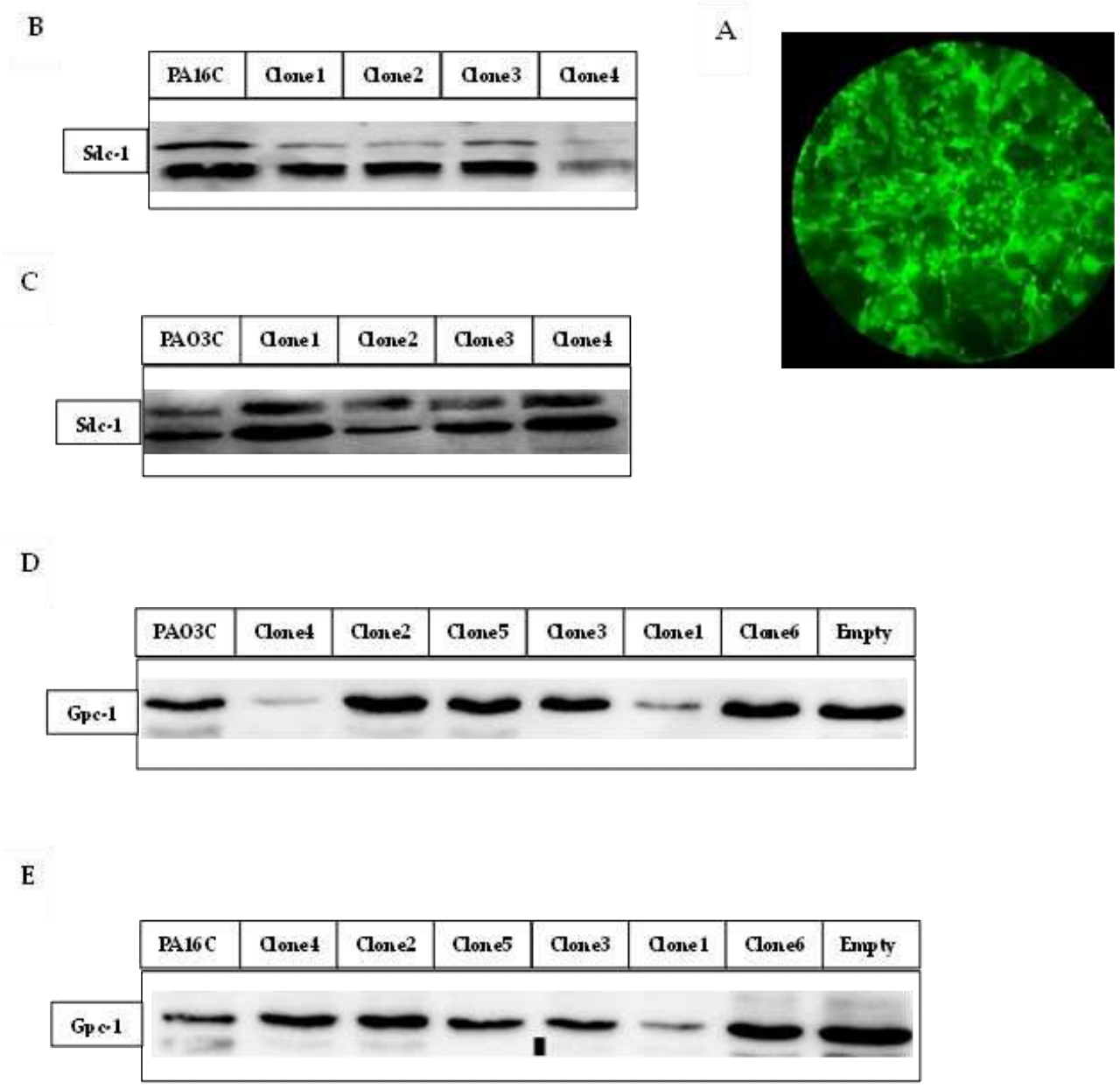

Fig. 32 Silenced cell lines data: ***A****) GFP signal picture of empty vector; B) WB of different shRNA clones used to silence Sdc-1 in PAO16C;* ***C****) WB of the clones used to silence Sdc-1 in PA3C. Clones used for reducing Gpc-1 expression in PA3C cells (****D****) and in PA16C (****E****).*

mTOR pathway involvement in HSPGs expression

AZD2014 is a small-molecule ATP competitive inhibitor of mTOR that inhibits both mTORC1 and mTORC2 complexes, while the complex 1 inhibitor, is Rapamycin, which phosphorylate substrates such as S6K1. Inhibiting mTOR genetically as well as pharmacologically, results in adaptive rewiring of oncogenic signalling with activation of canonical extracellular signal-regulated kinase and phosphoinositide 3-kinase-AKT pathways. To investigate the correlation between mTOR pathway and proteoglycans, treatment of all primary cell lines with AZD2014 (200nM) and Rapamycin (5mM) was performed at different time points (t=0, t=2h, t=8h and t=24h), followed by lysates preparation and western blot analysis. The number of bands resulting from Sdc-1 expression showed some variation along the different cell lines, due on the number of modifications, such as glycosylation, that occur in the cells. Finally, the concentrations of the drugs were decided from previous data on cell viability assays performed on all the cell lines from Brian C. Lewis lab.

Fig. 33A reported that HPNE showed no variations on Sdc-1 and Gpc-1 expression after the treatments, data that we expected due to the non-tumoral origin of the cell line. No significant difference was appreciable in the diagraphs below the WB results, where the histograms showed the same trend, except for AZD and RAP 24h treatment that reduced weakly the expression of Gpc-1 and for AZD8h and RAP8h that slightly lowered the expression of Sdc-1. Regarding PAO1C, Fig 33B showed a reduction on Sdc-1 levels only after 24h of RAP, while the other time points only reported increased levels. Gpc-1 seemed to be affected by both treatments starting from the 8h time point. Fig. 33C exhibited more variations in PAO3C cells, where both treatments increased the expression of Sdc-1 at 2h and 24h, while restored the basal level expression after 8h of drugs incubation. On the other hand, only AZD 24h and 8h were able to lower the expression of Gpc-1. Fig. 33D showed a strong reduction on Sdc-1 expression in PAO3C cells from both drugs even at the shorter time point, while Gpc-1 reduction was detectable after AZD 2h, 8h and 24h treatment. None of the Rapamycin time points showed significant effects. Fig. 33E showed a trend similar to PAO3C. In this case PAO4C cells had a strong reduction on Sdc-1 expression from both drugs and starting from the shorter time point, while Gpc-1 reduction was detectable after AZD and RAP 24h treatments. PAO14C results (Fig. 33F) showed a strong increase on Sdc-1 expression from both drugs at 2h and 8h of incubation and the same trend was followed by Gpc-1 expression. Fig. 33G reported the variation of expression on PA16C cells. The drop of the Sdc-1 expression occurred after 8h and 24h of treatment with both the inhibitors of mTOR, while Gpc-1 showed the strongest reductions after RAP 8h and AZD 24h incubation. Finally, Fig. 33H reported PA18C cells results, where no significant variations were notables between the different time points of drug incubation and the basal level of Sdc-1 expression. Gpc-1 showed a reduction especially when treated with AZD 8h.

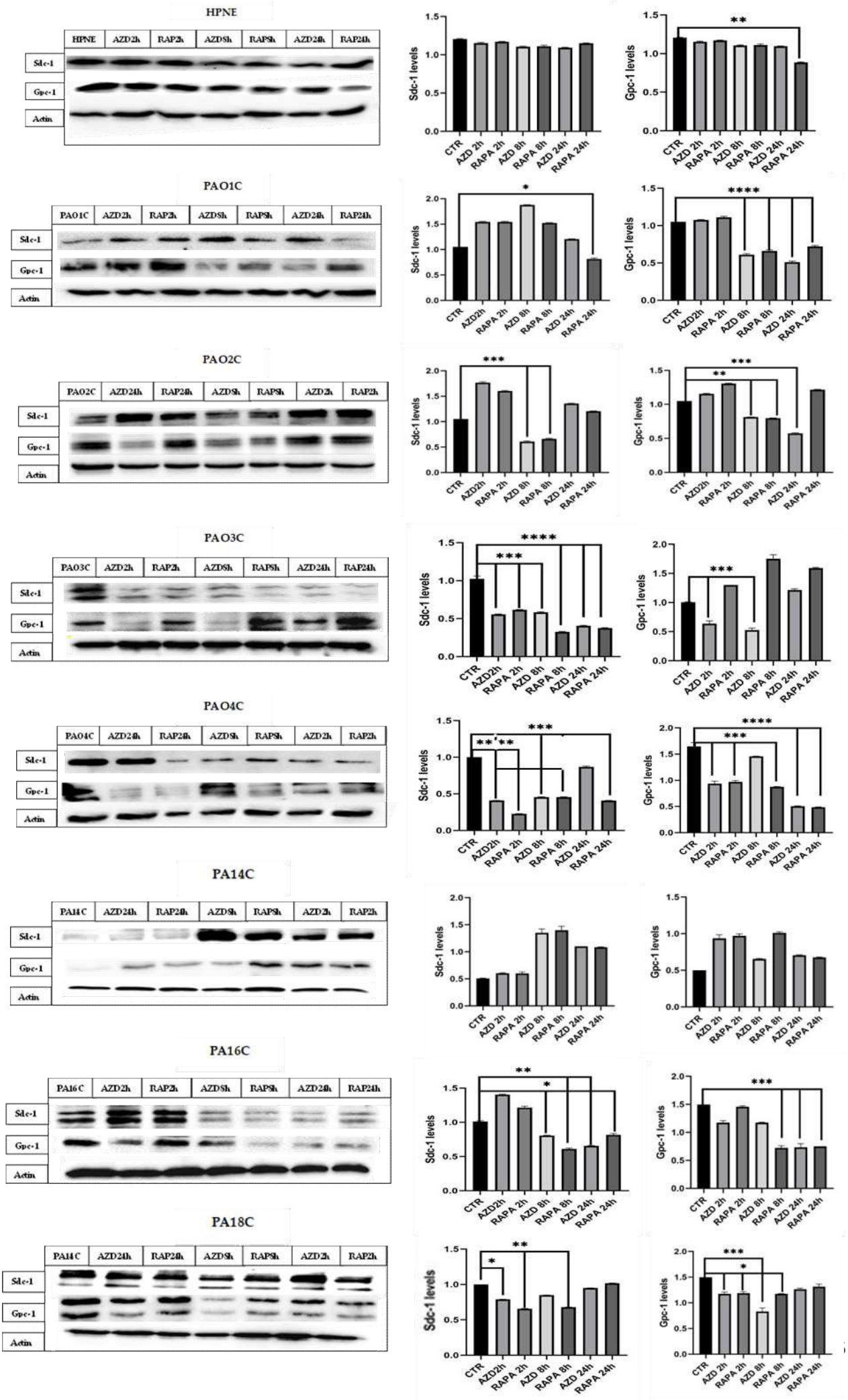
HPNE
HPNE AZD2h RAP2h AZD8h RAP8h AZD24h RAP24h
Sdc-1
Gpc-1
Actin
Sdc-1 levels
Gpc-1 levels
CTR
AZD 2h
RAPA 2h
AZD 8h
RAPA 8h
AZD 24h
RAPA 24h
PAO1C
PAO1C AZD2h RAP2h AZD8h RAP8h AZD24h RAP24h
PAO2C
PAO2C AZD24h RAP24h AZD8h RAP8h AZD2h RAP2h
PAO3C
PAO3C AZD2h RAP2h AZD8h RAP8h AZD24h RAP24h
PAO4C
PAO4C AZD24h RAP24h AZD8h RAP8h AZD2h RAP2h
PA14C
PA14C AZD24h RAP24h AZD8h RAP8h AZD2h RAP2h
PA16C
PA16C AZD2h RAP2h AZD8h RAP8h AZD24h RAP24h
PA18C
PA14C AZD24h RAP24h AZD8h RAP8h AZD2h RAP2h

Fig. 33 Western Blot of the different cell lines: ***A****) HPNE;* ***B****) PAO1C;* ***C****) PAO2C;* ***D****) PAO3C;* ***E****) PAO4C;* ***F****) PA14C;* ***G****) PA16C;* ***H****) PA18C. For all the cell lines the diagraphs show the syndecan-1 and glypican-1 curves together with the pictures of the bands analysed with ChemiDoc instrument. Sdc-1 and Gpc-1 can exist in two or one band depending on the cell lines, when two both the bands have been quantified (**** p value < 0.0001; *** p value <0.0005; ** p value < 0.0075; * p value = 0.0268; n=3; ANOVA, one-way, unpaired, parametric p-values).*

Level of expression of AKT and ERK in PA14C cell line overexpressing Sdc-1

The previous data on proteoglycans being partially affected by canonical mTOR drugs, such as AZD2014 and Rapamycin, raised questions about how the proteoglycans can affect the prior steps of the cascade such as AKT and ERK. In fact, HS chains of HSPGs binds the FGF ligand and receptor forming a ternary complex that promotes FGFR dimerization, and in turn activates signalling. Depending on the tumour type, HSPG-regulated FGF binding, and receptor dimerization triggers the activation of four main signalling pathways, including mitogen-activated protein kinase (MAPK)/extracellular signal-regulated kinase (ERK), phosphatidylinositol 3-kinase (PI3K)/protein kinase B (AKT), Janus kinase (JAK)/signal transducer and activator of transcription (STAT), and protein kinase C (PKC) pathways. Commonly, MAPK/ERK signalling cascade activated by FGFs is implicated in cell growth and differentiation, PI3K/AKT signalling cascade in cell survival and cell fate determination, and PKC in cell polarity (Fig. 34). In our case, PA14C cells overexpressing Sdc-1 and the parental control were plated and after 24h lysated to get the normal level of expression of these cells; while another sample was obtained after 14h of serum starvation which is already known to drop the expression of AKT and ERK and the last samples were obtained by replacement of serum media after 24h of starvation, that should raise again the level of these two proteins (Fig. 35 A-B). ERK cascade seemed to do not being affected by the overexpression of Sdc-1 in PA14C cells, which showed the same levels of protein's expression as the negative control, while AKT resulted to be affected by Sdc-1 overexpression in PA14C giving to the cells more sensibility to serum starvation.

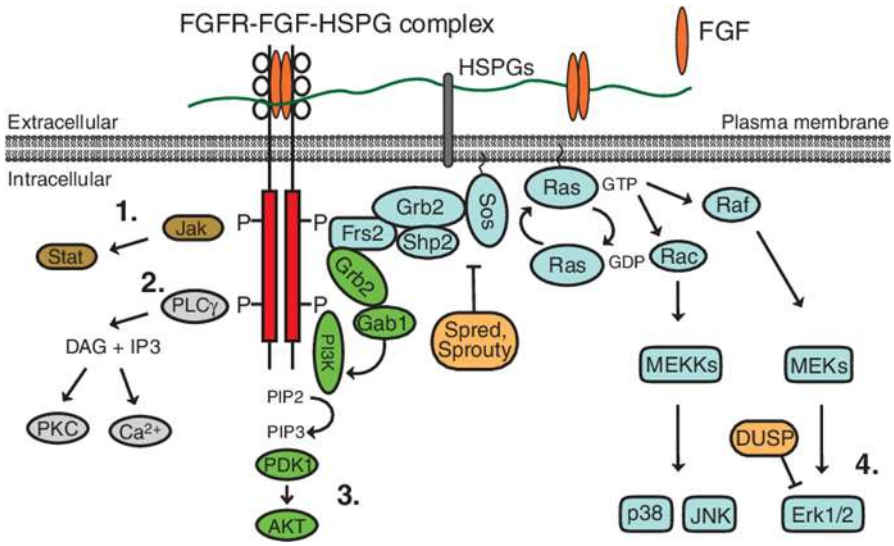

Fig. 34 Scheme of the pathway: *HSPGs enhance growth factor effect on MEK, AKT and PKC cascades.*

A

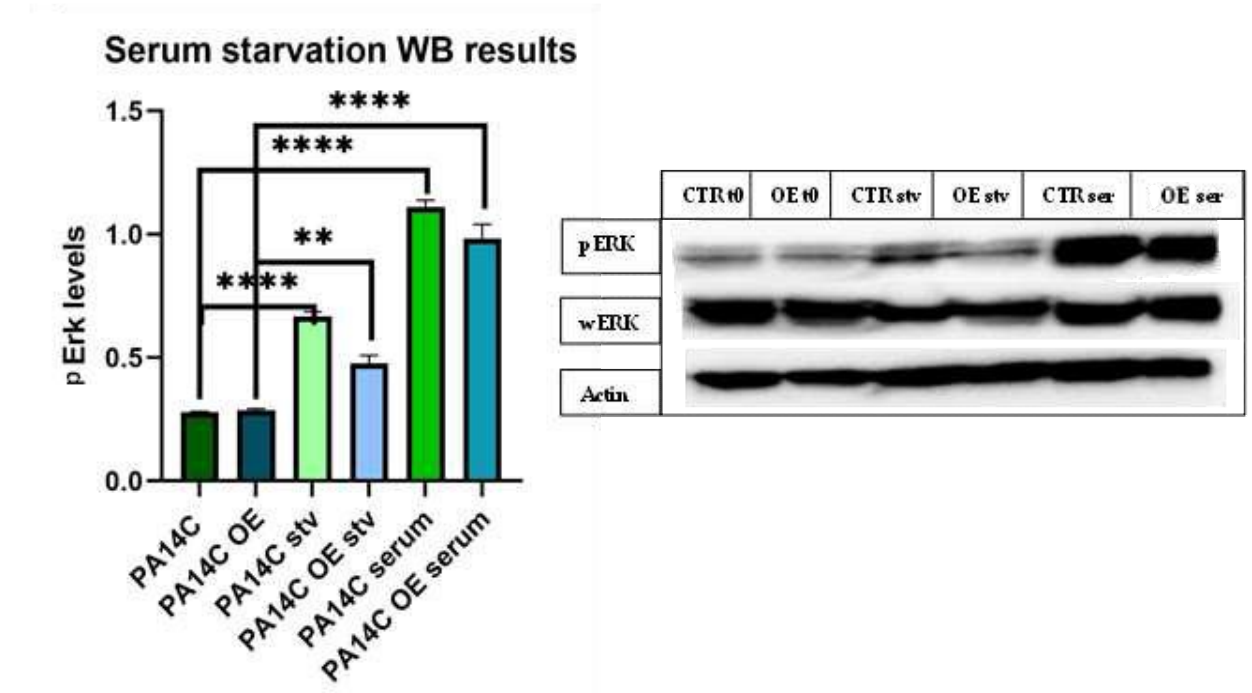

B

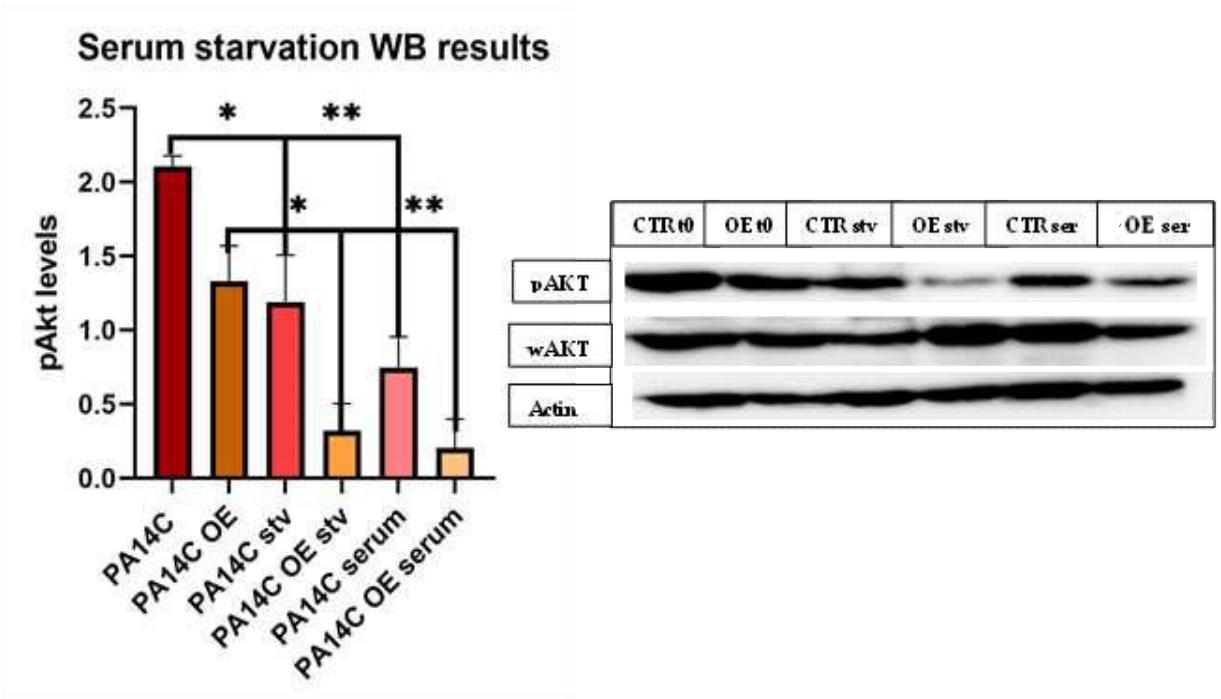

Fig. 35 WB results of serum starvation in PA14C OE Sdc-1 cells: A) *pERK levels are not affected by Sdc-1 surface overexpression, while the difference between OE starvation and OE serum restore compared with OE control results to be significant, as well as for PA14C control group (** p value = 0.0031; **** p value < 0.0001; n=3; ANOVA, one-way, unpaired, parametric p-values)* ***B)*** *pAKT is reduced by serum starvation in PA14C OE cells and even after serum replacement the re-activation of the pathway is weaker than PA14C cells (* p value = 0.021; *** p value < 0.0029; n=3; ANOVA, one-way, unpaired, parametric p-values). In both the assay, controls such as whole ERK and whole AKT together with β-actin were included.*

Exosomal mRNA extraction from PANC-1 and human cardiac fibroblasts

Exosomes are RNA and protein-containing tiny vesicles (30–150 nm) constantly secreted by all healthy and abnormal cells and found in abundance in all body fluids. They have a wide range of biological functions, including cell-to-cell communication and signalling and for that reason, they have a tremendous biomarker potential. An ideal biomarker should be easily assayed with minimally invasive or non-invasive medical procedures but possess high sensitivity and specificity. In this case, the use of PANC-1 (A1) and human cardiac fibroblasts (B1) had the purpose of identifying differential expression of exosomal RNA, which could be used in the future as possible biomarkers through liquid biopsies. Profiling of free RNAs and also circulating RNAs, have been used in several studies to identify novel and highly promising biomarkers for many pathologies, such as tumours and neurodegenerative diseases. Exosomes have been documented to contain circRNA, miRNA and lncRNAs. Circular RNA (circRNA) is a single stranded DNA closed in a circular loop, so 3′ and 5′ end resulted to be joined together. The unique structure of circRNAs provides them with a longer half-life and more resistance to RNase than linear RNAs, which makes them potential candidates for diagnostic biomarkers and therapeutic targets. PANC-1 (A1) and human cardiac fibroblasts (B1) showed 195 exosomal circRNA, while B1 174 circRNA. In the region where they overlap, are represented 5 circRNA in common between the two samples (Fig. 36).

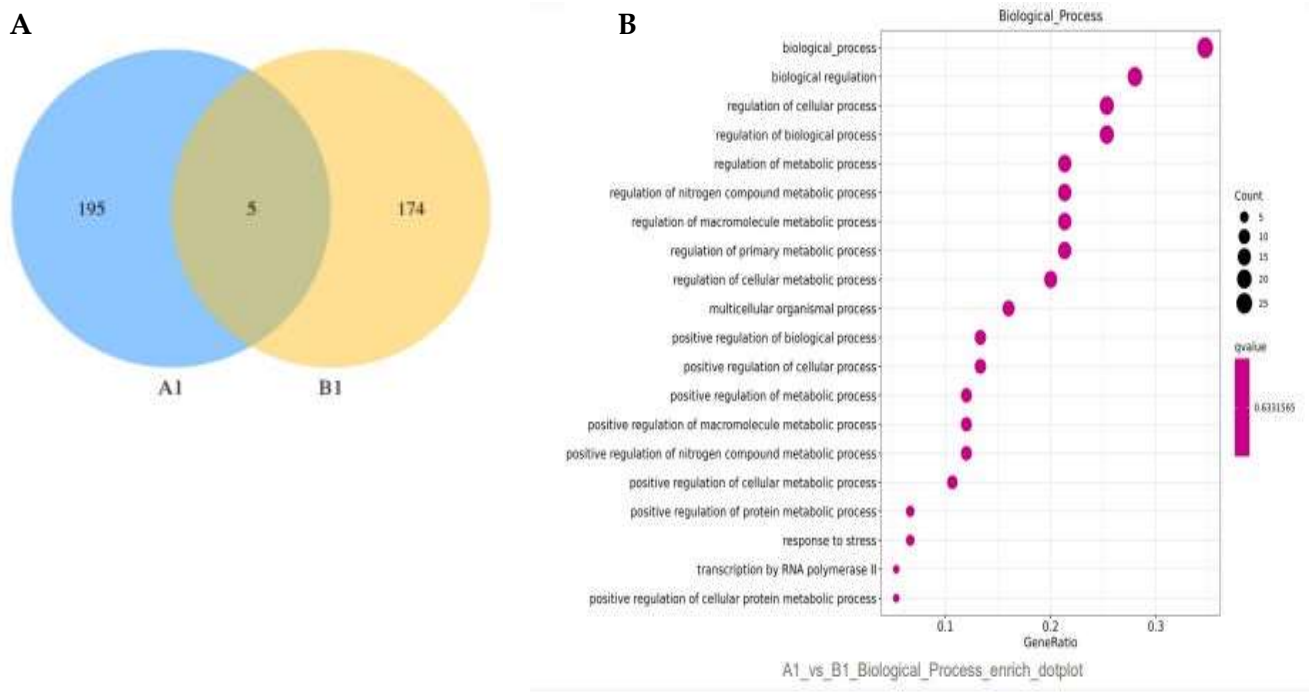

Fig. 36 Analysis A1 vs B1 samples: A*) Venn diagram on circular RNA counts among samples.* ***B****) Enrichment dot plot showing significant q value especially for the circRNA involved in biological process or regulation.*

In this project, threshold for defining differentially expressed genes was set as Fold Change no smaller than 2 and FDR<0.005. Fold change indicates ratio of expression levels between two samples A1 and B1. Gene set extracted by differential expression analysis (DEG) on circRNA is processed as independent statistical hypothesis testing on large number of circRNA expression (Table II).

Specifically, DEGs determines genotypical variability between two or more conditions of cells, helping identify genes that show significance differences.

TABLE II: Differential expression of circRNA in A1 and B1.

DEG Set	DEG Number	up-regulated	down-regulated
A1_vs_B1	160	105	55

Note: #DEG_Set: DEG-Set name;
All_DEG: Counts of DE-circRNA;
up-regulated: Number of up-regulated circRNA;
down-regulated: Number of down-regulated circRNA.

miRNAs are small, single stranded and non-coding RNA molecules involved in RNA silencing and post-transcriptional regulation of gene expression. miRNAs resemble the small interfering RNAs (siRNAs) of the RNA interference (RNAi) pathway, except miRNAs derive from regions of RNA transcripts that fold back on themselves to form short hairpins, whereas siRNAs are short non-coding double-stranded RNA (20-24 bp) and the human genome may encode over 1900 miRNA (Fig. 37). They interfere with the expression of specific genes with complementary nucleotide sequences by degrading mRNA after transcription, preventing translation. In Table II the differential expression showed 49 upregulated and 43 downregulated miRNAs in the two samples (A1 vs B1).

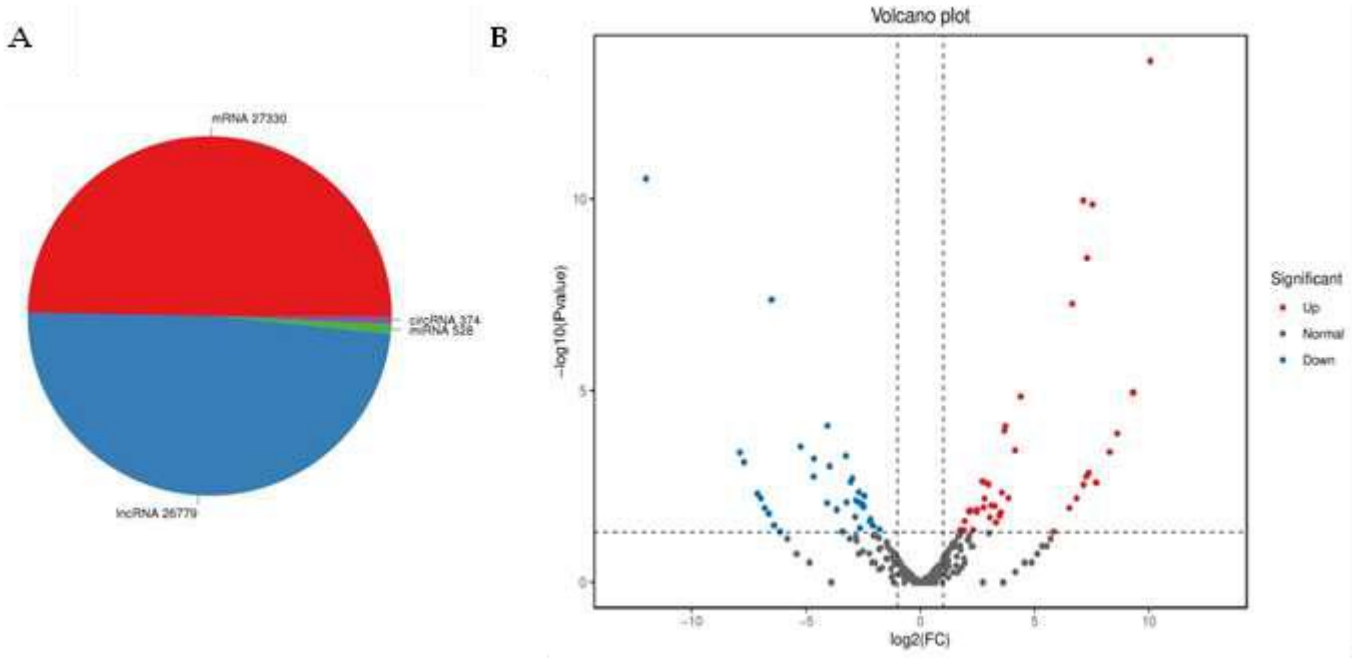

Fig. 37 miRNAs analysis: ***A****) Overview of RNA molecules identified in the samples, where miRNA and lncRNA are the most abundant classes.* ***B****) Volcano plot of miRNA analysis.*

TABLE III: Differential expression of miRNA in A1 and B1.

DEG Set	DEG Number	up-regulated	down-regulated
A1_vs_B1	92	49	43

As showed in Fig. 38A genes specifying long non-coding RNAs (lncRNAs) occupy a large fraction of the genomes of complex organisms. Long non-coding RNA (lncRNA) are 200 nucleotides long and they include intergenic lincRNAs, intronic ncRNAs, and sense and antisense lncRNAs. Most of them are just transcriptional noise and just a small portion of them have been demonstrated to be biologically relevant such as cell differentiation or physiological processes like cytokines expression, p53 response to DNA damage, inflammation.

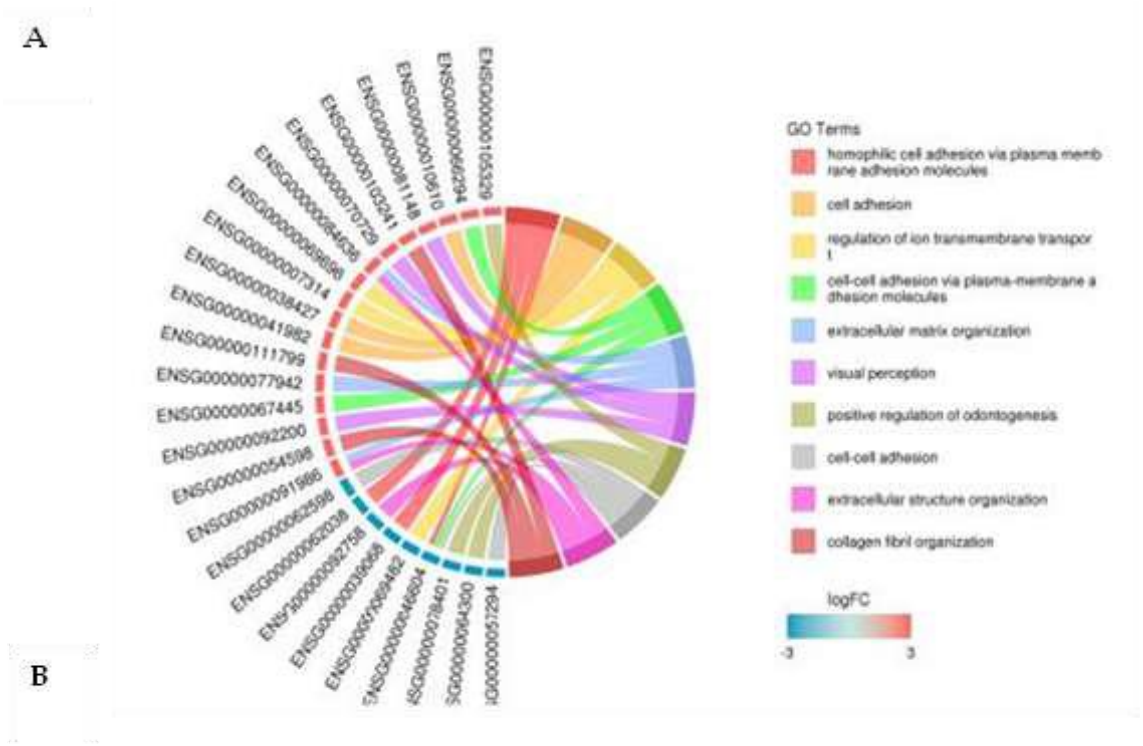

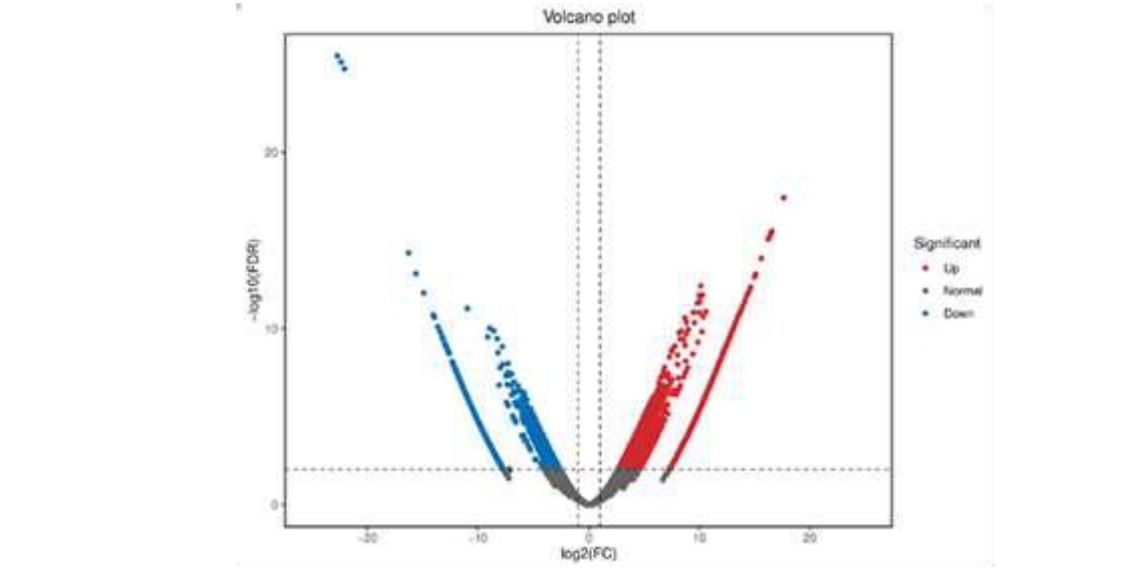

Fig. 38 lncRNA analysis: A) *Chordal diagram showing the involvement of the respectively upregulated or downregulated genes in the different cellular functions;* ***B)*** *volcano plot.*

TABLE IV: Differential expression of lncRNA in A1 and B1

DEG Set	DEG Number	up-regulated	down-regulated
A1_vs_B1	5,692	4,078	1,614

Fig. 38B showed the different types of lncRNA classified according to the sample's expression, where upregulated genes of lncRNA were more abundant than the downregulated also reported in table III. The chordal diagram showed through the use of different colour in which pathway were involved the upregulated and downregulated lncRNA, for example the collagen fibril organization was only upregulated A).

The volcano plot, represented the level of expression of lncRNA, specifically upregulated on the right side of the plot and downregulated on the left. The most interesting genes were the ones more distant from the cut-off. The black dots were genes whose expression levels didn't change between the two samples.

Lastly, focusing on miRNA expression distribution (Fig. 39), the volcano plot showed that the most significant genes were upregulated in A1 in comparison to B1, while only three genes were reported as downregulated.

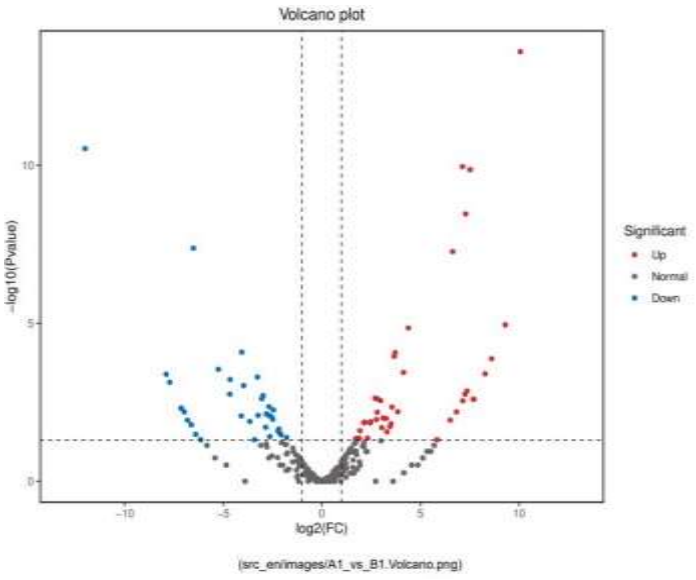

Fig. 39 miRNA analysis: *Volcano plot of the most significant miRNAs.*

These data are being analysed with the appropriate informatic instruments and will be object of a publication from Falciani lab, since they were done during my studies at the University of Siena.

Discussion

Pancreatic ductal adenocarcinoma (PDAC) has surpassed breast cancer as third leading cause of cancer-related death in the United States and the fourth in Europe. By 2030, it is widely predicted to become the second most common cause of cancer mortality. The factors driving the lethality of PDAC are numerous, centred on an inability to detect the disease until late in progression, often after distant metastasis. Moreover, outside of the minority (10%–15%) of cases ascribed to germline mutations or known risk factors, such as mucinous cystic lesions and chronic pancreatitis, there is no single attributable risk factor for most patients. Further complicating diagnosis, localized disease is largely asymptomatic or accompanied by ill-defined symptoms, there is a paucity of diagnostic biomarkers for earlier stage tumours, and the difficult-to-access anatomical location of the pancreas prevents routine office-based screening [24]. The most effective cancer treatment strategies presently in use are chemotherapy, radiotherapy, surgery, and if required, combinations of these approaches. However, various obstacles limit the efficacy of these treatments. Gene expression microarray analyses performed in pancreatic cancer (PC) cell lines showed more than 165 genes related to drug resistance. These genes were involved in a myriad of cell functions, including antioxidant activity, apoptosis, cell cycle regulation and transduction of signals, among others. For example, overexpression of integrin β1, an adhesion molecule involved in the interaction between cells and the extracellular matrix, has been linked to chemotherapy resistance in solid cancers, including PDAC through activation of PI3K pathway. Also, the EMT process is involved in drug resistance increasing the expression of E-cadherins and PI3K/AKT/mTOR pathways. Proteoglycans are an important part of this phenomenon regulating cell plasticity and stemness by directly controlling the activation of signalling cascades as co-receptors or regulating the availability of biological compounds such as growth factors and cytokines [51]. Syndecan-1 is up-regulated on PDAC, and it is a poor prognosis factor, especially when associated with increased levels of heparinase (HPA), which degrades the HS chains of syndecan-1. It promotes tumour progression and metastasis by enhancing the synthesis and shedding of syndecan-1 and specifically, HPA/syndecan-1 axis promotes the upregulation of FGF2, which in turn activates the PI3K/Akt pathway and EMT in cultured pancreatic cancer cell lines. Interestingly, syndecan-1 has been described to cooperate with KRAS to induce the malignant phenotype. A recent study demonstrates that syndecan-1 expression serves as a KRAS effector, inducing macropinocytosis in PDAC [3]. Also, Glypican-1 is overexpressed in PDAC and recently has been demonstrated that only cancer exosomes exhibit Gpc-1 on their surface in comparison to non-cancer exosomes. Surprisingly, the levels of Gpc-1 were able to distinguish between pancreatic cancer precursors lesions and patient with benign pancreatic disease, making it a good candidate for early detection of PDAC [52].

An important role in this scenario could be played by anti-cancer peptides. Their overall positive charge increases the affinity to cancer cells, which exhibit negative charge on the membranes, and induce cancer cell death through apoptosis or recruiting immune cells. They also show low tendency to promote drug resistance, less side effects and more tumour penetration properties. Nowadays MAP (multiple antigen peptides) are largely used in preclinical research due to their branched units bound to a functional group, which increase their stability against proteolytic degradation and allows multivalent binding [53]. In this work, BOPs were screened from the "Database of

Antimicrobial Activity and Structure of Peptides" (DBAASP v3.0) and selected for their amphipathic and cationic nature. They were synthesized in a tetra-branched structure and tested for stability in a pool of human sera for 0, 4 and 16 hours. As reported above, the chromatogram from HPLC analysis showed the persistency of BOP7 even at 16 hours, unexpected for short peptides. This data confirmed the importance of the repeating units, to stabilize the structure in comparison to a monomeric linear conformation that normally has a half-life of 30 minutes. The peptides were also tested in terms of safety for human red blood cells, in fact the hemolysis assay evaluates the hemoglobin release in plasma following an agent exposure and as reported above, even at the highest concentration of 100μM they didn't show any erythrocytes lysis. In order to verify the ability of binding pancreatic cancer cells, Mia-Paca2 and PANC-1 were used for immunofluorescence assays and flow cytometry. Particularly, the first showed that BOPs modified with biotin were able to bind cells surface (labelled with red signal) by emission of a green fluorescence, while flow cytometry not only confirm the binding but also gave us the information about the most effective concentrations. In fact, both confirmed their activity at 2μM and 10μM but not at 0.1μM, where the trend of the cytogram was similar to the one traced by the negative control (Fig. 18). Due to the cationic conformation of the peptides, we hypothesized that HSPGs could have been involved as possible target in the binding of BOPs on pancreatic cancer surface, thanks to their overall negative charge given by the glycosaminoglycan branches. To investigate this assumption, we performed another flow cytometry using RAW 264.7 which is a murine macrophage cell line used as a negative control due to their non-tumoral origin and PgsA-745, Chinese hamster cell line that lack of xylosyltransferase, an enzyme that is responsible of HSPGs synthesis. The BOPs peptides, particularly BOP7 and BOP9, showed cancer selectivity, confirmed by the low profile toward non-cancer cells. BOP2 on the other hand, had a poorer selectivity profile. To confirm that BOP7 and BOP9 were able to link HSPGs, a heparin-bio ELISA was performed. In fact, the vast majority of HS-binding proteins also invariably bind heparin, since its main repeat unit structurally resembles the protein binding sequences in heparan sulphate. Both the peptides were showing an effective binding at 5 μM while at the highest concentration of 10μM the binding was weaker, maybe due to the reaching of a plateau state. To support these data and to know more about the strength of the binding affinity, we made a flow cytometry using PANC-1, BOPs and two concentrations of heparin (5μg/ml and 20μg/ml). BOPs were displaced from PANC-1 binding, by heparin at 20μg/ml concentration, confirming the targeting of heparan sulphate chains.

Cytotoxicity towards pancreatic cancer cells was tested *in vitro* against PANC-1 and was measured as $8.3x10^{-6}$ M for BOP9 and $1.67x10^{-6}$ M for BOP7. BOP9 was then tested in a mouse model of metastasis. Nude mice and luminescent pancreatic cancer cells were used, and the tumour growth was monitored by imaging along 30 days of treatment with BOP9 (28 mg/kg). The peptide was able to reduce tumour growth in comparison to the controls, confirming the cytotoxic effect on pancreatic circulating cells (Fig. 28). The choice to create a metastatic model was due to the well-known involvement of HSPGs in EMT transition, extravasation of the primary tumour and metastasis. This possible role was also suggested by the encouraging data from the adhesion and migration assays, where BOP9 and BOP7 exhibited a significant adhesion and migration inhibition capacity. Taken together all these results confirmed the specific binding of BOP9 and BOP7 to HSPGs and their potential role as therapeutics. Since this seems to be true especially for BOP9, it would be interesting in the future to investigate its role in primary tumours, creating for example a pancreatic cancer

mouse model using BALB mice and injecting mouse pancreatic cancer cells. This would allow us to understand the effectiveness of the peptide in a model where the immune system is active and can contribute to the tumour inhibition or growth reduction, since several studies report peptide also as immunomodulator molecules. To predict the effect on the immune system, we could perform ELISA or single cell RNA experiments in which macrophages or T CD8+ cells or Treg cells could be screened in terms of cytokines and gene variation after treatment with BOPs. Another predictive model could regard the use of organoids to study drug penetration in a more complex model. In fact, it has been demonstrated that monolayer cell treatments show different results when used in 3D cell associations. BOPs could be also used as carrier of chemotherapeutics or in combination with other drugs to amplify their effect. Additionally, studying the phenotypic aspects of cancer cells, BOPs could also be used to investigate their effects on tube formations on endothelial cell lines and colony formation on pancreatic cancer cells. Lastly, since HSPGs are involved in macropinocytosis we could treat cells and look at their uptake ability variations.

During my period abroad, we used primary pancreatic cancer cells and metastatic cells collected in patient's liver and lung. All the cell lines express KRAS mutation G12D (except for PAO1C and PAO4C) known as the main driver-mutation in pancreatic cancer. HPNE is an immortalized cell line from healthy pancreatic tissues used as negative control for the next experiments. The expression of Syndecan-1 and Glypican-1 in these cells was evaluated by western blot, where PA14C, PAO4C and HPNE showed lower levels of Sdc-1 and PA18C, PA14C, PAO4C, PAO2C showed lower expression of Gpc-1 (Fig. 29). To verify the correlation between mTOR pathway and Syndecan-1/Glypican-1 we used two different drugs: Rapamycin which is known to inhibit specifically mTOR complex 1 by binding FRB domain and AZD2014 which is effective on mTOR complex 2. Complex 1 is responsible of the balance between anabolism and catabolism, promoting protein and lipids synthesis and cell growth. On the other hand, complex 2 plays an important role in proliferation and survival through activation of AKT and PI3K signalling by growth factor stimulation (such as insulin-growth factor). Downstream effectors are frequently mutated in cancer cells resulting in mTOR hyper activation. By using the two treatments at different time points (t=2h, t=8h, t=24) we observed different results along the cell lines (Fig. 30). HPNE cells didn't show any variation in the expression of both proteoglycans, being non-cancer cells. PAO1C and PAO2C showed a reduction in Glypican-1 expression after 8h of treatment with AZD2014. PAO3C reported lower levels of Sdc-1 and Gpc-1 during the whole treatment with both drugs. PAO4C showed a reduction on Gpc-1 levels already at 2h of incubation with AZD2014. PA14C didn't express any proteoglycans variations, except for an unexpected increase of HSPGs expression after 8h. PA18C results suggested modification in glypican-1 expression after 8h of treatment with AZD2014. Lastly, PA16C was the only cell line that showed a reduction of both proteoglycans starting from 8h of incubation with AZD2014. Taken together this data suggested that Gpc-1 could be related with mTOR complex 2 regulations, probably due to its interaction in heparin-binding growth factors (FGF and VEGFA) and their receptors, enhancing MARK and PI3K/AKT signalling. We then proceeded silencing PAO3C and PAO16C expression of Sdc-1 and Gpc-1, obtaining good reduction of Gpc-1 levels by using of the same plasmid in both cell lines. Sdc-1 was silenced using different plasmids, in PAO3C with clones 2 and 3 and in PA16C by using clone 4. Unfortunately, we couldn't investigate the specific effect of the knockout obtained. In the future it could be interesting to see how this reduction affects mTOR, PI3K and AKT pathways, since AKT phosphorylation is correlated with poor prognosis. We could expect

to observe reductions on colony formation, tube formation assays on endothelial cell lines and cancer cells migration like the results we could obtain for BOPs treatment. From literature, we know that in most of the tumours mTOR phosphorylation is higher in metastasis than in primary tumour, it could be interesting to verify it on pancreatic cancer cells.

Finally, we overexpressed Sdc-1 in PA14C cells, chosen because of the low baseline expression of this proteoglycan. Serum starvation is largely used to downregulate Erk and Akt pathway, that can be completely restored adding complete media after only 30 minutes of incubation. Sdc-1 transfected cells seemed to be more sensitive to serum starvation and showed less Akt phosphorylation and a weaker restore of AKT levels after serum addition in comparison to the parental cell line levels, which confirmed the essential role of HSPGs as enhancer of growth factors. ERK phosphorylation showed the same trend in OE and control cells, in fact both reported low basal levels, affected even more by serum starvation and completely recovered after complete media addition. Future projects could regard the treatment of PA14C OE Sdc-1 with BOP9 to observe variation on Akt and mTOR pathway, especially mTOR complex 2. Real time PCR could be an important confirmation of transcriptional variation in AKT levels.

Lastly, speaking in terms of useful markers for an early detection, traditionally, overexpressed proteins/epitopes such as CA 19-9, CA-50, CEA, and many others are being used as pancreatic cancer tumour markers. The main utility of these biomarkers was in the diagnosis of pancreatic cancer as well as to assess response to chemotherapy and to determine prognosis and to predict tumour recurrence. However, these markers had significant limitations such as lack of sensitivity, false-negative results in certain blood groups, as well as false-positive elevation in the presence of obstructive jaundice. To circumvent these limitations, an extraordinary amount of research is being performed to identify an accurate tumour marker. In the last part of this work, we extracted exosomal mRNA from pancreatic cancer cells and human cardiac fibroblasts to compare the expression of different classes of RNAs. Starting with circRNAs (Fig. 36) the comparison between the two cell lines showed that the most significant genes were the ones involved in biological processes. The Venn diagram also showed that the two samples have 5 genes of circRNAs in common, but the limitation of the Venn diagram is the lack of discrimination between up and downregulated genes. Another family which is increasingly receiving attention is the lncRNAs, due to the regulation activity that can exert in different pathways such as p53. The volcano plot reported as mostly upregulated the genes involved in the regulation of transcription. More details were given by the chordal graph where cancer cells had lower expression levels of genes regulating cell-cell adhesion, while higher levels of the ones into collagen fibril organization and external matrix regulation. Since Gpc-1 has been associated on pancreatic cancer exosomes surface as cancer progression promoter, we could investigate the effects of BOPs treatment on exosomes production. The future perspectives will involve the deeper analysis of specific genes of that up and downregulated pathways and the comparison of their expression using healthy pancreatic cancer cells, through qPCR. Finally, it could be interesting to treat the cells with some specific inhibitors to observe the effects on them.

As closing remarks, BOP7 and BOP9 showed evidence of reduction tumour progression and migration, through HSPGs binding, confirming their role as possible therapeutics. At the same time,

our work confirmed the correlation between Syndecan-1 and Glypican-1 with Akt pathway and indirectly with mTOR signalling, affecting pancreatic cancer progression.

Acknowledgements

The last three years of PhD have been an extremely exciting and rollercoaster period of my life, where I had the opportunity to experience the ups and downs of the role of being a junior researcher.

The first person I would like to thank is surely my thesis advisor, Dr. Chiara Falciani. Her guidance and support have helped me think critically and become a better researcher. She is not only a great scientist but also a very understanding human being who mentored me in both my scientific and non-scientific life, always ready to give me advice also regarding my experiences abroad and my life choices. This journey it's been the greatest choice I've ever made, and I would do it again if I could.

At the end of my PhD, I'm now realising that I had the opportunity to train students, participate to seminars, lectures, congresses and work on different fields and I discovered new passions and interests, but more importantly I've learnt how to embrace failure as part of the process of your growth. So, my gratitude goes to the whole lab team, starting from Giada that slowly opened up with me and become a friend more than a colleague. Of course, my students Eva, Alessandro and Benedetta that have been an active part of my experiments, not only as students but as reliable colleagues. I wish them all the best for their future in science. Thanks to a recently added member of Falciani lab, Tania. Your kindness and gentleness reflect the wonderful soul you are, I will miss our chats in the FACS room so badly. I hope you find the reward you deserve.

Speaking about the other labs members, thanks to the "old" part of the team, Laura and Giovanni for introduced me to the world of Bacteria and for being such a great "foodie" company. Elisabetta who I got to know better on my second year. Thanks for being a real friend, acting as my rational side. Thanks to Marta, for being an unexpected wonderful discover. You've been always there for me, making me feel home since the very beginning…please keep smiling.

To my lab-mate Clelia, I will never forget our chats and how easily we speak about silly things and then we switch to worldwide problems. I truly love the way we can be ourselves with no restrictions, you're such a pure heart!

Now my friends, some of them are part of my university life, like Gioia. We went through Covid-19 and PhD together, always meeting for a coffee and sharing our struggles and our joys even during our periods abroad. You know everything about me as I do, and I wish you the best for the new career you just started, I believe in you and I'm sure you will achieve great goals. I will always remember the day before I left Siena to move to US, when you drove me around the city so proud of the new car, but both crying because for the first time we knew we were going to end this journey separately. I love you so much.

Gabriella who believes in me more than I do, I can't still realize I have a nephew. Elisa, which always makes me laugh even when she is broken inside. Cristina, my secret soulmate, we fell in love from the very beginning, sharing everything and always being there supporting each other. Your achievements are also mine, but if there's one thing we can't do together, is watching movies, and you know why. Maria Giovanna, whose mom fed me with homemade figs pies every time she sent a pack! I promise to come to visit you and to trek Cervati together when I will have holidays. Good luck with your PhD, you're smart enough to smash it!

About my periods abroad, I loved Malta. I was totally surprised by this little Arabic-Italian Island with British heritage in the middle of nowhere. The best experience I've ever made so far, working with Christine and Maria that always guided me, sharing their knowledge, it's been a privilege. To my little cold polish girl, I loved the way you became my youngest sister and I never cried so much as I did in our last dinner together. Keep on chasing your goals and see you in Poland! All my Latin dance school friends, well….you know I will be back soon!

In USA I met Tanatcha and Suji that made me realize that Thai people are the purest gentle people in the world, I could never make it without your support; my roomies, Shefallika, Roja and Anouska, who made Worcester a better place and Jacoba and Wilson for being my Dominican best friends there! I felt blessed to have the opportunity to study and to learn from Dr. Brian C. Lewis a different approach to research. You opened the door of your lab, because as you said, "you saw something in me", I hope I haven't disappointed your expectations. Jeff and Maria, Remo and Luigia, literally my second family. You guys left me that I was only 16 years old and now our paths crossed again almost 13 years later…. Anyway, I'm still your little "cousin" coming from Italy and surprised about everything in USA, even about the size of the muffins.

Lastly, my boyfriend Andrea that always stood up for me, even when I felt lost and insecure, he always believed in me and supported every decision I've taken, without never limiting or influencing my choices. I truly believe love doesn't restrict the freedom and the identity of the other partner, thanks for calming my chaos.

My family, the most important persons I care about. My mother that keeps on asking me if I ate enough and to be safe when I travel, even if I'm almost 30 years old. You gave everything to your children, now it's time to enjoy life. My dad, who is my male version! We always fight because of our too similar personalities, but your honesty inspires me every day and if I keep this stubbornness, it's because you taught me that a person can change someone else's life. My brother that just like my mum, always has been the funny and the joyful part of the family. You're my best friend and even if we grew up, I still feel your little sister that looked at you with the eyes of unconditional love. Finally, my last gratitude is for myself, for never giving up and for leaning to stop being hard on myself. My self-criticism and perfectionism had burnt me out especially in USA where loneliness has amplified my defects. The best lesson I've received during this journey is to embrace yourself, to heal and to be your best version every day.

"Kindness is the language which the deaf can hear and the blind can see".

Mark Twain

References

[1] «A concise overview: structure and function of proteoglycans,» [Online]. Available: https://biologywise.com/structure-function-of-proteoglycans#:~:text=Proteoglycans%2C%20many%20a%20time%2C%20act,prevent%20their%20degeneration%20by%20proteases..

[2] I. V. Renato e S. Liliana, «Proteoglycan form and function: A comprehensive nomenclature of proteoglycans,» in *Matrix Biology*, Elsevier, 2015, pp. 11-55.

[3] B. Nausika, J. Bertran-Mas, A. Andreeva e C. E. Semino, «Syndecan and Pancreatic Ductal Adenocarcinoma,» *Biomolecules,* pp. 1-22, 2021.

[4] U. Karolina, K. Tanja, V. Veronika, K. Melitta, B. Heimo e H. Christine, «Expression of chondroitin sulphate proteoglycan 4 (CSPG4) in melanoma cells is downregulated upon inhibition of BRAF,» *Oncology reports,* vol. 45, n. 4, 2021.

[5] B. Maree e S. Kaye, «Betaglycan: A multifunctional accessory,» in *Molecular and Cellular Endocrinology* , Elselvier , 2011, pp. 180-189.

[6] H. Janna, R. Thomas e P. Linda, «Phosphacan and receptor protein tyrosine phosphatase b expression mediates deafferentation-induced synaptogenesis,» in *Hippocampus*, 2011, pp. 81-92.

[7] F. Jorge, «Glypicans: 35 years later,» *Proteoglycans research,* vol. 1, n. 2, 2023.

[8] H. J. Anthony, F. L. Brooke, B. J. Ifechukwude, B. J. Gregory e M. James, «Perlecan: a multi-functional, cell-instructive, matrix-stabilizing protoglycan with roles in tissue development has relevance to connective tissue repair and regeneration,» *Frontiers in cell and developmental biology ,* vol. 10, 2022.

[9] K. Chris, C. Liwen, W. J. Yao, Y. J. Albert e Y. B. Burton, «Structure and fuction of aggrecan,» *Cell Research,* vol. 12, pp. 19-32, 2002.

[10] W. N. Thomas, K. Inkyung, E. P. Stephen, H. A. Ingrid, C. Y. Mary, P. M. T. Oliver, A. E. Caris e F. W. Charles, «Versican- a critical extracellular matrix regulator of immunity and inflammation,» *Frontiers in Immunology ,* vol. 11, 2020.

[11] K. Jasvir e R. P. Dieter, «Extracellular Matrix (ECM) Molecules,» in *Stem cell biology and tissue engineering in dental sciences* , Academic press, 2015, pp. 25-45.

[12] I. J. Edwards, «Proteoglycans in prostate cancer,» *Nature reviews.*

[13] H. Michael, L. Zihan e R. Xi, «Extracellular matrix dynamics: tracking in biological systems and their implications,» *Journal of Biological Engineering ,* vol. 16, n. 13, 2022.

[14] S. P, «News medical life sciences,» [Online]. Available: https://www.news-medical.net/life-sciences/Structure-and-Function-of-Proteoglycans.aspx.

[15] A. D. Theresa, B.-C. R. Sara, J. M. Amalie, L. Caroline, S. B. Charlotte, S. T. Nicolai, C. M. Thomas, S. Ali e A. O. Mette, «The role of proteoglycans in cancer metastasis and circulating tumor cell analysis,» *Frontiers in cell and developmental biology ,* 2020.

[16] W. Jinfen, H. Meiling, H. Kaitang, L. Shudai e D. Hongli, «Roles of proteoglycans and glycosaminoglycans in cancer development and progression,» *international journal of molecular sciences,* vol. 21, n. 17, 2020.

[17] C. Vicente, D. D. Silva, P. Sartorio, T. Silva, S. Saad, H. Nader, N. Forones e L. Toma, «Heparan Sulfate Proteoglycans in Human Colorectal Cancer,» *Analytical Cell Pathology Journal,* 2018.

[18] W. Park, A. Chawla e E. O'Reilly, «Pancreatic cancer: a Review,» *JAMA,* vol. 326, n. 9, 2021.

[19] C. Mario, F. Marilisa, I. R.-C. Kryssia, C. Pellegrino, C. Ginevra, M. Chiara, B. Alberto, N. Antonio, L. Gioacchino, M. Tiziana, L. d. A. Gian e D. M. Francesco, «Epidemiology and risk factor of pancreatic cancer,» *Acta Biomedical ,* pp. 141-146, 2018.

[20] H.-F. Hu, Z. Ye, Y. Qin, X.-w. Yu, X.-j. Yu, Q.-F. Zhuo e S.-r. Ji, «Mutations in key driver genes of pancreatic cancer: molecularly targeted therapies and other clinical implications,» *Acta Pharmacologica Sinica,* 2021.

[21] D. K. Bartsh, M. Sina-Frey, S. Lang, A. Wild, B. Gerdes, P. Barth, R. Kress, R. Grutzmann, M. Colombo-Benkmann, A. Ziegler, S. A. Hahn, M. Rothmund e H. Rieder, «CDKN2A Germline mutations in Familiar pancreatic cancer,» *Annals of Surgery ,* vol. 236, pp. 730-737, 2002.

[22] I. A. Voutsadakis, «Mutations of p53 associated with pancreatic cancer and therapeutic implications,» *Annals oh Hepatobiliary pancreatic surgery ,* vol. 25, pp. 315-327, 2021.

[23] Z. Ezrova, Z. Nahacka, J. Stursa, L. Werner, E. Vlcak, P. K. Viziova, M. V. Berridge, R. Sedlacek, R. Zobalova, J. Rohlena, S. Boukalova e J. Neuzil, «SMAD4 loss limits the vulnerability of pancreatic cancer cells to complex I inhibition via promotion of mitophagy,» *Oncogene,* pp. 2539-2552, 2021.

[24] C. J.Halbrook, C. A.Lyssiotis, M. P. d. Magliano e A. Maitra, «PAncreatic cancer: advances and challenges,» *Cell ,* 2023.

[25] S. Stanciu, F. Ionita-Radu, C. Stefani, D. Miricescu, I.-I. Stanescu-Spinu, M. Greabu e M. J. Alexandra Ripszky Totan, «Targeting PI3K/AKT mTOR signaling pathway in pancreatic cancer: from molecular to clinical aspects,» *International Journal of Molecular Sciences,* 2022.

[26] W. J. Ho, E. M. Jaffee e L. Zheng, «The tumour micoenvironment in pancreatic cancer-clinical challenges and opportunities,» *Nature Reviews Clinical Oncology ,* pp. 527-540, 2020.

[27] Z. S. Kanji e S. Gallinger, «Diagnosis and management of pancreatica cancer,» *CMAJ,* pp. 1219-1226, 2013.

[28] A. B.-R. a. M. B. M. Cerezo-Magaña a, «The pleiotropic role of proteoglycans in extracellular vesicle mediated communication in the tumour microenvironment,» *Seminars in cancer biology ,* vol. 62, pp. 99-107, 2020.

[29] X. Fang, H. Lan, K. Jin e J. Qian, «Pancreatic cancer and exosomes: role in progression, diagnosis, monitoring, and treatment,» *Frontiers in Oncology ,* 2023.

[30] S. Guo, X. Wu, T. Lei, R. Zhong, Y. Wang, L. Zhang, Q. Zhao, Y. Huang, Y. Shi e L. Wu, «The role and therapeutic value of syndecan-1 in cancer metastasis and drug resistance,» *Frontiers in cell and developmental biology ,* 2021.

[31] W. Yao, J. L. Rose, W. Wang, S. Seth, H. Jiang, A. Taguchi, J. Liu, L. Yan, A. Kapoor, P. Hou, Z. Chen, Q. Wang, L. Nezi, Z. Xu, J. Yao, B. Hu, P. Pettazzoni, I. L. Ho e G. Draetta, «Syndecan1 is a critical mediator of macropinocytosis in pancreatic cancer,» *Nature ,* vol. 568, pp. 410-414, 2019.

[32] D. Yablecovitch, S. Ben-Horin, O. Picard, M. Yavzori, E. Fudim, M. Nadler, I. Levy, E. Sakhnini, A. Lang, T. Engel, M. Lahav, T. Saker, S. Neuman, L. Selinger, R. Dvir, M. Raitses-Gurevich e I. Laish, «serum syndecan-1: a novel biomarker fro pancreatic ductal adenocarcinoma,» *Clinical and traslational gastroenterology ,* 2022.

[33] Y. Zhu, D. Zheng, L. Lei, K. Cai, H. Xie, J. Zheng e C. Yu, «High expression of syndecan-4 is related to clinicopathological features and poor prognosis of pancreatic adenocarcinoma,» *BMC Cancer ,* 2022.

[34] M. K. Samantha McElyea, «The glycosaminoglycan syndecan-4 facilitates pancreatic cancer progression and biologic aggressiveness,» *Cancer research,* vol. 79, n. 12, 2019.

[35] D. Busato, M. Mossenta, M. D. Bo, P. Macor e G. Toffoli, «The proteoglycan Glypican-1 as a Possible Candidate for innovative targeted therapeutic strategies for pancreatic ductal adenocarcinoma,» *International Journal of Molecular Sciences,* 2022.

[36] S. A. Melo, L. B. Luecke, C. Kahlert, A. F. Fernandez, S. T. Gammon, J. Kaye, V. S. Leblue, E. A. Mittendorf, J. Weitz, N. Rahbari, C. Reissfelder, C. Pilarsky, M. F. Fraga e R. Kalluri, «Glypican 1 identifies cancer exosomes and detects early pancreatic cancer,» *Nature ,* 2015.

[37] S. Furini e C. Falciani, «Expression and role of Heparan Sulphated proteoglycans in Pancreatic Cancer,» *Frontiers in Oncology ,* 2021.

[38] S. Iriana, S. Ahmed, J. Gong, A. A. Annamalai, R. Tuli e A. E. Hendifar, «Targeting mTOR in Pancreatic Ductal Adenocarcinoma,» *Frontiers in Oncology ,* 2016.

[39] S. Iriana, S. Ahmed, J. Gong, A. A. Annamalai, R. Tuli e A. E. Hendifar, «Targeting mTOR in pancreatic ductal adenocarcinoma,» *Frontiers in Oncology,* 2016.

[40] M. Mortazavi, F. Moosavi, M. Martini, E. Giovannetti e O. Firuzi, «Prospects in targeting PI3K/AKT/mTOR pathway in pancreatic cancer,» *Critical reviews in Oncology/Hematology,* vol. 176, 2022.

[41] C. M. Li, P. Haratipour, R. G. Lingeman, J. J. P. Perry, L. Gu, R. J. Hickey e L. H. Malkas, «Novel peptide therapeutic approaches for cancer treatment,» *Cells,* 2021.

[42] P. G. Dougherty, A. Sahni e D. Pei, «Understanding cell penetration of cyclic peptides,» *Chemical Reviews,* 2019.

[43] B. B. B. R. Sarko D., N. E.M., L. K., E. M., A. A., H. U. e M. W, «The pharmacokinetics of cell-penetrating peptides,» *Molecular pharmacology,* 2010.

[44] C. Falciani, A. Pini e L. Bracci, «Oligo-branched peptides for tumor targeting: from magic bullets to magic forks,» *Expert opinion on biological therapy,* 2009.

[45] R. K. Chinnadurai, N. Khan, G. K. Meghwanshi, S. Ponne, M. Althobiti e R. Kumar, «Current research status of anti-cancer peptides: Mechanism of action, production, and clinical applications,» *Biomedicine & Pharmacotherapy ,* vol. 164, 2023 .

[46] R. Guerrini, E. Marzola, C. Trapella, M. Pela, S. Molinari, M. Cerlesi, D. Malfacini, A. Rizzi, S. Salvadori e G. Calo, «A novel and facile synthesis of tetrabranched derivates of nociceptin/orphanin FQ,» *Biomedical & Medicinal Chemistry ,* vol. 22, 2014.

[47] V. G. Joshi, V. D. Dighe, D. Thakuria, Y. S. Malik e S. Kumar, «Multiple antigenic peptide (MAP): a synthetic peptide dendrimer for diagnostic, antiviral and vaccine strategies for emerging and re-emerging viral diseases,» *Indian Journal of Virology ,* 2013.

[48] S. Silva, K. Kurrikoff, U. Langel, A. J. Almeida e N. Vale, «A second life of MAP, a model amphipatic peptide,» *International Journal of molecular sciences,* 2022.

[49] A. Gokhale e S. Satyanarayanajois, «peptides and peptidomimetics as immunomodulators,» *Immunotherapy,* 2014.

[50] N. T. T. Nhan, T. Yamada e K. H. Yamada, «Peptide-Based Agents for Cancer Treatment: Current Applications and future directions,» *International Journal of Molecular Sciences,* vol. 24, n. 16, 2023.

[51] Z. Karagiorgou, P. N. Fountas, D. Manou, E. Knutsen e A. D. Theocharis, «Proteoglycans determine the dynamic landscape of EMT and cancer stemness,» *Cancers ,* 2022.

[52] S. A. Melo, L. B. Luecke, C. Kahlert, A. F. Fernandez, S. T. Gammon, J. Kaye, V. S. LeBlue, E. A. Mittendorf, J. Weitz, N. Rahbari, C. Reissefelder, C. Pilarsky, M. F. Fraga e D. Piwnica-Worms, «Glypican-1 identifies cancer exosomes and detects early pancreatic cancer cells,» *Nature,* 2015.

[53] K. Sandler e J. P. Tam, «Peptide dendrimers: application and synthesis,» *Reviews in Molecular Biotechnology,* vol. 90, pp. 195-229, 2002.

[54] J. B.-M. A. A. a. C. E. S. Nausika Betriu, «Syndecan and Pancreatic ductal carcinoma,» *Biomolecules,* vol. 11, n. 3, 2021.

[55] Z. L. X. R. Michael Hu, «Extracellular matrix dynamics: tracking in biological systems and their implications,» *Journal of Biochemical engineering,* vol. 16, 2022.

[56] S. R. B.-C. A. M. J. C. L. C. B. S. N. T. S. T. M. C. A. S. M. Ø. A. Theresa D Ahrens, «The Role of Proteoglycans in Cancer Metastasis and Circulating Tumor Cell Analysis,» *Frontiers in Cell and Developmental Biology,* vol. 749, 2020.

[57] Z. Y. Y. Q. X. w.-X. X.-j. Y. Q. F. Z. S. r. J. Hai-Feng Hu, «Mutations in Key Drivers Genes of pancreatic cancer: molecularly targeted therapies and other clinical implications,» *Acta Pharmacologica sinica,* vol. 42, pp. 1725-1741, 2021.

[58] M. S.-F. S. L. A. W. B. G. P. B. R. K. R. G. M. C. B. A. Z. S. A. H. M. R. H. R. Detlef K.Bartsch, «CKDN2A Germline Mutations in Familiar Pancreatic Cancer,» *Annals of Surgery,* pp. 730-737, 2002.

[59] M. Distler, D. Aust, J. Weitz, C. Pilarsky e R. Grutzmann, «Precursor lesions for sporadic pancreatic cancer: PanIN, IPMN, and MCN,» *Biomed research International,* 2014.

[60] C. K. Weber, G. Sommer, P. Michl, H. Fensterer, M. Weimer, F. Gansauge, G. Leder, G. Adler e T. M. Gress, «Biclycan is overexpressed in pancreatic cancer and induces G1-arrest in the pancreatic cancer cell lines,» *Gastroenterology,* vol. 121, n. 3, pp. 657-667, 2001.

[61] G. S. P. M. H. F. M. W. F. G. G. L. G. A. T. M. G. Christoph K Weber, «Biglycan is overexpressed in pancreatic cancer and induces G-1 arrest in pancreatic cell lines,» *Gastroenterology Journal,* vol. 121, pp. 657-667, 2001.

[62] I. A. S. R. D. S. M. E. B. K. H. F. C. W. M. J. K. Tiago de Oliveira, «Syndecan-2 promotes perineural invasion and cooperates with K-ras to induce an invasive pancreatic cancer cell phenotype,» *Molecular cancer,* vol. 11, n. 9, 2012.

[63] D. Z. L. L. K. C. H. X. J. Z. C. Y. Yufei Zhu, «High expression of syndecan-4 is related to clinicopathological features and poor prognosis of pancreatic adenocarcinoma,» *BMC Cancer,* vol. 22, n. 1042, 2022.

[64] C. Vennin, P. Melenec, R. Rouet, M. Nobis, A. S. Cazet, K. J. Murphy, D. Herrmann, D. A. Reed, M. C. Lucas, S. C. Warren, Z. Elgundi, M. Pinese, G. Kalna, D. Roden, M. Samuel e P. Timpson, «CAF hierarchy driven by pancreatic cancer cell p53-status creates a pro-metastatic and chemoresistant environment via perlecan,» *Nature communications,* vol. 10, 2019.

[65] J. Zang, L. Darman, M. S. Hassan, U. V. Holzen e N. Awasthi, «Targeting KRAS for the potential treatment of pancreatic ductal adenocarcinoma: Recent advancements provide hope,» *Oncology reports ,* vol. 50, n. 5, 2023.

[66] A. Neville, A. Morina, T. Liskiewicz e Y. Yan, «Synovial joint lubrification- Does nature teach more effective engineering lubrification strategies?,» *Journal of mechanical engineering Science.*

[67] F. Xie, R. Li, W. Shu, L. Zhao e J. Wan, «Self-assemply of peptide dendrimers and their bio-application in theranostics,» *Material today bio,* 2022.

[68] F. S. T. Mirakabad, M. S. Khoramgah, K. Keshavarz, M. Tabarzad e J. Ranjbari, «Peptie dendrimers as valuable biomaterials in medical sciences,» *Life Sciences ,* 2019.